

Fretting Damage  
of  
High Carbon Chromium Bearing Steel

by

Masato Kuno, B.Eng, M.Eng.

Thesis submitted to the University of  
Nottingham for the degree of Doctor of  
Philosophy, May, 1988.

**BEST COPY**

**AVAILABLE**

Variable print quality

## ABSTRACT

This thesis consists of four sections, the fretting wear properties of high carbon chromium bearing steel; the effect of debris during fretting wear; an introduction of a new fretting wear test apparatus used in this study; and the effects of fretting damage parameters on rolling bearings.

The tests were operated under unlubricated conditions. Using a crossed cylinder contact arrangement, the tests were carried out with the normal load of 3N, slip amplitude of 50 $\mu$ m, and frequency of 30Hz at room temperature. The new fretting wear test rig consists of a sphere-on-plate arrangement, and the normal load and slip amplitude were variously changed. Using the new test rig, the tests were performed both at room temperature and 200°C, and tensile stresses were applied to the lower stationary specimens during the fretting wear tests.

In the fretting wear tests after tempering at 200, 230, 260 and 350°C in air, the high carbon chromium bearing steel showed low coefficients of friction due to a glaze type oxide film. In the fretting wear tests at 200°C, a very low coefficient of friction was obtained. Consequently, the oxide films on high carbon chromium bearing steel tempered at 200, 230, 260 and 350°C were thought to be protective in fretting damage.

Fretting wear volumes were measured using different specimen combinations and fretting oscillatory directions relative to the axes of the cylindrical specimens, although of the same material couples. It has been found that fretting

wear volume is significantly governed by frictional energy (fretting damage per unit area) and frequency of metal-to-metal contact, as determined by electrical contact resistance measurements. Metal-to-metal contact was observed throughout the whole stage of fretting wear even in the case of full slip fretting wear.

Fretting crack initiation is encouraged but fretting crack propagation rate is not significantly affected by high normal loads. Compressive residual stresses in the subsurface have little influence on crack initiation, but have a large influence on crack propagation rate. In the study of fracture induced by fretting wear, a critical slip amplitude which led to the shortest fracture life was identified. With the critical slip amplitude ( $35\mu\text{m}$ ), a higher coefficient of friction was obtained, and this result suggested a significant effect of coefficient of friction on fracture induced by fretting wear (or fretting fatigue).

The mechanisms of fretting wear and fretting fatigue were also discussed. Fretting wear is predominantly governed by the total tangential shear strain due to fretting oscillation. In contrast, fretting fatigue is dominated by the maximum alternating tangential shear strain energy. As coefficient of friction affects significantly both the total tangential shear strain and the maximum alternating tangential shear strain energy, it is thought to be the most important factor which needs to be controlled to reduce damage by both fretting wear and fretting fatigue.

## CONTENTS

CHAPTER		PAGE
1	<u>INTRODUCTION</u>	1
2	<u>LITERATURE REVIEW</u>	5
2-1	GENERAL ASPECTS OF FRETTING	5
2-2	THEORIES OF THE MECHANISM OF FRETTING WEAR	7
2-2-1	ADHESION THEORY	8
2-2-2	UHLIG'S THEORY	10
2-2-3	DELAMINATION THEORY	12
2-3	MINDLIN'S THEORY FOR FRETTING	15
2-4	THE EFFECT OF SOME VARIABLES ON FRETTING WEAR	17
2-4-1	MECHANICAL EFFECTS	17
2-4-1-1	AMPLITUDE OF SLIP	17
2-4-1-2	HARDNESS	18
2-4-1-3	SURFACE ROUGHNESS	19
2-4-2	CHEMICAL EFFECTS	21
2-4-2-1	DEBRIS AND OXIDE FILM	21
2-4-2-2	TEMPERATURE	22
2-4-2-3	ENVIRONMENT	24
2-5	INVESTIGATION OF FRETTING WEAR	27
2-5-1	CONTACT ELECTRICAL RESISTANCE DURING FRETTING WEAR	27

2-5-2	X-RAY RESIDUAL STRESS MEASUREMENT ON FRETTING SCAR	29
2-5-3	FRETTING WEAR PROCESS	31
2-5-3-1	VISIBLE OBSERVATION OF FRETTING WEAR PROCESS ON THE SURFACE	31
2-5-3-2	BEHAVIOUR OF CRACK IN FRETTING FATIGUE	32
2-5-3-3	DISCUSSION OF CRACK INITIATION DURING FRETTING OSCILLATION	34
2-6	THE EFFECT OF RESIDUAL STRESS ON FRETTING DAMAGE	36
2-7	TRIBOLOGICAL PROPERTIES OF CERAMIC MATERIALS	38
2-7-1	TRIBOLOGICAL PROPERTIES OF CERAMIC MATERIALS	38
2-7-2	FRETTING WEAR OF CERAMIC MATERIALS	40
2-8	FRETTING WEAR OF ROLLING BEARINGS	42
2-8-1	A PREVENTION OF FRETTING WEAR OF ROLLING BEARINGS	43
2-8-2	FRETTING PROPERTIES OF HIGH CARBON CHROMIUM BEARING STEEL	44

### 3 FRETTING WEAR IN SINTERED ALUMINA- AND TUNGSTEN CARBIDE COBALT CERMET-METAL COUPLES

3-1	INTRODUCTION	46
3-2	EXPERIMENTAL PROCEDURE	48
3-2-1	MATERIALS	48

3-2-2	TEST RIG	48
3-2-3	SCANNING ELECTRON MICROSCOPY	49
3-2-4	WEAR VOLUME	50
3-3	EXPERIMENTAL RESULTS	51
3-3-1	COEFFICIENT OF FRICTION	51
3-3-2	SCANNING ELECTRON MICROSCOPY	52
3-3-3	WEAR VOLUME	52
3-4	DISCUSSION	54
3-5	CONCLUSIONS	58

**4 THE EFFECT OF OXIDE FILM AND HARDNESS ON  
FRETTING WEAR IN HIGH CARBON CHROMIUM  
BEARING STEEL**

4-1	INTRODUCTION	60
4-2	EXPERIMENTAL PROCEDURE	62
4-2-1	MATERIALS	62
4-2-2	TEST CONDITIONS	62
4-2-3	WEAR VOLUME	63
4-3	EXPERIMENTAL RESULTS	64
4-3-1	COEFFICIENT OF FRICTION	64
4-3-2	WEAR VOLUME	64
4-4	DISCUSSION	65
4-4-1	COEFFICIENT OF FRICTION	65
4-4-2	WEAR VOLUME	67
4-5	CONCLUSIONS	70

**5 THE EFFECT OF OSCILLATORY DIRECTION AND  
SPECIMEN COMBINATION ON FRETTLING WEAR UNDER  
A CROSSED CYLINDER CONTACT CONDITION**

5-1	INTRODUCTION	72
5-2	EXPERIMENTAL PROCEDURE	74
5-2-1	MATERIALS	74
5-2-2	TEST CONDITIONS	74
5-2-3	WEAR VOLUME	75
5-2-4	ELECTRICAL CONTACT RESISTANCE	75
5-3	EXPERIMENTAL RESULTS	76
5-3-1	COEFFICIENT OF FRICTION	76
5-3-2	ELECTRICAL CONTACT RESISTANCE	76
5-3-3	WEAR VOLUME	77
5-4	DISCUSSION	79
5-5	CONCLUSIONS	83

**6 A NEW FRETTLING WEAR TEST APPARATUS**

6-1	INTRODUCTION	84
6-2	DESIGN	86
6-2-1	FRETTLING WEAR TEST MACHINE	86
6-2-2	SPECIMENS	86
6-2-3	TEMPERATURE CONTROL	87
6-2-4	NORMAL LOAD CONTROL	87
6-2-5	SLIP AMPLITUDE AND FREQUENCY CONTROL	88
6-2-6	COEFFICIENT OF FRICTION	88

6-2-7	APPLIED STRESS TO THE LOWER STATIONARY SPECIMEN	89
7	<u>FRETTING WEAR TEST ON HIGH CARBON CHROMIUM BEARING STEEL USING A NEW TEST APPARATUS</u>	
7-1	INTRODUCTION	90
7-2	EXPERIMENTAL PROCEDURE	93
7-2-1	MATERIALS	93
7-2-2	TEST CONDITIONS	93
7-2-3	FRETTING WEAR TEST AT 200°C	94
7-2-4	DEVELOPMENT OF FRETTING WEAR SCAR	94
7-2-5	FRACTURE INDUCED BY FRETTING WEAR	94
7-3	EXPERIMENTAL RESULTS	96
7-3-1	DEVELOPMENT OF FRETTING WEAR SCAR	96
7-3-2	ELECTRICAL CONTACT RESISTANCE	96
7-3-3	FRACTURE INDUCED BY FRETTING WEAR	97
7-4	DISCUSSION	98
7-4-1	DEVELOPMENT OF FRETTING WEAR SCAR	98
7-4-2	FRACTURE INDUCED BY FRETTING WEAR	100
7-4-2-1	CRITICAL SLIP AMPLITUDE	100
7-4-2-2	THE EFFECT OF TEMPERATURE	101
7-4-2-3	THE EFFECT OF THE NORMAL LOAD	102

7-4-2-4	THE EFFECT OF RESIDUAL STRESS	103
7-4-2-5	FRACTURE SURFACE	104
7-4-3	CRACK INITIATION AND WEAR DURING FRETTING OSCILLATION IN HIGH CARBON CHROMIUM BEARING STEEL, PARTICULARLY SPHERE-ON-PLATE ARRANGEMENT	106
7-4-3-1	CRACK INITIATION AND WEAR	106
7-4-3-2	DISCUSSION OF CRACK INITIATION	108
7-4-3-3	FRETTING WEAR AND FRETTING FATIGUE	111
7-5	CONCLUSIONS	112

## 8 PRACTICAL APPLICATION OF FRETTING DAMAGE PREVENTION FOR ROLLING BEARINGS

8-1	HIGH CARBON CHROMIUM BEARING STEEL	115
8-2	FRETTING WEAR AND FRETTING FATIGUE IN ROLLING BEARINGS	116

## ACKNOWLEDGEMENTS

## REFERENCES

## FIGURES AND TABLES

## 1. INTRODUCTION

The main cause of fretting wear is small amplitude oscillation between surfaces which are in contact with each other. Consequently, fretting wear damage can often be found in many machine components, for example rolling bearings. The typical form of fretting damage found on these rolling bearings is called "false brinelling". It is usually produced between the rolling elements and the raceways, and appears when the rolling bearings do not rotate but are subjected to small vibrations. The phenomenon may sometimes occur during transport of components. Another type of fretting damage which may be observed on rolling bearings is often found between the outer ring and the bearing cartridge or between the inner ring and the shaft. Fracture may be initiated by such fretting damage.[1]

The industrial demands of rolling bearings have increased with technological developments. In order to reduce cost, weight and size of the component machinery, smaller sizes of rolling bearings, e.g. miniature rolling bearings, have been frequently used in electrical goods such as video tape recorders, computer disc drives, compact cassette tape players, photocopiers etc. For such electrical components, the bearings are seldom subjected to continuous rolling, but often experience irregular and static conditions, e.g. on-off switching. This situation can promote surface damage, from fretting wear on the raceways in addition to the rolling elements. Indeed, since the rolling bearing is not operated constantly, control of lubrication becomes difficult creating

high levels of surface damage. Although the lubricating system of these bearings is strictly controlled, the operating condition may induce a tribological problem because of the intermittent operation. Once surface damage appears on the rolling bearing, there is a possibility of inducing a catastrophic fracture of the bearing, because the rigidity of the bearing is very low due to its compact design.

In addition, environmental conditions also need to be carefully assessed. The environment in which rolling bearings are frequently operated has become increasingly severe. For example, the  $dn$  value which users require has progressively increased. Here  $d$  represents the bore diameter of the rolling bearing,  $n$  the rolling speed (rpm) and thus the  $dn$  value is obtained. Under these conditions, therefore, an optimum lubricating countermeasure is necessary. The use of ceramic rolling bearings may also be a possible countermeasure, but manufacturing costs are high and the calculation control and also reliability of ceramic bearing life have not been fully examined. It is true that there are still many aspects which must be solved in order for ceramic bearings to be applied industrially. Consequently, rolling bearings made from high carbon chromium bearing steel will continue to be used in most applications and there is therefore a need to study their wear behaviour and tribological properties over a range of conditions.

In this work, the fretting wear of high carbon chromium bearing steel has been carried out with emphasis on fretting wear tests performed under unlubricated conditions. Many fretting wear

investigations of this steel are available, using balls as the test specimens. However, most of these studies refer to investigations of the opponent materials of the fretting couples, and few metallurgical researches have been presented to describe the fretting damage of the bearing steel. Moreover, some of the investigations [2]-[4] utilised high sliding amplitudes i.e. 200 - 400 $\mu$ m. Strictly, these amplitudes are too large for the wear to be called fretting, and should be referred to as reciprocating sliding. The amplitudes used in this work have varied from 5 - 100 $\mu$ m, these being more representative of typical fretting wear situations. Crossed cylinder and sphere-on-plate systems have been used as the test arrangements, and these have been fretted in air at room temperature and also at a specimen temperature of 200°C. In order to obtain the fretting characteristics of the high carbon chromium bearing steel and for comparison with other materials, fretting wear tests on other materials such as Al<sub>2</sub>O<sub>3</sub>, WC-Co, pure Cu, pure Al, pure Zn, pure Fe and various steels have also been carried out.

As a consequence of the fracture induced by fretting wear in rolling bearings, a new fretting wear test machine has been manufactured. Assuming there is a relationship between the fracture and the hoop stress which the rings of the rolling bearings are subjected to, the fretting wear test machine can apply tensile loads to the stationary specimen. Hence the fretting wear tests on the high carbon chromium bearing steel subject to tensile loads have been carried out. Consequently, the effect of tensile stress on bearing fracture

is investigated, and also the effects of fretting wear parameters on such failures are discussed.

## 2. LITERATURE REVIEW

### 2-1. GENERAL ASPECTS OF FRETTING

In 1911, the damage of Fretting was taken notice of by Eden, then in 1927, the term "fretting corrosion" was first used by Tomlinson [5].

According to a glossary of terms and definitions in the field of friction, wear and lubrication which was compiled by the Organisation for Economic Cooperation and Development (OECD), fretting is defined as a wear phenomenon occurring between two surfaces undergoing oscillatory relative motion of small amplitude. Fretting seems to be a quite simple type of wear according to the definition, however, the mechanism of fretting is very complicated and it almost impossible to explain in a few words. There seem to be three possible basic processes as follows in the mechanism of fretting.[6]

(a) Mechanical action disrupts oxide films on the surface exposing clean and possibly strained metal, which would be very reactive and in the presence of the atmosphere would oxidise rapidly during the half cycle after the disruption, to be re-disrupted on the return half cycle.

(b) The removal of metal particles from the surface in a finely divided form by a mechanical grinding action or by the formation of welds at points of contact which are subsequently broken at a surface other than the original interface, either by direct shearing or by a local fatiguing action. The atmosphere would play no part in this

process except where fatiguing was involved in which case it could introduce an element of corrosion fatigue.

(c) Oxide debris resulting directly from (a) or as a result of the oxidation of the metal particles in (b) is an abrasive powder which continues to damage the surfaces.

The main factors which affect fretting damage are the mechanical and chemical properties of materials, and the atmosphere in which fretting occurs. Therefore, researchers can be divided into two groups, those doing research from the mechanical aspect, and those from the chemical. Most of the researchers of the former group are interested in the mechanism of fretting, metallurgical effects and some mechanical effects i.e. amplitude of slip, velocity of sliding and magnitude of normal load, and stress analysis in the vicinity of the contact point. On the other hand, many researchers of the latter group have studied the effect of the oxide film and the environmental effects. Recently, researchers of both types have become very interested in ceramic materials, and have carried out fretting tests into both aspects, because those materials have special characteristics in terms of both physical and chemical properties.

## 2-2. THEORIES OF THE MECHANISM OF FRETTING WEAR

There are some theories on the mechanism of fretting wear as it is influenced by a large number of factors, in other words, fretting wear has some particular characteristics which other sorts of wear do not. Waterhouse [7] mentions that there are two obvious different factors in the circumstances between fretting wear and other forms of wear. One is that the relative velocity of the two surfaces in fretting is very much lower than that in unidirectional sliding. Another is that the surfaces are never brought out of contact, and therefore there is little opportunity for the products of the action to escape in fretting.

In general, the mechanism of fretting wear can be mainly divided into three theories as follows,

- (a) adhesion theory
- (b) Uhlig's theory
- (c) delamination theory.

Those theories are justified by several results. It is however true that the mechanism of fretting wear has not been completely clarified. It could be thought that the mechanism depends upon the fretting condition, the environmental circumstances, and the mechanical properties of the materials. Hence the aforementioned three mechanisms should not be independently considered, but it is important to comprehend the conditions to which each mechanism can be applied.

## 2-2-1. ADHESION THEORY

Most researchers [8][9][10] who infer this mechanism recently mention that the adhesion theory involves three stages of wear. Initially, it appears that extensive welds form between the surfaces, then the welded parts are broken off by local fatigue so that adhesive wear particles are developed. Secondly, oxidation of the adhesive particles occurs, then corrosive wear can develop. Finally, the oxidised adhesive particles are hardened by work hardening, so that abrasive wear can occur in the contact area. This theory is depicted in Fig. 2-1.[11]

The theory deals with a fracture mechanism at the local welded junctions. The fracture originates from fatigue. the wear particles are produced by fatigue, and the particles are oxidised, and eventually the particles play an important role in abrasive wear. This theory is based on adhesive wear (including local fatigue), oxidation of wear debris and abrasive wear. Indeed this theory includes various aspects as mentioned above, but the theory has been assumed for a restricted case; for instance the relation between the hardnesses of surfaces and the hardness of the wear debris during the abrasive wear in the fretting scar is ignored.

This mechanism can be applied to those materials which have a high coefficient of adhesion and a high work-hardenability. However, this fretting wear mechanism would not be adequate for the materials which have a high coefficient of adhesion and a low work-hardenability. The fretting wear mechanism of those materials would be mainly governed by the local welding.

Therefore, the effect of adhesive particles would be much less than that of adhesion.

It is also very important to discuss the nature of the fretting couple when the adhesion theory is under consideration. It is well known that the combination of materials is one of the most important factors which can control the magnitude of adhesion.[12]

## 2-2-2. UHLIG'S THEORY

Uhlig [13][96] proposes that there are chemical and mechanical factors in the mechanism of fretting. The chemical factor is the following. An asperity rubbing on a metal surface is considered to produce a track of clean metal which immediately re-oxidises, or upon which gas rapidly adsorbs. Then, the next asperity wipes off the oxide or initiates reaction of metal with adsorbed gas to form oxide. On the other hand, in terms of the mechanical factor, the asperities dig below the surface to cause a certain amount of wear by welding or shearing action in which metal particles are dislodged. Therefore, he has proposed the particular theory which combines the chemical factor with the mechanical one such as Fig. 2-2. In addition, he insists that any theories of fretting should account for several facts among which are the following.

(a) Fretting damage is reduced in vacuum or inert atmosphere.

(b) Debris formed by fretting of iron is largely of the composition  $Fe_2O_3$ .

(c) Greater damage occurs at low frequencies for a given number of cycles compared with high frequencies.

(d) Metal loss increases with load and relative slip.

(e) Greater damage occurs below room temperature compared with above room temperature.

(f) Damage is greater in dry air than in moist air.

According to Uhlig's theory, the equation of the weight loss :  $W_{corr}$  which oxide film is removed per single cycle can be described as follows.

$$W_{corr} = 2nlck \ln(s/2lfr + 1) \quad (2-1)$$

where  $n$  is the number of contacts or asperities per unit area of the interface,  $l$  is the distance moved by an asperity in half a cycle (the amplitude of slip),  $c$  is the width of the asperity,  $s$  is the distance between the asperities,  $f$  is the constant linear frequency, and  $k$  and  $r$  are constants.

The equation of the weight loss :  $W_{mech}$  due to mechanical wear is given by

$$W_{mech} = 2k'lL/P_m = k_2lL \quad (2-2)$$

where  $L$  is the load,  $P_m$  is the yield pressure, and  $k'$  and  $k$  are constants.

Uhlig expands the logarithmical term in equation (2-1), and he assumes a linear oxidation rate,

$$W_{corr} = ncks/fr. \quad (2-3)$$

The number of asperities along one edge of unit area is equal to  $n^{1/2}$ , and the total real area of contact is  $n\pi(c/2)^2 = L/P_m$ , therefore the following equation can be obtained,

$$W_{corr} = k_0L^{1/2}/f - k_1L/f \quad (2-4)$$

where  $k_0 = 2k/\tau(P_m\pi)^{1/2}$  and  $k_1 = 4k/\tau P_m\pi$ .

The total wear loss must be the summation of the  $W_{\text{corr}}$  and  $W_{\text{mech}}$ . Combining equations (2-2) and (2-4), the following equation can be obtained.

$$W_{\text{total}} = (k_0 L^{1/2} - k_1 L) c / f + k_2 l L c \quad (2-5)$$

### 2-2-3. DELAMINATION THEORY

The delamination theory of wear was introduced in 1973 by Suh [14]. The theory is based on the behaviour of dislocations at the surface, subsurface crack and void formation, and the subsequent joining of cracks by shear deformation of the surface. However, the theory is mainly applicable to wear mechanism where sliding speeds are very low, i.e. fretting.

The delamination theory of wear has been explained as follows.

(a) During wear, the material at and very near the surface does not have a high dislocation density, due to the elimination of dislocations by the image force acting on those dislocations which are parallel to the surface. Therefore, the material very near the surface cold-works less than that of the subsurface layer.

(b) With continued sliding there will be pile-ups of dislocations a finite distance from the surface. In time, this will lead to the formation of voids. The formation of voids will be enhanced if the material contains a hard second phase for dislocations to pile against. Voids form primarily

by plastic flow of matrix round hard particles when there are large secondary phase particles in the metal.

(c) With time, the voids will coalesce, either by growth or shearing of the metal. The end result is a crack parallel to the wear surface.

(d) When this crack reaches a critical length (dependent upon the materials), the material between the crack and the surface will shear, yielding a sheet like particle.

(e) The final observed shape of the particle will be dependent upon its length and internal strains.

Fig. 2-3 illustrates schematically the model of the delamination theory. Suh [14][15] mentions that there might be a "dislocation depleted zone" near the worn surface, and the thickness of the zone of the surface layer depends upon the surface energy of the metal and the magnitude of the drag stress acting on the dislocations. In general, the low dislocation density zone may be thicker for FCC metals than for BCC ones.

The delamination theory seems to be an application of a mechanism of rolling contact fatigue which has been stated by Lundberg and Palmgren [16]. They mention that the crack appears in the subsurface as the maximum shear stress and the maximum alternating stress cycle exist there, and nonmetallic inclusions at the subsurface become stress concentrated points during rolling contact fatigue. In rolling bearings, subsurface cracks which propagate parallel to the surface can

be often found after being rolling fatigued. It is also well known that rolling contact fatigue life increases with the hardness of the material. In addition, the subsurface cracks cannot be easily found in softer materials such as annealed steels although they are damaged by rolling contact fatigue. The damage of the softer material seems not to originate from the subsurface, but from the surface. Therefore the crack appearance and propagation at the subsurface (the delamination theory) should have a particular relationship with the hardness of the material.

Waterhouse et al [17] states that the production of loose wear particles by fretting of a sphere on a flat in a number of materials is by plate like particles of oxide coated metal. They are created by the spread of subsurface cracks. In addition, the thickness of the particles ranges from 1.3 to 3.5  $\mu\text{m}$ . They mention that these results are consistent with the delamination theory of wear.

Waterhouse [18] develops his theory further. Macroscopic adhesion occurs at the early stage of fretting wear, and subsequently breaking of local welds, then roughening of the surface. Consequently, adhesion falls off, the surfaces become smoother and removal of material from the surface occurs by the delamination. This process is a function of the nature of the materials and environment. This theory can be thought of as a combination of mechanisms of the adhesion theory and the delamination theory.

### 2-3. MINDLIN'S THEORY FOR FRETTING

Mindlin [19] assumes the theory of elastic contact of two spheres using Hertzian contact stress theory. Fig. 2-4 simply illustrates stress distributions of the surfaces [20], where  $\mu$  is the coefficient of static friction. When the tangential load,  $T$ , is less than  $\mu N$ , the central stick area which is called non-slip region is obtained, but microslip occurs at the extremities of the contact region where  $q = \mu N$ . This is a main reason of occurrence of fretting damage [20 - 24].

According to the theory, a sphere contacting on a plate, the ratio of radius between the slip region and the non-slip region can be shown as equation (2-6).

$$b/a = \{1 - (T/\mu N)\}^{1/2} \quad (2-6)$$

If the coefficient of tangential force,  $\phi$ , is used instead of  $T/\mu N$ , the following equation can be obtained.

$$b/a = (1 - \phi)^{1/2} \quad (2-7)$$

Sato et al [25][26] carry out the fretting test by a steel ball on a glass, and they measure the ratio between  $b/a$  and  $\phi$  as Fig. 2-5. Nishioka et al [22] obtain the value of  $b/a$  with using cylindrical shoes and a plate in the fretting test. Fig. 2-6 is obtained by their experiment, and the ratio of the radius between the slip region and the non-slip region is given by,

$$b/a = \{1 - (T/\mu N)\}^{1/2} = (1 - \phi)^{1/2} \quad (2-8)$$

Sato et al [23][25][26][32][71] analyse the distribution of stresses and strains at the contact surface with using a steel ball on a flat glass. The schematic diagram is shown in Fig. 2-7.

## 2-4. THE EFFECT OF SOME VARIABLES ON FRETTING WEAR

### 2-4-1. MECHANICAL EFFECTS

#### 2-4-1-1. AMPLITUDE OF SLIP

It is very obvious that the amplitude of slip has great effect on fretting wear rate. Hence, the amplitude of slip is one of the main factors for fretting wear. However, there are two main theories about the effect of the amplitude of slip for fretting. One is that fretting wear is independent of the amplitude of slip [27]. Another is that there is a critical amplitude of slip at which the fretting behaviour remarkably changes [28 - 31]. Recently, many researchers have pointed out the existence of a critical amplitude of slip.

Ohmae et al [28] carried out the fretting wear test in air on mild steel. Their results are shown in Figs. 2-8 and 2-9. According to the results, under the condition of a constant number of cycles, the wear volume is very small at the amplitude of slip less than about  $70\mu\text{m}$ , and increases remarkably at larger than about  $70\mu\text{m}$ . In addition, under the condition of a constant sliding distance, the wear volume is extremely small at small amplitude of slip (less than about  $70\mu\text{m}$ ), the wear volume rises rapidly at over  $70\mu\text{m}$ , and the wear volume shows a constant behaviour at amplitudes larger than  $300\mu\text{m}$ . They propose that the mechanism of fretting wear at much larger amplitude of slip becomes similar to reciprocating sliding wear. Sato et al [29][31 - 33] discuss the critical amplitude of slip in the fretting wear test for a bearing steel ball (756VHN) on a glass (620VHN), and obtained Fig. 2-10 which shows the

vertical displacement due to fretting wear after  $5 \times 10^4$  cycles. The result indicates that there is a critical amplitude of slip, the value being  $3\mu\text{m}$  in the fretting wear test for the bearing steel ball on glass.

#### 2-4-1-2. HARDNESS

Research on the effect of hardness on fretting wear has already been carried out by many researchers, but as yet agreement.

Graham [34] shows an equation as follows.

$$V = k_1 (1/\log H) \quad (2-9)$$

where  $V$  is the fretting wear volume,  $H$  is the hardness and  $k_1$  is constant. In contrast, Wright [35] indicates that  $V$  is proportional to  $1/H^{2.5 \pm 0.5}$

Generally, Waterhouse [36] mentions that hardness can act two possible ways in fretting wear. Initially, higher hardness implies higher ultimate tensile strength and higher fatigue strength. Secondly, oxide debris is produced at the contact point, and then it may lead to abrasive wear, therefore the higher the surface hardness, the higher the abrasive resistance [37].

Kayaba et al [38] carried out the fretting wear test in air on specimens of various hardnesses, and they state that hardness has minor influence on fretting wear. However, Sato et al [39] studied the effects of hardness in air, oxygen gas, argon gas, water and sea water on a high carbon chromium steel (JIS SUJ2). They always used the hardest

specimen as the moving component, and the various hardness specimens as the stationary component. From their experiments, they have obtained a relationship between fretting wear volume and the relative hardness which is the ratio of the hardness of the moving specimen to that of the stationary one. The results are shown in Fig. 2-11. According to the results, fretting wear volume increases with decreasing relative hardness in air, argon gas, water and sea water. On the other hand, fretting wear volume decreases with relative hardness in oxygen gas. Therefore, it is very obvious that the effect of hardness on fretting wear depends upon the atmosphere, in other words, the chemical effect is one of the most sensitive factors in fretting wear.

#### 2-4-1-3. SURFACE ROUGHNESS

It is well known that the finer the surface roughness is, the more serious is fretting damage at room temperature.[40]

It is true that the real area of contact is dependent upon the normal load. However, the magnitude of the normal load which the asperities show to be the transition from elastic to fully plastic behaviour must be clarified. The plasticity index,  $\Omega$ , is clearly indicative of the onset of plastic deformation.[97][98]

$$\Omega = (E'/H) (\sigma/\beta)^{1/2} \quad (2.10),$$

$$1/E' = \{1 - (1/m_1)^2\} / E_1 + \{1 - (1/m_2)^2\} / E_2,$$

where  $H$  represents the indentation hardness value of the material,  $\sigma$  the standard deviation of the peak height distribution of the surface,  $\beta$  the asperity radius and  $E_1$  and  $E_2$  the Young's moduli,  $1/m_1$  and  $1/m_2$  the Poisson's ratios. Therefore, the plasticity index is one of the most important factors when the effect of surface roughness on fretting wear damage is discussed.

Considering a fretting couple which consists of the same material, the asperities are crushed plastically by the opposing specimen. They deform plastically when a contact pressure is roughly  $3Y$ , where  $Y$  is the yield strength of the material. The specimen as a whole yields in bulk at a normal pressure of  $Y$ . Therefore, the maximum ratio of the real area of contact between surfaces to the normal area is about  $1/3$ . Strain hardening of the asperities may decrease the ratio further.[88] Consequently the rough surfaces are smoothed by fretting oscillation.

In the case of fretting wear between a rough surface specimen and a smooth surface specimen, the hardness of both the specimens being equal, it is expected that the wear damage on the smooth surface specimen is more severe than that on the rough surface specimen. Small cracks could appear on the smooth surface specimen when the specimens are very hard. This phenomenon has been observed in a rolling contact fatigue test.[41]

On the other hand, at elevated temperature the wear damage on the smooth surface specimen is smaller than that on the rough surface specimen. This may be due to the oxide film being less adherent to a rough surface.[42]

## 2-4-2. CHEMICAL EFFECTS

### 2-4-2-1. DEBRIS AND OXIDE FILM

Considering ferrous materials, the oxide particles, which are termed "cocoa", can be seen due to fretting wear. Many researchers have investigated it, because it plays a very important role in fretting mechanism. The major chemical component of the debris is a ferric oxide,  $\alpha\text{-Fe}_2\text{O}_3$  [43][44] and  $\text{Fe}_3\text{O}_4$  by X-ray analyses, and they are affected by atmosphere, in particular, moisture in air. Godfrey [45] mentions that the colour changes from black to red-brown of the debris occurs with increasing moisture. Iwabuchi et al [46] suggest that the colour of fretting wear debris depends upon the ambient pressure. Mainly, the red-brown debris is produced at  $1.0 \times 10^5$  and  $1.3 \times 10^3 \text{Pa}$ , and the black debris at  $2.7$  and  $1.3 \times 10^{-3} \text{Pa}$ . Additionally, they mention that the red oxide is  $\alpha\text{-Fe}_2\text{O}_3$  and the black one is  $\text{Fe}_3\text{O}_4$ , and a few wear particles which are not oxide, but metallic, are detected at  $1.3 \times 10^{-3} \text{Pa}$ .

The particle size of the debris has been investigated by many researchers [47][48 - 50], and the value has a very wide range by each of them. Roughly speaking, the particle size is  $0.1 - 10 \mu\text{m}$ . According to Shima et al [50], the wear particles in the contact area are considerably large and flake-like, which may be the particles which are covered with oxide film. On the other hand, the debris exuded from the contact area is a very fine oxide. It seems that metallic large debris produced by the local fracture of the fretted surfaces are crushed and ground between the surfaces to become very fine oxide particles.

Rowe [51] suggests that the surface oxides repeatedly form on metal surfaces by fretting in air, therefore, the oxides may play a very important role during fretting wear. Harris et al [52] mention that certain oxides can be effective in reducing the coefficient of friction, hence, the oxides may play a role in reducing fretting wear. However the oxides which can reduce wear loss depend upon their thickness, their mechanical properties, and the value of their residual stress. Bowden et al [53] state that the main factor is the relative mechanical properties of the oxide and the underlying metal. As an example, hardness differences between them are shown in Fig. 2-12 [54].

#### 2-4-2-2. TEMPERATURE

Many researchers have investigated fretting wear at various temperatures. However, there are very few references of fretting wear study at low temperature (lower than room temperature). Fretting behaviour at elevated temperature has great deal to do with oxidation rates, for instance the transition temperature at which fretting wear behaviour significantly changes.

On copper, the transition temperature occurs at 50°C, and on steel at 140°C. The transition temperature is independent of frequency and load.[55] Hurricks [56][57] notes that the transition temperature depends upon a critical oxide thickness, the temperature at which this forms depending upon the oxidation characteristics of the metal, and oxidation occurring during the

high temperature fretting process tends to heal the deformed surface zones incurred initially and so drop the wear rate. Indeed, Waterhouse [58] studying the fretting wear test of high temperature alloys in  $\text{CO}_2$  claims that fretting wear depends upon the development of a glaze type oxide which is a smooth, mirror like surface. On titanium alloys, the oxide film is protective and very thin at  $600^\circ\text{C}$ , so that the wear volume becomes so slight as to be incapable of forming the characteristic glaze oxide layer.[59] On nitrogen bearing austenitic stainless steel, the wear volume drops dramatically at  $400^\circ\text{C}$  and above, with no measurable wear at  $600^\circ\text{C}$ , and a smooth protective oxide is formed which has the spinel structure.[60] Bill [61] has investigated the fretting wear of high purity iron, nickel and titanium at several temperatures. The results (Fig. 2-13) indicate that all three metals show reduction in fretting wear as temperature is increased from  $23^\circ\text{C}$  to about  $200 - 300^\circ\text{C}$ . Further, increases in temperature to  $650^\circ\text{C}$ , however, lead to increased fretting wear for iron and nickel. On the other hand, titanium shows increased fretting wear as the temperature is increased to  $500^\circ\text{C}$ , beyond which remarkably reduced fretting wear is observed. He mentions that for titanium, oxidation kinetics become rapid enough above  $500^\circ\text{C}$  for the oxide film to fully support the contact and fretting which takes place entirely on a  $\text{TiO}_2$  surface of good integrity.

### 2-4-2-3. ENVIRONMENT

The environment in which fretting wear tests have been carried out can be roughly divided into two groups. One is an oxidising environment such as  $O_2$  gas, air,  $CO_2$ , corrosive solutions etc. The other is an unoxidising atmosphere such as Ar gas, vacuum, lubricant oils etc.

As mentioned in Chapter 2-4-1-2, Sato et al [34] obtained the results which are shown in Fig. 2-11. Although the same materials are used in the fretting wear test, the results show that the fretting wear volume depends upon the atmosphere. It is very obvious that the atmosphere is one of the most effective factors in fretting wear, and particularly the atmosphere has a great deal to do with oxidation.

When the fretting wear test of high carbon chromium steel (JIS SUJ2) and ceramics ( $Al_2O_3$  and  $Si_3N_4$ ) is carried out in sea water, Sato et al [62] mention that the corrosion products behave as a lubricant and reduce the fretting damage. Indeed, Pearson et al [63] state that dilute aqueous solutions provide a lubricant quality which accounts for reduced adhesion and lower friction. On the other hand, they point out that in the absence of cathodic protection, corrosion products trapped inside the fretting scars soon give rise to an increase in the value of the coefficient of friction. Sato et al [62], further mention that the fretting damage is not greatly influenced by the different environments (air, deionised water, 3.07%NaCl solution, synthetic sea water and natural sea water) at very small amplitudes such as 14  $\mu m$ . Iwabuchi et al concentrated on the effects of ambient pressure in

the fretting wear of 0.45%C steel [44] and SUS 304 stainless steel [64] when sufficient oxygen is supplied. According to the results, on 0.45%C steel, friction behaviours are divided into three types depending upon the ambient pressure :  $1.0 \times 10^5 - 10\text{Pa}$ ,  $10 - 10^{-1}\text{Pa}$  and below  $10^{-1}\text{Pa}$ . They explain them as follows. The coefficient of friction increases with a decrease in ambient pressure below  $1\text{Pa}$ . The critical pressure in fretting is found to be  $10\text{Pa}$ , above which the oxidation rate is independent of the ambient pressure and  $\alpha\text{-Fe}_2\text{O}_3$  is formed. Fretting wear decreases with ambient pressure below the critical pressure where  $\text{Fe}_3\text{O}_4$  is formed. Adhesive transfer of metallic debris occurs below  $10^{-1}\text{Pa}$ . In contrast, on SUS 304 stainless steel the critical pressure is also  $10\text{Pa}$ , above which the pressure does not affect the frictional behaviour and the wear properties, and below which the coefficient of friction increases and the wear volume decreases. In addition, there is another critical pressure, the transition pressure at which the transition from the oxidative wear regime to the adhesive wear regime occurs. The pressure depends upon the slip amplitude because of the limitation in the oxygen supply to the interface. The critical pressure for SUS 304 stainless steel is  $2.7\text{Pa}$  and  $10^{-1}\text{Pa}$  at the slip amplitudes of  $35\mu\text{m}$  and  $110\mu\text{m}$  respectively.

Bill [61] investigated the fretting wear of high purity iron, nickel and titanium under varied environmental conditions (Fig. 2-14). Iron and titanium show the maximum fretting wear at 10 and 30 per cent relative humidity respectively. In contrast, nickel shows a minimum in fretting wear at about 10 per cent relative humidity. He states

as follows: for iron and nickel, increased humidity has as its predominant influence by increasing debris mobility. For titanium, more rapid fatigue of the fretting surfaces is seen to accompany increases in humidity levels. Incidentally, all three metals show substantially reduced fretting in dry  $N_2$  compared with dry air.

## 2-5. INVESTIGATION OF FRETTING WEAR

### 2-5-1. CONTACT ELECTRICAL RESISTANCE DURING FRETTING WEAR

Considering the mechanism of fretting wear, the role of the wear debris is very important. As mentioned above, the wear debris accumulates between the specimens, and sometimes acts as abrasive particles. Fretting wear is affected by not only the wear debris but the oxide film on the specimen. In order to investigate the behaviours of both the wear debris and the oxide film, the contact electrical resistance has often been measured.

The factors which affect contact resistance should be time, normal load, frequency, amplitude, atmosphere, materials etc. Hence, the effects of these factors can be determined by the behaviour of the contact resistance.

Fenner et al [46] state that increasing the humidity reduces the resistance. They also point out that the contact resistance is low in a protective atmosphere such as nitrogen and denotes metal-to-metal contact, but the resistance rises in air as oxide debris is formed.

Antler [65] has carried out the fretting wear tests using various materials and test conditions. He mentions very clearly the relationship between the contact resistance and various fretting wear parameters. He concludes as follows;

(1) Base metal contacts rapidly oxidise and produce debris which, because of the small amplitude of movement, tends to accumulate in the

contact zone. As a consequence, contact resistance increases.

(2) The contact resistance is determined by the composition of the interface. When fretting involves dissimilar metals the interface composition changes because of transfer, wear and film formation. In general, the direction of net metal transfer is from soft to hard surfaces. The dissimilar metal systems reduce the wear loss as it is very difficult for the asperities of the dissimilar couples to fracture oxide films and re-establish metal-to-metal contact.

(3) The lower frequency, the fewer the number of cycles for base metals to attain a given increase in contact resistance.

(4) Increasing the contact normal load tends to stabilise the contact resistance.

(5) Contact resistance transients during fretting may be significantly higher than the contact resistance at rest. The contact resistance across the wear track is variable when the surfaces are covered with fretting films and tends to be at or near the end of the track because of the accumulation of insulating debris at these locations.

Pendlebury [66][67] has used mild steel, and has measured the contact resistance continuously during the fretting wear test at room temperature ( $20 \pm 2^\circ\text{C}$ ,  $60 \pm 6\% \text{RH}$ ). He points out that the results of the contact resistance measurements show that metal-to-metal contacts of widely different durations can be recognised, and the metallic wear

particles are successively formed, which are partially comminuted to oxide.

#### 2-5-2. X-RAY RESIDUAL STRESS MEASUREMENT ON FRETTED SCAR

Recently, X-ray fractography has been increasingly investigated, and a few researchers have tried to use it for fretting studies.

Fig. 2-15 [68] shows the distributions of the residual stress and the half value breadth of the X-ray intensity curve below the outer raceway surface of a ball bearing where fretting wear occurred. As the penetrating depth of the radiation is about  $10\mu\text{m}$  [69], the information from the X-ray residual stress measurement for the bearing includes some effects of its rolling contact fatigue because the bearing has been driven. Hence the residual stress at the surface indicates a high compressive stress, and the value of the half value breadth is low even at the unfretted part of the bearing. Actually, the residual compressive stress value at the surface of the fretted part is lower than that of the unfretted part, and the half value breadth at the surface of the fretted part is higher than that of unfretted part. The X-ray parameters show that the surface fatigue damage of the unfretted part is greater than that of the fretted part although the unfretted surface should not be fatigued as much as the fretted surface. The reason why it is obviously contrary to the fact can be thought that the fretted surface is not an initial contact surface, therefore, the most fatigued layer of the

fretted part might have been worn away after the level of fatigue damage at the initial contact surface has reached a certain critical value.

The distribution of the residual stress in the fretted area indicates formation of compressive stress below the surface due to fretting although the initial contact surface was worn, if it is compared with the unfretted part. The formation of compressive stress is usually much bigger than the result when the surface damage is obtained by rolling contact fatigue. Hence, a typical X-ray parametric example can be mentioned that the half value breadth at the vicinity to the surface indicates a very low value such as  $5^\circ$ , and a slight formation of compressive residual stress exists at the subsurface.

Sato K. et al [70] have obtained the X-ray diffraction patterns at both the fretted surfaces and subsurfaces of 0.45%C steel. The specimens have been fretted under the stress ratio :  $R = -1$ . An  $\alpha$ -Fe (220) has been diffracted by using Fe- $K\alpha_1$  X-rays. Although they do not describe it, the diffraction patterns from the surface show continuous rings, but those patterns at the subsurface are spotty. As those patterns at the matrix are also spotty and the hardness at the fretted area is about 1.2 times harder than that at the unfretted area, the surface has been deformed and roughened by fretting, consequently the grains at the surface have been finely recrystallised. They mention that the damaged layer due to the fretting is about a grain size. Therefore, from these references it is obvious that the fretting damage at the surface is much more severe than the subsurface.

### 2-5-3. FRETTING WEAR PROCESS

#### 2-5-3-1. VISIBLE OBSERVATION OF FRETTING WEAR PROCESS ON THE SURFACE

Sato et al [23][25][26][32][71] analyse the distribution of stresses and strains in the contact surface by using a steel ball on a flat glass. They have observed the fretting wear process with an optical microscope and a motion picture camera. From the results, they mention that wear of the steel may be initiated at the point of the maximum strain energy,  $(q\delta)_{max}$ , on the surface. In contrast, cracks on the surface of the glass specimen will be initiated at the point of maximum principal tensile stress,  $\sigma_{max}$ , at the outer edge of the contact region (Fig. 2-7). In Fig. 2-7, (A), (B) and (C) indicate the places of crack occurrence. (A) is the area where the damage is produced by the maximum tangential stress, (B) is by the maximum strain energy,  $(q\delta)_{max}$ , and (C) is by the maximum principal stress,  $\sigma_{max}$ .

They [24][29] describe the process of crack propagation. When the slip amplitude is small enough, both the stick and slip regions can be recognised. In the slip region a tangential force occurs on both the surfaces, and it may cause microscopic adhesion. Combined normal and tangential forces lead to an increase in the contact area at the high spots on the surface. The cracks are produced in the glass surface at the outer edge of the slip region, because the peak in the tensile stress occurs at the outer edge of the slip region. The driving force for the crack propagation should be the alternating load at the surface which is produced by the bidirectional

tangential force. The behaviour of the crack propagation depends upon the magnitude of the tangential force. Many cracks can be found in the fretting contact area when the macroscopic slip exists. They state that those cracks are produced by the migration of the maximum principal stress due to the macroscopic fretting oscillation. Compared with the microscopic fretting oscillation, more wear debris is created in the macroscopic one, and the debris easily escape from the fretting contact area.

#### 2-5-3-2. BEHAVIOUR OF CRACK IN FRETTING FATIGUE

As mentioned in the previous section, Sato et al have investigated the crack appearance and propagation at the surface as they have carried out, not fretting fatigue but fretting wear. The work on fretting wear was predominantly studied from the aspects of contact mechanics. It is however true that a mechanism of fretting wear, particularly the early stage of fretting wear, is based on a fatigue mechanism. Hence, it is necessary that a study on fretting wear should be discussed in relation to the fundamental knowledge of the mechanism of fretting fatigue.

In general [72]-[74], the processes of the appearance and propagation of fretting fatigue crack can be divided into three stages as follows;

(1) The crack is produced at the vicinity of the fretting contact edge by combined normal and tangential forces.

(2) The crack grows at an angle of about 45° to the surface. The crack propagation is governed by both the alternating fatigue stress and the the aforementioned combined stress due to fretting oscillation. Incidentally the stage is called  $S_I$ .

(3) The direction of the crack growth is approximately perpendicular to the surface with increasing depth. The driving force of the crack growth at this stage is predominantly the alternating fatigue stress. The deeper the crack propagates, the less is the effect of the combined stress due to fretting oscillation. This stage is called  $S_{II}$ . The crack propagation rate  $da/dN$  increases significantly with the crack growth.

Applying the mechanism of fretting fatigue to fretting wear, only (1) should be focussed on. However, for example, in the case which a fretted material is subjected to a static stress, both the (1) and (2) should be discussed.

The effects of fretting wear factors such as amplitude, normal load, temperature, environment, surface roughness etc. have been investigated in most of the studies on fretting fatigue.

Some researchers [35][75][76] have pointed out that the effect of normal load on fretting fatigue life is significant. Indeed, the tangential force plays a very important role in fretting fatigue mechanism, and there is a linear relationship between the tangential force and the normal load. As mentioned above, the real area of contact is also governed by the normal load. Hence the normal

load should be the most significant parameter when the appearance of the cracks is discussed.

### 2-5-3-3. DISCUSSION OF CRACK INITIATION DURING FRETTING OSCILLATION

Ruiz et al [103][104] have carried out investigations of fretting damage in dovetail joints. The schematic diagram of the specimen and the distributions of the stresses and parameters are shown in Fig. 2-16. They have always found the location of the crack at the position of maximum value of the parameter  $(\sigma_T + \tau\delta)$  which is named the fatigue/fretting damage parameter. Here  $\sigma_T$  represents the tangential stress,  $\tau$  the shear stress and  $\delta$  the relative slip displacement at the interface. The fatigue/fretting damage parameter is based on the fretting damage parameter,  $\tau\delta$ , which is proposed by them. In summary, they have assumed that fretting cracks result mainly from the combination of the tangential stress and the strain due to the slip amplitude. The fretting damage parameter,  $\tau\delta$ , corresponds to  $q\delta$  in Sato et al's work [23][25][26][32][71] (see Chapter 2-5-3-1).

Halling [105] has described the distributions of the stresses and strains during fretting oscillation (when  $T < \mu P$ ), as shown in Fig. 2-17. Here  $T$  represents the total tangential stress,  $T'$  the tangential stress,  $T''$  the tangential traction,  $e$  the total strain,  $e'$  the strain due to  $T'$  and  $e''$  the strain due to  $T''$ . According to his theory, the critical slip amplitude can be explained by altering the coefficient of friction,  $\mu$ . His

distribution diagram of the total strain,  $e$ , shown in Fig. 2-17 is, however, challenged by the author, as shown in Fig. 2-18, where  $U$  represents the shear strain energy. This shear strain energy,  $U$ , corresponds to the fretting damage parameter proposed by Ruiz et al [103][104].

The author assumes that the shear strain energy,  $U$ , is the most effective factor to produce fretting cracks. This discussion is described in Chapter 7.

## 2-6. THE EFFECT OF RESIDUAL STRESS ON FRETTING DAMAGE

It is well known that fatigue life is improved by the compressive residual stress at the surfaces of machine components. [110][111] It is thought that the compressive residual stress reduces the fatigue crack propagation rate. Generating a high compressive residual stress in components also induces a high dislocation density. Gray et al [112] have carried out fatigue tests using shot peened Ti alloys. They have noted that the propagation rate of the short cracks is influenced by both the compressive residual stress and the high dislocation density. The compressive residual stress significantly reduces the crack propagation rate but the high dislocation density creates the opposite effect. They have described that the negative effect of the high dislocation density is overcompensated by the beneficial action of the compressive residual stress at room temperature. Conversely, at high temperatures, the fatigue life is mainly governed by the high dislocation density due to a relaxation of the compressive residual stress. Therefore, the effect of residual stress on fatigue life is very dependent upon temperature.

Few investigations have been made regarding the relationship between surface residual stress, slip amplitude and fretting fatigue life. Kudva et al [109] have carried out this study with using various steel specimens thermo-chemically treated. They have found a critical slip amplitude for the fretting fatigue tests, which is dependent upon the surface residual stress. Labedz [113] has investigated the relationship between the residual

stress and the volume of the fretting wear scar and also the residual stress and the maximum depth of the fretting wear scar. There is a proportional relationship between the residual stress and the maximum depth of the fretting wear scar. However, the depth shows a minimum value at  $-750\text{MPa}$ , and the depth increases again at  $-900\text{MPa}$ . The wear volume is very small when the residual stress is compressive. Compared with the results for a tensile residual stress field, a very small wear volume is shown when the residual stress is  $+450\text{MPa}$ . Hence, when the residual stress is  $+450\text{MPa}$ , the wear volume is small although the maximum depth of the fretting wear scar shows a large value. He has suggested that this result may come from a particularly favourable mechanical condition of the surface layer.

## 2-7. TRIBOLOGICAL PROPERTIES OF CERAMIC MATERIALS

### 2-7-1. TRIBOLOGICAL PROPERTIES OF CERAMIC MATERIALS

The application of ceramic materials have significantly expanded in the industrial field. Tribologically speaking, the ceramic materials can be used at elevated temperature as they are chemically very stable. Compared with metallic materials, the coefficients of thermal expansion, the specific gravities and the thermal conductivities of the ceramic materials are extremely small. In addition to them, the elastic moduli of the ceramic materials are larger than those of metallic materials. Hence, the ceramic materials have great advantages mechanically as well. For instance, in rotating machinery the centrifugal force of ceramic materials is much smaller than that of metallic materials even if the machine element made of the ceramic materials rotates with high speed, because the specific gravity of the ceramic materials is roughly half that of steel. The accuracy of the elements made of ceramic materials is higher than that of metallic materials, because the elastic moduli of the ceramic materials are approximately 1.5 higher than those of metallic materials.

The ceramic materials which have been applied to the tribological area are alumina ( $Al_2O_3$ ), silicon carbide (SiC), silicon nitride ( $Si_3N_4$ ) and partially stabilised zirconia with magnesium (PSZ).

Habeeb et al [77] have investigated tribological properties of those ceramic materials with using a four ball test at 90°C in lubricated

environment. From the results, the coefficients of friction of both the  $\text{Al}_2\text{O}_3$  couples and the PSZ couple show high values. The wear loss versus speed of the  $\text{Al}_2\text{O}_3$  is significantly high compared with other ceramic materials. The PSZ shows a low wear loss at low speed, but the wear loss significantly increases with the speed, and it shows the highest wear value above 1000 (rpm) among the ceramic materials. Interestingly there are some opinions in disagreement with their result. For example, Hannink et al [99] state that it is certain that PSZ is a useful tribological material and its properties are used to best advantage in unlubricated situations, in abrasive or corrosive environments and at moderately high temperature. The coefficients of friction of both SiC and  $\text{Si}_3\text{N}_4$  are almost similar to the coefficient of friction of steel. The SiC and  $\text{Si}_3\text{N}_4$  show low wear loss values. Therefore the tribological properties of SiC and  $\text{Si}_3\text{N}_4$  are superior to those of  $\text{Al}_2\text{O}_3$  and PSZ. Buckley et al [78] point out that SiC at high temperature can result in the graphitisation of the ceramic surface with the graphite functioning to reduce abrasion and friction, hence a lubricating film is provided from the material itself.  $\text{Si}_3\text{N}_4$  has been recently applied to rolling bearing. It is well known that the frictional properties of  $\text{Si}_3\text{N}_4$  are quite similar to those of steel. Some reports [77][79] mention that the wear rate of  $\text{Si}_3\text{N}_4$  is the smallest among the ceramic materials which have been applied tribologically. It is however true that the friction behaviour of  $\text{Si}_3\text{N}_4$  depends upon the environment, particularly humidity.[80] The surface of  $\text{Si}_3\text{N}_4$  is active, hence the frictional properties of this material are

governed by the condition of lubrication, environment and contaminants on the surface. In general, contaminants on the surface of ceramic materials affect their tribological behaviour.[78]  $\text{Si}_3\text{N}_4$  is one of the most sensitive to the chemical condition of the surface.

Considering the application of ceramic materials, in many cases ceramic materials are in contact with metallic materials. Aronov et al [76] mention that the wear rate of a ceramic and metallic couple increases linearly with the normal load. Even if the normal load were small, the contact stress between the couple could be very large, because the elastic moduli of ceramic materials are roughly 1.5 larger than those of metallic materials. Therefore the magnitude of the normal load has to be very carefully controlled.

## 2-7-2. FRETTING WEAR OF CERAMIC MATERIALS

Very few references on fretting wear of ceramic materials are available. Klaffke has investigated the fretting wear of ceramic vs. steel. The fretting arrangement which he used is a sphere-on-plate. The stationary sphere is always high carbon chromium steel (800 VHN), and the oscillating disc is made of  $\text{Si}_3\text{N}_4$ , PSZ,  $\text{Al}_2\text{O}_3$  and SiSiC (Si-infiltrated SiC). However, the slip amplitude in Klaffke's experiments [81][82] is  $200\mu\text{m}$  and  $400\mu\text{m}$  which are too high for fretting, it should be called reciprocating sliding. Nevertheless, they have obtained some very interesting results. The damage between  $\text{Si}_3\text{N}_4$  and steel ball and between SiSiC and steel ball occur mainly on the ceramic

materials, however the damage between  $Al_2O_3$  and steel ball shows on the steel ball. The damage between PSZ and steel ball is very small, and the damage on the steel ball is almost same amount as on the PSZ. The latest work of Klaffke et al [82] have used roughly the same configuration, and they have focussed on the fretting wear behaviour of SiC. The results mention that the fretting wear in dry air (5%RH) is much greater than that in medium (50%RH) or humid (95%RH) air, and at medium and humid air the fretting wear between SiC and SiC is less than the fretting wear between SiC and steel. Hence it is obvious that the fretting wear of SiC depends upon humidity. The results agree with Ishigaki's work [80]. Ishigaki shows the relationship between coefficient of friction and relative humidity of several ceramic materials. From the results, the coefficient of friction of SiC in dry air is approximately 30% higher than that at medium or humid air.

## 2-8. FRETTING WEAR OF ROLLING BEARINGS

Fretting damage which can be seen on rolling bearings is mainly called "false brinelling" or "flute" [83]. Some typical fretting damage on roller bearings is shown in Fig. 2-20 [84][85].

Later research has attempted to develop a satisfactory theory for the mechanism by which adhesion occurs between metals. The study consists of the physical metallurgy of the bodies and the physics and chemistry of the surfaces. In the study, the items [86] which must be avoided in order to prevent severe adhesive wear are described as follows.

- (a) Specific metals and metal combinations
- (b) Close metallurgical relations and alloying tendencies between the couple
- (c) Similar crystal structure and crystallographic orientation

The ordinary rolling bearings correspond to all of them, because the bearings consist of raceways and rolling elements which are usually made of the same steel. Indeed, the bearings are usually used under lubrication, but when there are some local points where there are metal-to-metal contact without lubricant, they show significant wear damage such as surface originating type flaking. The lubrication for the bearings during driving under mild conditions may create only a small number of problems. However, when the rotatory motion of the bearings is stopped and when the bearings are transported, metal-on-metal contact

points are likely to appear between the raceways and the rolling elements. Then if the bearings are subjected to oscillation, microslip appears between them and they eventually show fretting damage.

#### 2-8-1. A PREVENTION OF FRETTING WEAR OF ROLLING BEARINGS

The prevention of fretting wear of rolling bearings can be divided into two aspects.

One is the chemical aspect. Culp [87] mentions that the best lubricating grease for fretting wear is low viscosity, soft consistency and high degree of oil separation. On the other hand, Ito [4] states that fretting wear damage is impeded by high viscosity lubricants. These results do not agree with each other. In general, lubricants which have a high film strength prevent bearing elements developing metal-to-metal contact, hence the film strength of lubricants would be the most important factor.

The other is the mechanical aspect. Considering the fretting damage between the outer ring of the bearing and the housing, the most common countermeasure is that the clearance between the outer ring and the housing is made as small as possible. In addition, there is another way to avoid the fretting wear between the outer ring and the housing, which is to place some materials which have high elastic moduli, high damping capacity and high coefficient of friction between them. On the other hand, in the case of the fretting wear between the rolling elements and the

raceways of the bearings, the countermeasure usually used is that the rolling bearings are subjected to preload. The length of the space between the outer ring and the inner ring is usually longer than the diameter of the rolling elements. However, the clearance is sometimes designed smaller than the size of the rolling elements in order to avoid vibration. This means preloading. The preload sometimes produces the improvements of bearing life and load capacity. It is however true that the bearings are subjected to high normal load, hence it may lead to high tangential stress and strain and some lubricating problems. As mentioned above, a high normal load induces significant fretting damage and decrease of fretting fatigue life. Therefore the magnitude of the preload must be very carefully controlled.

## 2-8-2. FRETTING PROPERTIES OF HIGH CARBON CHROMIUM STEEL

Aoki et al [3] investigated the fretting wear by rolling contact of high carbon chromium steel (JIS SUJ2 steel) under unlubricated conditions. The results are shown in Figs. 2-21. The depth of the fretting wear is defined as Fig. 2-21a, and the mean depth is from the most severe damaged part, F. As shown in Fig. 2-21b, there is no significant difference in relationship between the depth of damage and the relative humidity (from 10% up to 85%). They mention that the applied load is quite comparable to the practical condition and is very heavy, so that the lubricating effects of moisture cannot be obtained. On the influence of

amplitude, Fig. 2-21c, it is found that fretting does not occur below a certain amplitude, the critical amplitude. The tendency of the curve is quite similar to Ohmae's result [28] on pure iron. On the other hand, the influence of load shows that the damage increases with the applied load,  $Q$  (Fig. 2-21d). Theoretically speaking, fretting damage should be proportional to  $Q^n$ , ( $n > 1$ ), as the maximum amplitude of the differential slip is proportional to  $Q$ . However, the result shows that the damage significantly increases with the applied load,  $Q$ . Incidentally, according to the relationship between the depth of damage and the number of fretting cycles (the accumulated cycles of oscillation) (Fig. 2-21e), the damage is proportional to the  $\log$  number of fretting cycles.

### 3. FRETTING WEAR IN SINTERED ALUMINA- AND TUNGSTEN CARBIDE COBALT CERMET-METAL COUPLES

#### 3-1. INTRODUCTION

Ceramic materials are increasingly being used in industry for machine components because they have special characteristics not displayed by metals, for example corrosion resistance, oxidation resistance, electrical resistance, heat resistance, wear resistance and low density.  $Al_2O_3$  is one of the ceramic materials most frequently used in industry. In many applications ceramic components are in contact with metals, e.g. in frictional components of machinery such as bearings and gears. As a result, research on the friction and wear between ceramic-metal couples has increased in the past few years.[78]

Some ceramic materials of ionic bond type have a characteristic which tends to lead to self-adhesion during wear.[80] However,  $Al_2O_3$ , which displays mostly covalent characteristics, does not develop significant adhesion when sliding on itself in air, but when sliding against softer materials wear of the latter occurs by abrasion. This is particularly true if the counter-surface is a metal. In the process of wear between dissimilar metals, oxidation may occur upon both surfaces. Consequently it becomes very difficult to estimate the wear behaviour of each surface separately as the oxidation process involves complex factors which depend not only upon material properties but also upon the environment. However, for wear tests between  $Al_2O_3$  and metals, it becomes possible to investigate the wear characteristics of the metal in isolation, because

$\text{Al}_2\text{O}_3$  is already fully oxidised and much harder than the metal, so that the adhesion and oxidation of the  $\text{Al}_2\text{O}_3$  component may be ignored.

Fretting has certain notable differences compared with unidirectional sliding. In the latter case, the contact area on one of the surfaces, i.e. the moving surface, has momentary contact and then is exposed to the surrounding atmosphere until the subsequent contact is made and so on. In fretting, the two surfaces are experiencing an oscillatory movement of often only a few micrometres, so that access of the atmosphere is restricted to much of the contact area. It follows, therefore, that wear results obtained in unidirectional sliding tests are not always reliable indications of the behaviour of sliding surfaces in fretting. In this work, fretting wear tests have been carried out between  $\text{Al}_2\text{O}_3$  and some selected metals and alloys. A cermet, tungsten carbide - cobalt (WC-Co), which has characteristics similar to those of ceramics, was also used as an alternative to  $\text{Al}_2\text{O}_3$ .

## 3-2. EXPERIMENTAL PROCEDURE

### 3-2-1. MATERIALS

The ceramic materials were a 99.5% sintered  $Al_2O_3$  and a Co-bonded WC (WC-Co), while the metal specimens were a titanium alloy (Ti-6Al-4V), pure metals (Fe, Al, Cu and Zn) and steels (0.64% C steel, 1.5%Mn steel, 316 austenitic stainless steel and high carbon chromium bearing steel (JIS SUJ2)). The chemical composition and mechanical properties of these materials are shown in Table 3-1 and Table 3-2, respectively. The pure Fe was ARMCO-iron. The microstructures of the specimens are shown in Fig. 3-1.

The metallic specimens were all polished by the same method, hence the same surface roughness was always obtained.

### 3-2-2. TEST RIG

Fig. 3-2 is a schematic diagram of the fretting rig, which has been described in detail by Hamdy et al.[89] The fretting contact consists of a cross-cylinder arrangement. the lower cylinder (5mm dia., 30mm long) was fixed. In nearly all the tests this was the metal specimen. The upper cylinder (5mm dia., 15mm long) was fixed to the end of the fretting arm and this was the ceramic specimen, i.e.  $Al_2O_3$  or WC-Co and referred to as the rider. The fretting arm is vibrated by means of an electromagnetic vibrator, which is mounted in a trunnion. The fretting arm is strain-gauged in such a way that both the normal load applied to

the contact and the tangential force can be measured. The normal load is transmitted to the contacting specimens. The amplitude of slip is measured by an accelerometer and a feedback system maintains the amplitude at a constant level. The experimental conditions were as follows,

normal load	:	3N
peak-to-peak amplitude	:	50 $\mu$ m
frequency	:	30Hz
environment	:	in laboratory
temperature	:	17 - 22°C
humidity	:	51 - 59%RH
number of cycles	:	5.18 x 10 <sup>e</sup> cycles

The output from the strain gauges was recorded on a UV recorder, from which the coefficient of friction at various stages in a test could be calculated.

### 3-2-3. SCANNING ELECTRON MICROSCOPY

All specimens were cleaned in acetone in an ultrasonic cleaner after fretting in order to remove loose debris from the vicinity of the scar. The specimens were mounted and carbon coated. The scanning electron microscope was not only used for observing the scar but was also used for qualitative analysis. Distributional photographs of elements in the vicinity of the scar could be obtained by an X-ray microanalyser.

#### 3-2-4. WEAR VOLUME

After observation by scanning electron microscopy, the geometry of the scar was measured by parallel profilometer traces at  $22\mu\text{m}$  intervals. The horizontal magnification of the traces was constant at  $\times 100$ , and the vertical magnification was either  $\times 1000$  or  $\times 2000$ .

Using a planimeter, the area of each trace,  $a$ , was obtained. The calculation of average wear volume,  $V$ , used the following equation,

$$V = (\Sigma a/n) (n-1) d \quad (3-1),$$

where  $n$  is the number of parallel traces,  $(\Sigma a/n)$  is the average area of the depth profile of the scar, and  $d$  is the spacing of the traces.

In fretting between  $\text{Al}_2\text{O}_3$  and JIS SUJ2 steel of various hardnesses, the projected area and the mean depth of each scar were calculated. The projected area,  $A$ , was calculated from each profile of the scar by the following equation,

$$A = \Sigma (l_i + l_{i+1}) d / 2 \quad (i=1, 2, 3, \dots, n-1) \quad (3-2),$$

where  $l$  is the horizontal length of the scar. The mean depth was obtained by dividing the volume of the scar by the projected area.

### 3-3. EXPERIMENTAL RESULTS

#### 3-3-1. COEFFICIENT OF FRICTION

Fig. 3-3a - Fig. 3-3f show the variation in coefficient of friction during the course of the tests.

In a small number of cases in fretting against  $Al_2O_3$  there was a pronounced peak within the first hundred cycles of fretting. This is particularly so for the Zn specimen. Fig. 3-3c, and the Fe specimen in the solitary test where the metal specimen was the moving component, Fig. 3-3a. In metal-to-metal sliding and fretting such a peak is usually ascribed to the rupture of oxide films on the metal leading to metal-to-metal contact. In both these metals plastic deformation occurs resulting in metal transfer to the  $Al_2O_3$  so that in the early stages the sliding is that of metal-to-metal. However, it would also be expected that Al, together with the test where Fe was the fixed specimen, would show the same behaviour. In both cases the peak is not as pronounced, although Al does show a very high coefficient of friction which persists for two hundred cycles before it begins to fall, Fig. 3-3b.

Most of the other traces maintain a more or less constant friction value throughout the tests, although in certain cases notably Cu, 316 stainless steel, Fig. 3-3c, and 1.5%Mn steel, Fig. 3-3d, there is a rise in friction after  $10^4$  cycles. These are materials with a greater capacity for work-hardening but this would lead one to expect exactly the opposite effect, i.e. a drop in friction. This matter is discussed below.

In fretting against WC-Co, the ferrous materials show less pronounced variations in coefficient of friction.

### 3-3-2. SCANNING ELECTRON MICROSCOPY

Figs. 3-4 and 3-5 show the scars produced on the components of an  $\text{Al}_2\text{O}_3$  / 0.64%C steel couple and an  $\text{Al}_2\text{O}_3$  / JIS SUJ2 steel couple, as examples, with distributional photographs of the elements Al and Fe. It can be seen that Fe is transferred to the surfaces of the  $\text{Al}_2\text{O}_3$ . Even the hardest material among the specimens, JIS SUJ2 steel, Fe is transferred to the surface of the  $\text{Al}_2\text{O}_3$  (Fig. 3-4c).

### 3-3-3. WEAR VOLUME

Wear volume is usually taken to be the summation of material lost from the scars on both materials in contact. However, in this work the measured volumes on  $\text{Al}_2\text{O}_3$  and WC-Co were insignificantly small and taken to equal zero. Hence, the wear volumes measured were the volumes of material lost from the metallic component of the wear couple.

The scars on the surfaces of both pure Al and pure Zn were too large to be measured by the profilometre. In addition, in the fretting wear test of the  $\text{Al}_2\text{O}_3$  / WC-Co couple the wear volumes were so small as to be undetectable in the profilometre traces.

Table 3-3 shows the values of both the volume of scar and the initial maximum Hertzian contact stress ( $P_{max}$ ). With the softer materials the calculated value of  $P_{max}$  was not achieved because it exceeded the compressive yield stress of the material and plastic deformation occurred.

### 3-4. DISCUSSION

In the fretting tests against  $Al_2O_3$ , there appears to be some correlation. In the case where the Fe specimen is the moving component the wear is much higher and the friction is also initially higher but the friction values attain the same value after  $10^4$  cycles, although the Fe as fixed specimen shows a further drop in friction in the later stages of the test. The reason for the higher wear rate is that the contact spot on the moving specimen is of constant area, whereas the contact spot on the stationary specimen is moving backwards and forwards due to the amplitude of fretting oscillation. The frictional energy dissipated in the fretting is thus concentrated in a smaller volume and the consequent temperature rise somewhat higher than when it is the stationary specimen resulting in greater oxidation. Also loose oxide debris is more likely to fall off on the upper moving specimen and thus lessen the protective action of the oxide. Previous workers have found that the transfer of material and the resultant wear is not always equally divided between the moving and stationary specimens. [38][46][63][64][90]

In the case of fretting against WC-Co, Table 3-3, the wear volumes are noticeably lower and this is thought to be due to the presence of Co which is the bonding agent for the WC-Co and which could be acting as a lubricant since the tribological properties of Co are known to be superior to those of FCC and BCC metals [91][92]. However, Co was not detected in the scars on the counter-faces. Even the 316 stainless steel which shows the

highest wear volume against WC-Co has much lower wear than when fretted against  $Al_2O_3$ . Of the four steels this steel shows the highest wear volumes against both  $Al_2O_3$  and WC-Co. Although the coefficient of friction attained a more or less constant value of 0.7 against WC-Co, Fig. 3-3f, it rose to a value in the region of 1.0 against  $Al_2O_3$ , Fig. 3-3c. It has the lowest hardness of the steels as well as having greater resistance to oxidation, so that there is less oxide debris to prevent metal transfer to the  $Al_2O_3$ . The situation develops where the coefficient of friction is characteristic of metal-to-metal contact and wear occurs by an adhesive wear process. Indeed, during the fretting tests, some stick-slip action was observed. This explanation is also thought to apply to the 1.5%Mn steel which is a corrosion resistant steel widely used in marine environments.

The harder steels, 0.64%C steel and JIS SUJ2 steel, show lower wear volumes against both  $Al_2O_3$  and WC-Co, particularly against WC-Co. Figs. 3-6a and b show the very small scars on the WC-Co / JIS SUJ2 steel couple. Debris on the steel was analysed and found to contain tungsten (Figs. 3-6c and d) and therefore likely to be tungstic oxide  $WO_3$  since the debris was yellow in colour. This would also contribute to the low friction and wear that obtain when WC-Co is fretted against steels.

When  $Al_2O_3$  was fretted against WC-Co, the coefficient of friction was very low and no measurable wear was observed. However, the scars were visible on both materials as can be seen in Figs. 3-7a and b.

The scars were too large on the very soft metals pure Al and Zn to assess by the profilometer, but obviously wear was very great. Pure Cu showed a high coefficient of friction rising to values of 1.2 characteristic of metal-to-metal friction, and with it a high wear volume. This contrasted with the behaviour of pure Fe where the friction and wear was much lower, although the mechanical properties of the two materials are not dissimilar. The reason appears to be, as in the case of the 316 stainless steel, that Cu is a noble metal and does not therefore grow a sufficiently thick oxide film to prevent metal transfer to the  $Al_2O_3$ .

Titanium and its alloys have generally poor tribological properties and suffer particularly in fretting conditions. In the present case of fretting against  $Al_2O_3$ , it shows a high coefficient of friction but a low wear volume. In earlier work where this alloy was fretted against itself, a coefficient of friction of 0.5 at  $10^4$  cycles falling to 0.3 at  $10^6$  cycles was observed but this was not reflected in the wear rate which continued to rise [93]. Both Ti and Al, although reactive metals, have good corrosion resistance due to their very protective oxide films. Fretting against  $Al_2O_3$  appears to disrupt the films and lead to high coefficients of friction characteristic of metal-to-metal. The fretting of the Ti alloy against  $Al_2O_3$  appears to give exactly opposite results to those when fretting on itself.

There appears to be little correlation between crystal structure and the friction and wear behaviour in these tests. There is some indication that resistance to oxidation may influence the coefficient of friction but not necessarily the

wear. It is to be expected that the mechanical properties of these materials would be more relevant to their behaviour.

The greater correlation was found between wear volume and the ratio of the Hertzian contact stress in the initial contact area to the hardness (VHN). The results of the specimens against  $Al_2O_3$  and WC-Co are shown in Figs. 3-8a and b, respectively. The correlation breaks down where the yield point of the material is exceeded and plastic deformation is occurring as is the case with the fretting of the pure Fe. The reason for including the hardness in the correlation is that although in such contacts the overall behaviour of the material obeys the Hertzian formulae, at the very intimate contact points in the surface, i.e. the asperities, very local plastic deformation of these areas occurs, as has been demonstrated by Johnson and O'Connor [94]. In fretting it is these asperity contacts which are mainly concerned in the resultant damage process.

### 3-5. CONCLUSIONS

The following conclusions are drawn from this investigation of the fretting wear of a variety of metallic materials against  $Al_2O_3$  and Co-bonded WC (WC-Co).

(1) The wear volumes of the metallic specimens fretted against WC-Co are very small, because the cobalt bonding agent and the tungstic oxide in WC-Co have a lubricating effect which greatly reduce the wear volume.

(2) Fretting wear is greatly increased when the metal is the moving component. It could be thought that a local strain due to the migration of the shear stress leads to this result.

(3) The soft metals Al and Zn show the highest wear volumes and the hardest alloys the lowest.

(4) The materials which are corrosion resistant, such as 316 stainless steel and pure Cu, do not built up a layer of oxide debris and consequently show high coefficients of friction characteristic of metal-to-metal contact, and the wear volumes are high due to metal transfer and adhesive wear.

(5) For the harder materials where no significant plastic deformation occurs during fretting, there is a correlation between the wear volume and the ratio of the maximum Hertzian contact stress in the contact region and the hardness of the material (VHN).

(6) The harder steels such as 0.64%C steel and high carbon chromium bearing steel show lower wear volumes against both  $Al_2O_3$  and WC-Co, particularly against WC-Co. The debris on the steels were likely to be tungstic oxide  $WO_3$ . This would be contribute to the low friction and wear.

#### 4. THE EFFECT OF OXIDE FILM AND HARDNESS ON FRETTING WEAR IN HIGH CARBON CHROMIUM BEARING STEEL

##### 4-1. INTRODUCTION

High carbon chromium bearing steel (JIS SUJ2 steel) is very well known for its application for rolling bearings. When this steel is used for the elements of rolling bearings, the surface of the steel is machined to a very smooth finish, consequently large fretting wear damage is likely to be produced on the surface.[40]

As the high carbon chromium bearing steel is a through hardened steel, the hardness can be easily changed by tempering. The hardness of the high carbon chromium bearing steel may be changed between 750 and 500 VHN if the steel is tempered at between 180°C and 400°C. Unless a carbide precipitates, there is no significant difference in the mechanical properties between the steel tempered at 180°C and the steel tempered at 400°C. Therefore, the hardness of this steel can be changed without a change in mechanical properties by tempering.

The Hertzian contact stress is governed by elasticity of the material. Hence, as long as there is no significant difference in the mechanical properties, a constant value of the Hertzian contact stress is given at a constant normal load. Results from Chapter 3 have shown that there is a correlation between fretting wear volume and the ratio of the maximum Hertzian contact stress the contact region and the indentation hardness value of the material ( $P_{max.}/VHN$ ). If this steel is tempered at various

temperatures, the ratio between the  $P_{max}$  and the VHN can be changed. Consequently the relationship between fretting wear volume and the  $P_{max}/VHN$  can be confirmed by using the same steel, and also the effect of hardness can be discussed.

The effect of hardness on fretting wear has been studied by some researchers, and it is said that fretting wear damage in general decreases as hardness is raised.[95] However, these works may include the interaction of oxidation between the specimens during fretting wear tests. As mentioned in the previous chapter, the interaction may be ignored in fretting wear tests between  $Al_2O_3$  and metals, therefore, the effect of hardness on fretting wear can be studied by this experimental method much more obviously than by the conventional one. Hence in this work,  $Al_2O_3$ /JIS SUJ2 couples were fretted, and for comparison JIS SUJ2/JIS SUJ2 couples also were tested.

In order to investigate the effect of oxide film on the high carbon chromium bearing steel on fretting wear damage, the specimens of this steel were tempered both in air and in a vacuum.

## 4-2. EXPERIMENTAL PROCEDURE

### 4-2-1. MATERIALS

The high carbon chromium bearing steel (JIS SUJ2) and the  $Al_2O_3$  specimens were prepared by the same process as the specimens which were used in the tests outlined in Chapter 3. In order to change the hardness of the high carbon chromium bearing steel specimens, the specimens were tempered under various conditions. In addition, heat treatment was performed in air and in a vacuum. Fig. 4-1 describes the process used in the preparation of the high carbon chromium bearing steel specimens. Table 4-1 shows the tempering conditions and hardness of the specimens. The high carbon chromium bearing steel specimens which were tempered in air show temper colours, but those specimens which were tempered in a vacuum do not.

Incidentally, the microscopic structures of the high carbon chromium bearing steel specimens tempered at 400°C both in air and in a vacuum show no carbide precipitates.

### 4-2-2. TEST CONDITIONS

The test was carried out by using the same test rig, conditions and experimental methods that were used in the test described in Chapter 3. The fretting wear couple consisted of both  $Al_2O_3$  vs. the steel specimens and the steel specimens vs. themselves.

The maximum Hertzian contact stresses used in the tests are as follows,

Al<sub>2</sub>O<sub>3</sub> / JIS SUJ2 : 1276.8 MPa  
JIS SUJ2 / JIS SUJ2 : 1109.5 MPa

#### 4-2-3. WEAR VOLUME

In the case of the Al<sub>2</sub>O<sub>3</sub> / JIS SUJ2 steel fretting couples, only the scars of the JIS SUJ2 steel specimens were considered, because the wear on the Al<sub>2</sub>O<sub>3</sub> specimens was immeasurably small.

## 4-3. EXPERIMENTAL RESULTS

### 4-3-1. COEFFICIENT OF FRICTION

In fretting between  $Al_2O_3$  and the JIS SUJ2 steel of various hardnesses, all of them show similar trends in coefficient of friction (Fig. 4-2a - Fig. 4-2f). Comparing the specimens which were tempered in air with the specimens which were tempered in a vacuum, the coefficient of friction of the former specimens nearly always show higher value than that of the latter. However, the coefficient of friction of the specimen which was tempered at 400°C in air (T5A) is lower than that at 400°C in a vacuum (T5V).

Figs. 4-3a and b show that the coefficient of friction of between steel specimens tempered in a vacuum and in air, respectively. The friction behaviours of the steel specimens couples tempered at 200°C, 230°C and 400°C (T1V, T2V and T5V) (T1A, T2A and T5A) are shown in Figs 4-3a and b, as being representative.

### 4-3-2. WEAR VOLUME

Table 4-2 shows the values of the volume, projected area and mean depth of scars on the high carbon bearing steel specimens of various hardnesses which fretted against  $Al_2O_3$ . Table 4-3 shows the results of the fretting wear tests of the JIS SUJ2/JIS SUJ2 steels. The fretting wear scar on the T5A lower stationery specimen was too small to be measured by a talysurf profilometer, but it was visible.

#### 4-4. DISCUSSION

##### 4-4-1. COEFFICIENT OF FRICTION

In the fretting test of  $Al_2O_3$  / JIS SUJ2 steel of various hardnesses, the values of the coefficient of friction of the specimens which were tempered in vacuum are always higher than those of the specimens which were tempered in air. However, the relation between the T5V (tempered at  $400^\circ C$  in vacuum) and the T5A (tempered at  $400^\circ C$  in air) shows a difference from the other couples. On the specimens which were tempered in air temper colours can be seen, while those which were tempered in vacuum do not show them. Hence, it is obvious that the former specimens were oxidised during tempering.

Some researchers [52][56]-[60][100] point out that there is a transition temperature where the oxide composition changes from  $Fe_2O_3$  to  $Fe_3O_4$ . The transition temperature of steels is approximately  $200^\circ C$ . It is well known that the  $Fe_3O_4$  film is a glaze type oxide film and the coefficient of friction of this oxide film is lower than that of the  $Fe_2O_3$  film. In this experiment, all of the steel specimens which were tempered in air should be covered with the  $Fe_3O_4$  film. Hence, the difference of the friction behaviour between the  $Fe_2O_3$  film and the  $Fe_3O_4$  film cannot be discussed.

The thickness of the oxide film can be estimated from the colour [101]. Both the temper colours and the oxide film thickness of the specimens which were tempered in air are as follows

T1A	straw colour	0.440 $\mu$ m
T2A	light violet	0.660 $\mu$ m
T3A	light blue	0.710 $\mu$ m
T4A	blue	0.725 $\mu$ m
T5A	dark blue	>0.725 $\mu$ m

In the steady stages of the fretting wear, the values of the coefficient of friction of the all of the specimens which were tempered in air show about 0.8, but the T5A shows a quite high value, 1.0 (see Fig. 4-2a - Fig. 4-2f). It could be thought that there is a critical thickness of oxide film which affects the coefficient of friction; in this work the value, 0.725 $\mu$ m was obtained. In other words, when the thickness of the oxide film is less than 0.725 $\mu$ m, the coefficient of friction shows a relatively low value. On the other hand, when the thickness is more than 0.725 $\mu$ m, the coefficient of friction shows a relatively high value.

In the fretting wear tests between high carbon chromium bearing steel specimens, the friction behaviour of the steel specimens tempered in air is different from that of the steel specimens tempered in a vacuum. Fig. 4-3b shows that the friction behaviour of the specimens tempered in air does not indicate an obvious difference among these specimens. On the other hand, a significant difference of the friction behaviours among the specimens tempered in a vacuum can be recognised in Fig. 4-3a. In particular, the coefficient of friction of these specimens at the early stage of fretting wear shows an obvious difference. It is thought that the oxide film influences the results. In fretting wear tests between steel

specimens tempered in air, the early stage of the fretting wear may be an oxide film-to-oxide film contact. While in the fretting wear tests between the steel specimens tempered in vacuum, the early stage of the fretting wear may be less oxide film-to-oxide film contact. The oxide film on the steel specimens tempered in vacuum may be gradually produced by fretting oscillation. Consequently the coefficient of friction of these specimens after  $10^5$  cycles may show similar behaviour.

#### 4-4-2. WEAR VOLUME

The relationship between the wear volume and the hardness of both the  $Al_2O_3$ /JIS SUJ2 steel couples and the JIS SUJ2 steel/JIS SUJ2 steel couples is shown in Fig. 4-4a and b. In the fretting wear tests between the  $Al_2O_3$  and the JIS SUJ2 steel specimens tempered in air, there is no obvious relation between the wear volume and the hardness. On the other hand, the fretting wear tests between the  $Al_2O_3$  and the JIS SUJ2 steel specimens tempered in a vacuum shows that the fretting wear volume decreases with increasing hardness. In the fretting wear tests between the JIS SUJ2 steel specimens, there is no significant difference in the fretting wear damage on the lower stationary specimens, but there is on the upper moving specimens, as shown in Fig. 4-4b. Consequently, the results show that the fretting wear volume decreases with decreasing hardness, as shown in Table 4-3. This result does not agree with the result of the fretting wear between the  $Al_2O_3$  and the JIS SUJ2 steel specimens tempered at

various temperatures. Considering only the fretting damage on the lower stationary specimens in the fretting wear tests between the JIS SUJ2 steel specimens, the result shows that the fretting wear volume becomes less with increasing the hardness. As shown in Chapter 3, the wear on the pure Fe specimen which was used as an upper moving specimen was much greater than that on the pure Fe specimen which was used as a lower stationary specimen. Therefore, this result indicates that the fretting wear mechanism on the upper moving specimens is different from that on the lower stationary specimens in the crossed cylinder arrangement. This aspect will be discussed in the following chapter.

Fig. 4-4b shows that fretting wear of the JIS SUJ2 steel specimens tempered in air is larger than that of the steel specimens tempered in vacuum. In Figs. 4-3a and b, the coefficient of friction of the fretting couple between the JIS SUJ2 steel specimens tempered in air is higher than that of the couple between the steel specimens tempered in a vacuum. Hence, oxide film may be produced at the early stage of fretting wear. Subsequently, the oxide film may be removed. However, in the fretting wear tests between the steel specimens tempered in air, the steel specimens have already been fully oxidised, therefore the early stage of the fretting wear of the couples may be the removal of oxide film. Consequently, the large wear volume is produced.

The oxide film on the T5A specimen is thick, approximately  $>0.725\mu\text{m}$ , hence the thick oxide film may impede the removal of the film due to fretting wear, resulting in the very low fretting wear.

In the fretting wear tests between the  $Al_2O_3$  and the JIS SUJ2 steel specimens tempered in a vacuum, there is a relation between the wear volume and the  $P_{\text{max.}} / \text{hardness}$ , but the specimens tempered in air indicate a constant value of wear volume, as shown in Fig. 4-5a. This result shows that the oxide film formed before fretting wear test nullifies the effect of hardness on fretting wear volume.

Fig. 4-5b is the relationship between the wear volume and the  $P_{\text{max.}} / \text{hardness}$  of the JIS SUJ2 steel specimen couples. The volume of scar is the summation of wear volume on both the upper and lower specimens. Although Figs. 3-10 and Fig 4-5a show that the relationship between the wear volume and the  $P_{\text{max.}} / \text{VHN}$  ratio is directly proportional, Fig. 4-5b shows an inversely proportional relationship. In fact, the wear volume on the pure Fe specimen fretted against  $Al_2O_3$  as an upper moving specimen shows a similar result in Fig. 3-10a. Therefore, the inversely proportional relation in Fig. 4-5b may not result from the difference between the material couples,  $Al_2O_3$ /JIS SUJ2 and JIS SUJ2/JIS SUJ2. As mentioned above, the fretting wear mechanism on the upper moving specimens seems to be different from that on the lower stationary specimens. This subject will be discussed in Chapter 5.

#### 4-5. CONCLUSIONS

The following conclusions are drawn from the investigation of the effect of oxide film and hardness on fretting wear in high carbon chromium bearing steel.

(1) In the fretting wear test of the high carbon chromium bearing steel (JIS SUJ2 steel), the behaviour of the coefficient of friction is different between the specimens which were tempered at 200, 230, 260 and 350°C in air and the specimen which was tempered at 400°C in air. The thicknesses of the oxide films of these specimens could be estimated from their temper colours as 0.725µm and over 0.725µm, respectively,. There appears to be a critical thickness of the oxide film which affects the behaviour of the coefficient of friction at about 0.725µm for the steel.

(2) In the specimens which were tempered in air, the fretting wear volume shows a nearly constant value, so that there is no noticeable relation between the wear volume and the hardness of the matrix. Hence, the oxide film formed before fretting wear test overrides the effect of hardness on fretting wear volume.

(3) In the specimens which were tempered in vacuum, the fretting wear volume increases with the ratio of  $P_{max} / VHN$  and with decreasing the hardness. However, the relationship between the wear volume and the  $P_{max} / VHN$  is inversely proportional in the fretting wear test between high carbon chromium bearing steel specimens

tempered at various temperatures in a vacuum and in air. This result may be the result of the difference of the fretting wear mechanism between the upper moving specimens and the lower stationary specimens in crossed cylinder arrangement.

5. THE EFFECT OF OSCILLATORY DIRECTION AND  
SPECIMEN COMBINATION ON FRETTING WEAR  
UNDER A CROSSED CYLINDER CONTACT CONDITION

5-1. INTRODUCTION

In Chapter 3, in the fretting wear tests between some selected metallic materials and  $Al_2O_3$ , the fretting wear volume on the pure Fe specimen, which was used as an upper moving component, was much greater than that on the pure Fe specimen which was used as a lower stationary component. In addition, in Chapter 4, in the fretting wear between high carbon chromium bearing steel specimens, it was confirmed that the fretting wear volumes on the upper moving specimens were greater than those on the lower stationary specimens. The author suggested that the cause might be due to differences in the access of the atmosphere and the concentration of frictional energy between the components (i.e. moving and stationary components). In fretting wear tests, a difference in fretting wear volume between the components of the contact can often be obtained although the same material is used for both of them. [38][46][63][64][90][102] The reason has been thought to be the effect of oxidation on the fretting contact region. Many fretting wear tests have been carried out between a sphere and a flat plate [38][46][64][90] and between cylindrical specimens in a crossed cylinder contact arrangement. [63][102]

According to these test results, it should not be simply considered that this phenomenon results entirely from oxidation during fretting wear. The effect of specimen geometry must be considered

when discussing fretting wear. If the fretting wear test is carried out between a sphere and a flat plate, the fretting wear mechanism of the two components may be different. Considering this difference in fretting wear volume of the components, it is therefore very useful to use a crossed cylinder contact in the test, because this form of contact consists of elements of both sphere-on-plate and sphere-on-sphere contact arrangements. By changing the combination of components and the direction of fretting oscillation it becomes possible to investigate various parameters of fretting wear.

In this work, high carbon chromium bearing steel (JIS SUJ2) and alumina ceramic material ( $\text{Al}_2\text{O}_3$ ) were used as the fretting wear test components. The fretting wear tests were carried out by a crossed cylinder contact arrangement in laboratory air. In addition, high carbon chromium bearing steel couples were used to measure the electrical contact resistance during the fretting wear tests.

## 5-2. EXPERIMENTAL PROCEDURE

### 5-2-1. MATERIALS

The specimens used in this experimental work were a 99.5% sintered alumina ( $\text{Al}_2\text{O}_3$ ) and a high carbon chromium bearing steel (JIS SUJ2 steel). The JIS SUJ2 steel specimens were quenched at  $810^\circ\text{C}$  and tempered at  $180^\circ\text{C}$  for 2 hours in air after machining, and then the specimens were polished to  $1\mu\text{m}$  finish. The fretting couples JIS SUJ2/JIS SUJ2 and  $\text{Al}_2\text{O}_3/\text{Al}_2\text{O}_3$  were used as well as  $\text{Al}_2\text{O}_3/\text{JIS SUJ2}$  in this test.

### 5-2-2. TEST CONDITIONS

The test was carried out by using the same rig and experimental method that were used in the test described in the previous chapters. Two test conditions were used for the fretting wear tests, as shown in Fig. 5-1. In test condition (1), the upper specimen moves parallel to the axial direction of the lower stationary specimen. On the other hand, in test condition (2), the moving direction of the upper specimen is perpendicular to the axial direction of the lower stationary specimen. In the fretting wear tests between the  $\text{Al}_2\text{O}_3$  and the JIS SUJ2 steel, the combination of the fretting couples used in this work is shown in Fig. 5-2

The maximum Hertzian contact stress ( $P_{\text{max}}$ ) of the  $\text{Al}_2\text{O}_3/\text{Al}_2\text{O}_3$  couple is 1528.8MPa when the normal load is 3N.

### 5-2-3. WEAR VOLUME

In the case of the fretting couples between the  $\text{Al}_2\text{O}_3$  and the JIS SUJ2 steel, only the scars of the JIS SUJ2 steel specimens were considered, because the fretting wear on the  $\text{Al}_2\text{O}_3$  specimens was immeasurably small.

### 5-2-4. ELECTRICAL CONTACT RESISTANCE

Both upper and lower specimens were connected with a constant current supply when the JIS SUJ2 steel couples were used in the work, and were supplied with a DC current of  $1\mu\text{A}$ . The electrical contact resistance during fretting oscillation was recorded on a chart recorder up to  $2 \times 10^4$  cycles.

### 5-3. EXPERIMENTAL RESULTS

#### 5-3-1. COEFFICIENT OF FRICTION

Figs. 5-3a - 5-3c show the coefficients of friction of the fretting couples under both fretting wear test conditions. The results show different friction behaviour in these combinations although the same material couple is used. Under test condition (1)-B (Fig. 5-3a), the coefficient of friction indicates a peak at the early stage of the fretting wear. This behaviour can quite often be seen in fretting wear tests, but the rest of the fretting wear tests do not indicate such a peak. In the fretting wear tests of the JIS SUJ2/JIS SUJ2 couples, the friction behaviour between test conditions (1)-S and (2)-S is totally different (Fig. 5-3b). The coefficient of friction in test condition (2)-S is about twice that of test condition (1)-S. Fig. 5-3c shows the coefficients of friction of  $Al_2O_3/Al_2O_3$  couples under both test conditions (1)-C and (2)-C. The friction behaviour is very similar between test condition (1)-C and (2)-C.

#### 5-3-2. ELECTRICAL CONTACT RESISTANCE

The traces of the electrical contact resistance during the fretting oscillation under both test conditions (1)-S and (2)-S are shown in Figs. 5-4a and b. Near zero contact resistance indicates metal-to-metal contact. It is very obvious that the fretting contact situation between these test conditions is different although the material of

the component is the same. Under test conditions (1)-S, metal-to-metal contact can be recognised at the early stage of the fretting wear, up to  $4 \times 10^3$ , and the periodical peaks can be seen after  $8 \times 10^3$  cycles. On the other hand, under test condition (2)-S, a little electrical contact resistance can be seen from the beginning of the fretting wear, and the electrical contact resistance gradually increases with a large fluctuation about a mean. The electrical contact resistance decreases at about  $1.7 \times 10^4$  cycles, and then increases again. More frequent falls to zero resistance are apparent in this case.

### 5-3-3. WEAR VOLUME

Table 5-1 shows the average volumes, projected areas and mean depths of the scars on the JIS SUJ2 steel specimens fretted against the  $Al_2O_3$  specimens. In all the test conditions, the volumes of the scars are significantly different. The volume of the scar produced on the JIS SUJ2 steel specimen under test condition (1)-B is more than twice that produced on the JIS SUJ2 steel specimen under test condition (1)-A. On the other hand, the volume of the scar produced on the JIS SUJ2 steel specimen under test condition (2)-A is nearly twice that produced on the JIS SUJ2 steel specimen under test condition (2)-B.

Table 5-2 shows the results of the fretting wear tests of the JIS SUJ2/JIS SUJ2 couples. The results show the same tendency as the results shown in Table 5-1. The wear volume of the upper specimen is larger than that of the lower specimen

under test condition (1)-S. Under test condition (2)-S, the wear volume of the lower specimen is much larger than that of the upper specimens, and the mean depth of the lower specimen under test condition (2)-S is significantly deep.

#### 5-4. DISCUSSION

The coefficients of friction of the fretting wear couples between the  $\text{Al}_2\text{O}_3$  specimen and the JIS SUJ2 steel specimen and between the JIS SUJ2 steel specimens under four test conditions are shown in Figs. 5-3a and 5-3b, respectively.

In Fig. 5-3a, compared between test conditions (1)-A and (1)-B, the coefficient of friction of (1)-B is higher than that of (1)-A. Fig. 3-3a also shows a similar result, where the coefficient of friction is high when the  $\text{Al}_2\text{O}_3$  is used as the lower stationary specimen under test condition (1). As mentioned in Chapter 3, it may be thought that loose oxide debris is more likely to fall off on the upper moving specimen and thus lessen the protective action of the oxide. Indeed, the coefficient of friction under test condition (2)-B also shows a similar tendency. In these tests, the JIS SUJ2 steel specimens are always worn and the shape of the scars is concave. On the other hand, the shape of the scars on the  $\text{Al}_2\text{O}_3$  specimens is convex due to adhesion of the steel. Considering fretting contact geometry, the elliptical scars on the JIS SUJ2 steel specimens under test conditions (1)-A and (2)-B have major axes parallel to the longitudinal axis of the specimens, while the scars on the JIS SUJ2 steel specimens under test conditions (1)-B and (2)-A have major axes perpendicular to the axis of the specimen. As Sato et al [33] state, maximum tangential force increases with decreasing of the radius of the specimen surface curvature, and the contact stress near the contact edge is extremely high when the radius of the specimen surface curvature is small. Hence, the coefficient of friction at the early

fretting wear stage under test condition (1)-B and (2)-A is high. Comparing test conditions (1)-B and (2)-A after  $10^4$  cycles, these test conditions show different friction behaviours. The results might come from the different oxidation behaviour under the test conditions mentioned above and the effect of adherent or remnant debris. As the shape of the scar on the JIS SUJ2 steel specimen under test condition (2)-A is concave, debris easily remains there, and thus the debris may act as a roller bearing. Consequently, the coefficient of friction shows a low value.

The coefficients of friction under test conditions (1)-S and (2)-S are shown in Fig. 5-3b. The friction behaviours are totally different between test condition (1)-S and (2)-S. Fig. 5-3c shows the coefficients of friction of  $Al_2O_3/Al_2O_3$  couples under both test conditions, (1)-C and (2)-C, respectively. The fretting wear scars on the  $Al_2O_3$  specimens are invisible, and debris has not been detected after fretting under test conditions (1)-C and (2)-C. Interestingly, the friction behaviour is very similar between test condition (1)-C and (2)-C.  $Al_2O_3$  is already fully oxidised, hence oxidation during the fretting wear test can be ignored. According to the results shown in Fig. 5-3-c, it is obvious that the coefficient of friction in fretting wear is significantly affected by the behaviour of debris. The scar on the lower stationary specimen under test condition (2)-S is very deep, as shown in Table 5-2. Compared with the scar on the lower stationary specimen under test condition (1)-S, it may, therefore, be difficult to fill the scar with the debris. Subsequently, the debris may mainly dwell at the bottom of the scar. Metal-to-metal contact

is frequently induced at the periphery of the fretting contact area as less debris exists there. Consequently, a high coefficient of friction is produced, as shown in Fig. 5-3b. The difference of the coefficients of friction at the very early stage of the fretting wear (up to  $10^2$  cycles) between test condition (1)-S and (2)-S may be induced by a contaminant on the surfaces. As described in Chapter 2-8, it is well known that severe adhesive wear is produced when material couples which have similar metallurgical properties are in contact.[86] Both test conditions (1)-S and (2)-S correspond to this situation. Indeed, compared with other fretting couples, the friction behaviours of the couples under test conditions (1)-S and (2)-S indicate quite high coefficients of friction.

The electrical contact resistance during fretting wear is shown in Fig. 5-4. Peaks after  $5 \times 10^3$  cycles correspond to the accumulation of debris. Metal-to-metal contact can be recognised even after  $2 \times 10^5$  cycles in Figs. 5-4. This result is similar to that reported by Pendlebury [67]. He states that metal-to-metal contact continues to occur in fretting wear even after long running times.

Tables 5-1 and 5-2 show details of the fretting scars tested under various conditions. In fretting wear test between the  $Al_2O_3$  and the JIS SUJ2 steel, the scars on the steel specimens under test conditions (1)-B and (2)-A are larger than the others. As mentioned in Chapter 3, the fretting contact spots on the steel specimens are always constant, therefore the frictional energy

concentrates in the spots. Table 5-2 also shows similar results. The debris at the early stage of the fretting wear under test condition (2)-S may be produced from the lower stationary specimen, because the surface damage (i.e. the frictional energy) on the lower specimen due to fretting oscillation is larger than that on the upper specimen under test condition (2)-S as the damage is concentrated in a smaller area. In contrast, it may be produced from the upper moving specimen under test condition (1)-S for the same reason. Hence, the disruption of the local welds might be on the lower stationary specimen side due to the frictional energy under test condition (2)-S. On the other hand, the disruption under test condition (1)-S might be on the upper moving specimen side.

The most interesting result is that the volumes of the scars on the steel specimens are extremely large when the steel specimens are used as a lower stationary specimen under test condition (2), see the results in Tables 5-1 and 5-2. Indeed the lower stationary specimens under test condition (2)-A and (2)-S are subjected to high frictional energy, but these scars are too large compared with others. It would be considered that the frequency of metal-to-metal contact under test condition (2) is higher than that under test condition (1) as shown in Fig. 5-4b, and in addition the lower stationary steel specimens are subjected to high frictional energy. Consequently such large wear volumes are obtained.

## 5-5. CONCLUSIONS

The following conclusions are drawn from the investigation of the effect of oscillatory direction and specimen combination on fretting wear under a crossed cylinder contact condition.

(1) The friction behaviour is totally different between test conditions (1) and (2). The coefficient of friction during fretting oscillation is significantly governed by the behaviour of debris.

(2) Measuring electrical contact resistance under test conditions (1) and (2), metal-to-metal contact was detected even after  $2 \times 10^5$  cycles. Metal-to-metal contact appears even after long running times in fretting wear which Pendlebury has also observed. More frequent metal-to-metal contacts occur under test condition (2).

(3) The most effective factors on fretting wear volume are frictional energy and frequency of metal-to-metal contact during fretting oscillation.

(4) Consequently, fretting wear damage is significantly dominated by fretting contact arrangement, specimen combination and oscillatory direction.

(5) Where debris and metal-to-metal contact are not factors, as in fretting  $Al_2O_3$  on  $Al_2O_3$ , the coefficient of friction is identical under test conditions (1) and (2).

## 6. A NEW FRETTING WEAR TEST APPARATUS

### 6-1. INTRODUCTION

New materials have increasingly been applied to engineering components, and in many cases the fretting wear properties of those materials are not well known at the moment. In order to take account of the more severe working circumstances of those new materials it is essential that the test conditions themselves are increased in severity. As these new materials have special characteristics, new criteria should be created for measuring the properties. In addition, metals and alloys which have been used in the past for engineering materials have recently been used in more severe environments, and therefore the fretting wear properties under these situations need to be determined. Hence a fretting wear test rig which can operate under these conditions has been developed.

Fretting damage will be significant in hostile environments and conditions of high load under which engineering components are now expected to operate. Rolling bearings belong to these engineering components. The evaluation of their performance under severe circumstances has been increasingly demanded: and the test rig aims to cover even the most severe factors found in present service. In previous work the fretting specimens were not themselves stressed, whereas real engineering components are usually subjected to stress. This fretting wear test rig is capable of applying a tensile stress to the stationary specimen, enabling the relation between the

applied tensile stress and fretting wear  
parameters to be obtained.

## 6-2. DESIGN

### 6-2-1. FRETTING WEAR TEST MACHINE

Figs. 6-1 and 6-2 show a schematic diagram of the fretting apparatus and a photograph of it, respectively. The fretting contact consists of a sphere-on-plate arrangement. The plate is stationary and the upper spherical rider oscillates. A 25.4mm diameter sphere is usually used for the upper specimen, and the size of the lower stationary specimen can be arranged according to the geometry of the lower specimen holder.

### 6-2-2. SPECIMENS

In the test, the upper specimen is a commercial 25.4mm diameter steel ball (high carbon chromium bearing steel). The upper spherical specimen is fixed to the fretting arm which is oscillated by an eccentric cam. The lower stationary specimen is 1mm thick, 10mm wide and 100mm long, polished to 1 $\mu$ m finish and finally attached to the specimen holder. In addition, a tensile stress can be applied to the lower stationary specimen during the fretting wear test, as shown in Fig. 6-3.

### 6-2-3. TEMPERATURE CONTROL

A furnace is used for elevated temperature fretting wear tests. The temperature capacity is 1200°C to raise the specimen temperature up to 800°C. The furnace consists of two parts. The upper part can be removed when the fretting wear test is carried out at room temperature. Both the upper and lower specimens are located in the uniform heat zone of the furnace, and a thermocouple is set up there to measure the furnace temperature.

A commercially available thyristor unit temperature controller is used to keep the temperature constant, control the heating speed, and displays the furnace temperature. Another thermocouple is placed underneath and in contact with the lower stationary specimen to measure the specimen temperature. This thermocouple is linked with a specimen temperature display and a chart recorder. The furnace temperature is determined by the required specimen temperature. the specimen temperature is simultaneously measured during the test.

### 6-2-4. NORMAL LOAD CONTROL

As shown in Fig. 6-1, the normal load is applied to the fretting arm by the loading arm. The loading arm is strain-gauged to determine the applied normal load. The relationship between the strain of the loading arm and the applied load has been obtained beforehand. The magnitude of the load can be adjusted by turning the locking nut.

The strain gauges are connected with an amplifier, and the applied normal load is indicated on the normal load display. The normal load corresponds to half the indicated load as the loading arm is located at the centre of the fretting arm. By this mean, the normal load can be controlled precisely.

#### 6-2-5. SLIP AMPLITUDE AND FREQUENCY CONTROLS

The fretting oscillation is produced by the eccentric cam. The slip amplitude, from 5 $\mu$ m to 50 $\mu$ m, can be achieved by adjustment of the setting of the eccentric cam. In some fretting wear rigs the fretting oscillation is impeded by the large normal load, but the magnitude of the slip amplitude is independently controlled in this rig.

#### 6-2-6. COEFFICIENT OF FRICTION

The fretting arm is strain-gauged to measure the tangential force. the test can be carried out at elevated temperatures as the part of the strain-gauged fretting arm is hollow to allow the circulation of cooling water. the strain gauges are linked with an amplifier to record the tangential force on a U.V. recorder. the recorder trace on the U.V. recorder is the average of the peak-to-peak tangential force. Hence, the tangential force, q, at half cycle can be obtained by using the following equation;

$$q = K ( W - I ) / 2 \quad (6.1),$$

where K is the tangential force calibration factor, W the width of the recorded trace and I the width of the recorded inertia force trace. the coefficient of friction,  $\mu$ , is given by the following equation;

$$\mu = q / N \quad (6.2),$$

where N is the normal load.

#### 6-2-7. APPLIED STRESS TO THE LOWER STATIONARY SPECIMEN

As shown in Fig. 6-3, a tensile stress can be applied to the lower stationary specimen. Fig. 6-4 shows the geometry of the specimen used in the test. In Fig. 6-5, the upper spherical specimen is positioned at the centre of the lower gauge length in the stationary specimen. A tensile stress is applied via a loading screw. One of the ends of the jigs holding the specimen is linked with a load cell. the capacity of the load cell is approximately 8900N. The magnitude of the applied tensile stress can be adjusted by turning the nuts, and the load is indicated on the applied load display.

## 7. FRETTING WEAR TESTS ON HIGH CARBON CHROMIUM BEARING STEEL USING A NEW TEST APPARATUS

### 7-1. INTRODUCTION

High carbon chromium bearing steel quenched and then tempered at low temperature is used as a material for rolling bearings. The microstructure is tempered martensite, and the hardness is approximately 800 VHN. The hardness is carefully controlled as there is a close correlation between the hardness and the rolling contact fatigue life. Hardness of the material is the most effective mechanical factor to prevent the raceways from surface damage. On the other hand, it is well known that there is a proportional relationship between brittleness and hardness. Hence, toughness of the material is decreased if hardness is increased. In fact, surface damage on the raceway and rolling elements is the most common problem in rolling bearing life, and fracture of the rings is seen in practice.

Fracture of the rings of rolling bearings is predominantly the result of heavy radial and axial loads and occurs even in lubricated conditions on the raceways. Surface damage should not arise as long as the rolling bearings are sufficiently well lubricated and the operating condition is controlled. It is observed that surface damage primarily occurs on the raceway, from which fracture is initiated. Therefore, in order to obviate fracture, the most effective countermeasure is to prevent the raceways suffering the initial surface damage. However, the circumstances where rolling bearings are used are extremely varied and becoming increasingly severe,

as mentioned in the previous chapters. In particular, miniature rolling bearings and solid lubricant rolling bearings are likely to be surface-damaged, because these bearings are not continuously operated for long periods. Hence, these bearings are often subjected to a situation in which fretting wear is likely to occur.

Rolling bearings are usually subjected to a hoop stress as they are placed between shafts and housings. The hoop stress is large when the rolling bearings are used in machinery where accuracy is particularly required. The hoop stress of the outer ring is usually compressive, while that of the inner ring is usually tensile when the rolling bearing is installed as a machine component. For example, when the machine containing the rolling bearings is transported, vibration is likely to cause fretting damage on them. Fracture resulting from fretting damage tends to occur when the inner ring of the rolling bearing is subjected to a tensile hoop stress.

As mentioned in Chapter 6, the new fretting wear test apparatus can apply tensile load to the lower stationary specimens. The applied tensile load to the lower stationary specimens can be adjusted to equal the tensile hoop stress which is experienced by rolling bearing rings. Therefore, the fracture mechanism induced by fretting wear on the high carbon chromium bearing steel can be investigated with this test apparatus. The relationships between the factors which can be considered as affecting the fracture, i.e. applied tensile load, normal load (maximum Hertzian contact stress), slip amplitude and temperature, have been studied. In this study, the fretting wear tests have been carried out under

unlubricated condition. The specimen temperatures used were room temperature and 200°C, because 200°C is considered to be approximately the maximum temperature to which ordinary rolling bearings are subjected.

## 7-2. EXPERIMENTAL PROCEDURE

### 7-2-1. MATERIALS

As described in Chapter 6, the upper moving specimen is a commercial 25.4mm diameter high carbon chromium bearing steel ball. The lower stationary specimen is also made of the high carbon chromium bearing steel, and is polished to 1 $\mu$ m finish. The geometry of the lower stationary specimen is shown in Fig. 6-4.

The stress distribution below the surface of the lower stationary flat specimen has been measured by X-ray residual stress measurement, and is shown in Fig. 7-1.

### 7-2-2. TEST CONDITIONS

Details of the test apparatus are described in Chapter 6. The experimental conditions were as follows,

normal loads	:	135 - 437N
maximum Hertzian contact stresses	:	812 - 1200MPa
slip amplitudes	:	5 - 50 $\mu$ m
applied tensile stresses to the lower stationary specimens	:	0 - 600MPa
specimen temperatures	:	in laboratory (17 - 22°C) 200°C

### 7-2-3. FRETTING WEAR TEST AT 200°C

The fretting wear tests at 200°C were carried out using the following method. After the specimen temperature had reached 200°C, it was held constant for 30min., and then the upper and lower specimens were placed in contact. Therefore, the condition of the surfaces of the specimens is assumed to have reached equilibrium and to be chemically constant.

### 7-2-4. DEVELOPMENT OF FRETTING WEAR SCAR

The fretting wear tests were individually carried out. Hence in each test the fretting contact situation at the beginning stage of the test is identical. Fretting wear scars produced on the lower stationary flat specimens without an applied tensile stress were examined to investigate the development of the fretting wear scar. The test conditions used in this work were as follows,

normal load	:	437 N,
maximum Hertzian contact stress	:	1200 MPa,
frequency	:	50 Hz,
amplitude	:	8 $\mu$ m.

### 7-2-5. FRACTURE INDUCED BY FRETTING WEAR

A tensile stress was applied to the lower stationary flat specimen during the fretting wear

test at both laboratory temperature and 200°C (specimen temperature), as described in Chapter 6-2-7. In the test at 200°C, the applied tensile stress was applied to the lower stationary specimen 30 min. after reaching the test temperature, and then the upper and lower specimens were placed in contact. Various slip amplitudes, normal loads and applied tensile stresses were used, as shown above. The test was predominantly carried for up to 10<sup>6</sup> cycles, and when specimens had not failed at 10<sup>6</sup> cycles the test was discontinued. An example of a failure induced by fretting wear is shown in Fig. 7-2.

### 7-3. EXPERIMENTAL RESULTS

#### 7-3-1. DEVELOPMENT OF FRETTING WEAR SCAR

Examples of the development of the fretting scar are shown in Figs. 7-3a and 7-3b. The outer circumferences of the fretting scars in Fig. 7-3a show the same diameter, although the width of the annulus of damage varies. On the other hand, the size of the scar significantly changes with increasing number of cycles in Fig. 7-3b. Fig. 7-3c shows the relationship between the number of cycles and the width of the annulus, (a-b).

#### 7-3-2. ELECTRICAL CONTACT RESISTANCE

An example of the electrical contact resistance is shown in Fig. 7-4. This fretting wear test was carried out under the following condition,

normal load	:	135 N,
maximum Hertzian contact stress	:	822 MPa,
frequency	:	60 Hz,
amplitude	:	25 $\mu$ m,
temperature	:	24°C,
humidity	:	54%RH.

The slip amplitude used in this test, 25 $\mu$ m is large enough for bulk sliding to occur with no non-slip area in the fretting contact area, as shown in Fig. 7-5. Nevertheless, metal-to-metal contact can be recognised throughout the whole stage of the fretting wear.

### 7-3-3. FRACTURE INDUCED BY FRETTING WEAR.

The fracture lives tested under various applied tensile stresses, normal loads and slip amplitudes at both laboratory temperature and 200°C are plotted on the diagrams shown in Figs. 7-6. The specimens have not fractured at 200°C as shown in Fig. 7-6c. According to Figs. 7-6a and b, short fracture life is the result of high normal load and occurs at a slip amplitude of 35 $\mu$ m in laboratory air.

#### 7-4. DISCUSSION

##### 7-4-1. DEVELOPMENT OF FRETTING WEAR SCAR

According to Figs. 7-3a and 7-3b, it is obvious that the the development process of the fretting wear scar is governed by the numerical relationship between  $T$  and  $\mu P$ . Fig. 7-3a is a typical example when  $T < \mu P$ , while Fig. 7-3b is an example when  $T > \mu P$ .

When the slip amplitude is small enough for the fretting wear scar to contain a non-slip region (when  $T < \mu P$ ), the fretting wear scar results from the following process. Initially, a small annular slip region is worn by microslip. The damage starts at the edge of fretting contact area as the relative slip is greatest there. Subsequently, the annular slip region is enlarged towards the centre of the annulus, while the outer diameter of the annulus remains constant. Sato et al [25] have also reported a similar wear process. Finally, the enlargement of the annular slip region is ceases because the total tangential strain falls to zero at the edge of the non-slip region (Fig. 2-18 curve (B)-(6)), and the scar shows no further development. At this stage, little debris is produced.

It is very obvious that non-slip region exists in the fretting wear scar when  $T < \mu P$ . Referring to Fig. 2-18, the non-slip region is subjected to the tangential traction strain,  $e''$ , which is the opposite direction of the tangential strain,  $e'$ . The maximum tangential traction strain,  $e''_{max}$ , exists at the boundary between the non-slip region and slip region. The total tangential shear

strain,  $e$ , is greatest at the fretting contact edge and is zero at the boundary between the non-slip region and slip region. Hence, the fretting wear towards the centre of the annulus again falls off due to the reduced total tangential shear strain,  $e$ . It is possible that the total tangential shear strain,  $e$ , may be related to the production of debris in fretting wear. Therefore, the total tangential shear strain,  $e$ , seems to be the most effective factor in the fretting wear process when  $T < \mu P$ .

A typical example of the relationship between the number of cycles and the width of fretting wear annulus is shown in Fig. 7-3c. According to this result, the development of the fretting wear annulus has settled down at  $10^5$  cycles, and the fretting wear may not progress appreciably further from this stage..

On the other hand, when the contact region entirely slips (when  $T > \mu P$ ), the size of the scar dramatically enlarges outwards. Referring to Fig. 7-8, the tangential shear strain,  $e$ , is greatest at the periphery of the fretting contact area. The periphery of the contact area is subjected to a significant strain as the contact region entirely slips. Figs. 7-4 show the electrical contact resistance during the fretting oscillation when  $T > \mu P$ . It can be recognised that debris exists between the specimens during the fretting oscillation. However, metal-to-metal contact throughout the whole stage of the fretting wear also can be recognised. Metal-to-metal contact would predominantly occur at the periphery of the fretting contact area as the scar increases in size.

## 7-4-2. FRACTURE INDUCED BY FRETTING WEAR

### 7-4-2-1. CRITICAL SLIP AMPLITUDE

According to the results in Figs. 7-6, the normal load (maximum Hertzian contact stress), the applied tensile stress, the residual stress of the material and the slip amplitude are effective in fracture induced by fretting wear at room temperature. The existence of a critical slip amplitude can be recognised at approximately  $35\mu\text{m}$ . Some researchers [22][106]-[109] have also found a critical amplitude in fretting fatigue. Nishioka et al [22][106]-[108] have obtained approximately  $20\mu\text{m}$  for the critical slip amplitude using carbon steels. On the other hand, in Kudva et al's study [109], where the residual stress of the specimens was changed by heat treatments such as carburising, decarburising and quenching-tempering, they mentioned that the critical amplitude lies between 20 and  $60\mu\text{m}$  and depends upon the residual stress in the specimen surface, as shown in Fig. 7-7. In Figs 7-6a and b, the critical slip amplitude is always  $35\mu\text{m}$  although the surface residual stress is changed by the applied tensile stress to the specimen. This result does not agree with Kudva's result [109]. Their results may include some other factors, for example the microscopic structures are different in the specimens used in their study. The relationship between coefficient of friction and slip amplitude obtained in this study is shown in Table 7-1. The coefficient of friction at  $35\mu\text{m}$  of slip amplitude is approximately twice that at other amplitudes.

Referring to Fig. 7-8 (when  $T \gg \mu P$ ), if the coefficient of friction,  $\mu$ , increases then the tangential stress,  $T$ , also increases under a constant contact stress condition. Simultaneously, the total tangential shear strain,  $e$ , due to  $T$  increases, and thus a high tangential shear strain energy,  $U$ , is created. Consequently, the critical slip amplitude in fracture induced by fretting wear is obtained.

#### 7-4-2-2. THE EFFECT OF TEMPERATURE

It is well known that oxide films lead to low coefficient of friction, and are often referred to as "glaze oxide" at higher temperatures. The crystallographic structure of these oxide films is a spinel.[58] Figs. 7-9 show the scars obtained by fretting under the same condition but at different temperatures. It is very obvious that the width of the annular scar fretted at room temperature is much larger than that at 200°C. Using Mindlin's theory (eq. 2-6), the coefficients of friction,  $\mu$ , are 0.5 and 0.21, respectively. This, therefore, confirms the effect of oxide film on fretting wear at an elevated temperature. According to this result, it can be seen that the critical slip amplitude in fretting fatigue is nullified by the oxide film.

No specimen has been fractured at 200°C in these tests. This result indicates that coefficient of friction is one of the most effective factors in fracture induced by fretting wear. This may suggest an appropriate

countermeasure for the prevention of this type of fracture.

#### 7-4-2-3. THE EFFECT OF THE NORMAL LOAD

As mentioned in the previous chapters, the significant effect of the normal load on fretting fatigue has been pointed out. [35][75][76] In the experimental rig used in this study, the slip amplitude can be controlled independently from the normal load. Hence, the results do not include the effect of reducing amplitude. Considering the crack initiation due to fretting oscillation, it is obvious that the total tangential stress,  $T$ , and the total tangential shear strain,  $e$ , which are subjected to a high contact stress leads to a high tangential strain energy,  $U$ , and consequently crack initiation is encouraged as shown in both Fig. 2-18 (when  $T < \mu P$ ) and Fig. 7-8 (when  $T > \mu P$ ). As mentioned above, some researchers [35][75][76] have pointed out that a high normal load induces significant fretting damage and decrease of fretting fatigue life. It has also been reported that a high normal load impedes rapid crack propagation in subsurface.[115] It is very obvious that a high normal load leads to high tangential stress and strain. It may, therefore, be thought that crack initiation is encouraged but crack propagation rate in subsurface is reduced by high normal load. The effect of high normal load on crack initiation may be larger than that on crack propagation.

#### 7-4-2-4. THE EFFECT OF RESIDUAL STRESS

As mentioned in Chapter 2-6, Kudva et al [109] have found a critical slip amplitude in fretting fatigue tests. They have suggested that the critical slip amplitude depends upon the different surface treatments and stress states. A critical slip amplitude has also been found in this study. However, the critical slip amplitude shows a constant value which is approximately  $35\mu\text{m}$  although the surface stress is mechanically changed. It may, therefore, be thought that the critical slip amplitude is independent of the stress state, but dependent upon thermo-chemical surface treatments such as carburising.

Fig. 7-10 shows the stress distributions below the surface when the lower tensile specimen is subjected to various applied tensile stresses. Although the specimen is subjected to +600MPa, the residual stress on the specimen surface is still compressive. In contrast, the depth where there is a change over to tensile residual stress is significantly dependent upon the applied tensile stress. Hence, the initiation of the cracks induced by fretting wear may be controlled by the tangential shear strain energy,  $U$ , described in Chapter 7-4-2-1, but the propagation of the cracks may be governed by a combination of the tangential stress and the resultant subsurface tensile stress. It appears that the initiation of fretting wear cracks is little affected by the residual stress in the subsurface, but the subsequent crack propagation rate in fretting fatigue is very dependent upon the stress state. Nishioka et al [107][108], Fair [123] and Mutoh et al [124] have

also reported that residual stresses have little influence on crack initiation in fretting fatigue.

The residual stress in the surface of the specimen tempered at 200°C is -270.6MPa, as shown in Fig. 7-1. The residual stress in the surface is +330MPa if a tensile stress of +600MPa is applied to the specimen. The specimen has not been fractured nor have cracks been found although the surface indicates a high tensile residual stress. As described in Chapter 2-4-2-2, the coefficient of friction at 200°C is much lower than that at room temperature. It, therefore, appears that coefficient of friction is more effective than surface residual stress in crack initiation.

#### 7-4-2-5. FRACTURE SURFACE

A typical fracture surface is shown in Fig. 7-11. The fracture surface can be mainly divided into three zones, (a), (b) and (c) in Figs. 7-11 and 7-12.

The shear mode zone (Fig. 7-12a) is heavily rubbed and oxidised. This zone is dominated by the combined stresses of the tangential stress and applied tensile stress. However, it is predominantly controlled by the tangential stress very near the surface. A typical fatigue fracture appearance can be seen in the opening mode zone (Fig. 7-12b). This zone is predominantly governed by the applied tensile stress. Fig. 7-12c shows the rapid fracture zone which indicates a transgranular fracture surface.

The driving force for fracture induced by fretting wear is mainly dominated by the fretting

damage on the surface as the applied tensile stress is static in this test. In summary, the tangential shear strain energy,  $U$ , seems to be a quite effective factor in initiating a crack in the specimen. It is, therefore, necessary to discuss the mechanism of crack initiation in fretting wear.

7-4-3. CRACK INITIATION AND WEAR DURING FRETTING  
OSCILLATION IN HIGH CARBON CHROMIUM BEARING  
STEEL, PARTICULARLY SPHERE-ON-PLATE  
ARRANGEMENT

7-4-3-1. CRACK INITIATION AND WEAR

As shown in Chapter 2-5-3-1, Sato et al [26][29] have mentioned that there are three crack initiation points in the fretting wear scar (see Fig. 2-7). These three points correspond to the places where there is maximum shear stress, maximum strain energy and maximum principal stress, respectively. According to their reports, the crack initiation point may depend upon the mechanical properties of the specimen.

Considering the mechanism of fracture induced by fretting wear in the high carbon chromium bearing steel, crack initiation is governed by the tangential shear strain energy,  $U$ , which corresponds to the shear strain energy in Sato's study, as mentioned in the previous chapters. Referring to Fig. 2-18(A), the tangential shear strain energy,  $U$ , shows maximum and minimum values in the slip region when  $T < \mu P$  and the sliding is unidirectional. However, the tangential shear strain energy,  $U$ , assumes a cyclic alternating value in the slip region since fretting is reciprocating motion. Hence the place which experiences the maximum/minimum tangential shear strain energy indicates the minimum/maximum tangential shear strain energy during fretting oscillation. Consequently, these points are subjected to the most severe fretting fatigue damage. Indeed, Figs. 7-2 and 7-13a show very clear curved cracks. The points where the radii of

the curves are a minimum (i.e. on the horizontal centre line) indicate the position of maximum alternating tangential shear strain energy,  $U_{max}$ . Fig. 7-13b shows a typical fretting wear scar which has cracks when  $T \geq \mu P$ . This is evidence that the position of the crack initiation due to fretting wear is independent of the numerical relationship between  $T$  and  $\mu P$ . As described in Chapter 7-4-2-1, there are points where the alternating tangential shear strain energy is a maximum in the fretting wear scar even if  $T$  is equal to or greater than  $\mu P$ . (see Fig. 7-8) It is, however, very important to obtain the numerical relationship between the fretting wear rate and the crack propagation rate when fracture induced by fretting wear is discussed. As described in Chapter 7-4-1, fretting wear is predominantly dominated by the total tangential shear strain,  $e$ . On the other hand, fretting crack initiation in fracture induced by fretting wear (or fretting fatigue) is governed by the maximum alternating tangential shear strain energy,  $U_{max}$ . It is true that the cracks induced by fretting oscillation are worn away by fretting wear before they have time to propagate if the fretting wear rate is greater than the crack propagation rate. In summary, it is very important to obtain the numerical relationship between the total tangential shear strain,  $e$ , and the tangential shear strain energy,  $U$ . Indeed, Waterhouse [104] has pointed out that fretting fatigue damage can be minimised by increasing the slip amplitude. Increasing the slip amplitude results in a large total sliding distance during fretting oscillation. Consequently, the fretting wear rate is encouraged and overcompensates the crack

propagation rate. It is, therefore, important to determine the depth of the fretting crack initiation and its growth per cycle and their relation to the depth of the fretting wear scar and its increase per cycle when fracture induced by fretting wear is discussed. This aspect is also important in the discussion of fretting fatigue.

#### 7-4-3-2. DISCUSSION OF CRACK INITIATION

Figs. 7-14a - 7-14e show fretting cracks in the surface. The cracks shown in Figs. 7-14a - 7-14c belong to the fretting wear scar illustrated in Fig. 7-13a ( $T < \mu P$ ), and those shown in Figs. 7-14d and 7-14e belong to the fretting wear scar illustrated in Fig. 7-13b ( $T > \mu P$ ). Interestingly, the cracks which exist in the fretting wear scar have a inclination from the surface plane (see Figs. 7-14b, 7-14c, 7-14d and 7-14e). In contrast, the cracks which exist out side of the fretting scar propagate perpendicularly to the surface plane, as shown in Fig. 7-14a. The mechanism of the crack propagation near the surface in fretting wear scar may be similar to that of the stage I in fatigue. At the place where is not subjected to shear stress due to fretting oscillation, the mechanism may be predominantly governed by the applied tensile stress, which is similar to the mechanism of the stage II even if the place is near the surface. It is well known that the stage I is significantly dominated by the combined stress between the tangential stress and the applied tensile stress. Broszeit et al [116] have reported that a maximum shear stress due to

contact stress is  $0.62P_{\text{max}}$  at the place where is  $0.47a$  below the surface in the case of a point contact. Here  $P_{\text{max}}$  is the maximum Hertzian contact stress,  $a$  the radius of the contact circle. Therefore, the depth of the maximum tangential shear stress due to contact stress is  $0.165\text{mm}$  from the surface when  $P_{\text{max}}$  is  $1000\text{MPa}$ . The cracks shown in Fig. 7-14e are nearly at the centre of the fretting wear scar, and reach a depth of approximately  $0.165\text{mm}$  with an inclination of approximately  $70^\circ$  from the surface. According to Figs. 7-14a - 7-14e, it is obvious that the inclination of the crack depends upon the distance of the centre of the fretting wear scar. The steepest inclination is at the centre of the fretting wear scar.

Edwards [117] and Rooke et al [118] have suggested  $K^f/K^\sigma = 0.4/a$ , and that the frictional force (i.e. tangential shear force) contributes significantly to the stress intensity factor ratio,  $K^f/K^\sigma$ , if the crack length,  $a$ , is approximately  $1\text{mm}$  or less. Here  $K^f$  represents the stress intensity factor due to frictional force,  $K^\sigma$  the stress intensity factor due to applied stress and  $a$  the crack length in millimeters. It may, however, be inapplicable to discuss this study with the stress intensity factor ratio, as the specimen used in this study is  $1\text{mm}$  in thickness.

Nowell and Hills have made a computer programme to obtain the distribution of the fretting/fatigue damage parameter in fretting wear scar, which is based on the equations proposed by Ruiz et al [103][104]. The contour key, C, of the fretting/

fatigue damage parameter is given by the following equation,

$$C = \sigma\tau\delta\beta / (a P_{\max})^3 \quad (7.1).$$

Here  $\sigma$  represents the tensile stress in the surface parallel to the fretting oscillatory direction [119],  $\tau$  the tangential stress at the surface due to the fretting oscillation [19],  $\delta$  the half amplitude of the microslip during fretting cycle [120],  $\beta$  the shear modulus,  $a$  the radius of the contact circle and  $P_{\max}$  the maximum Hertzian contact stress.

Fig. 7-15a is the contour diagram of the fretting damage parameter calculated by the computer programme when the tangential force is 118.5N, normal load 437N, coefficient of friction 0.50 and the ratio between the slip region and non-slip region,  $b/a$ , 0.77 at room temperature. It is very obvious that the fretting damage parameter (i.e. value of the tangential shear strain energy) reaches a maximum in the slip region, according to Fig. 7-15a. The contour diagram of the fretting/fatigue damage parameter of the specimen illustrated in Fig. 7-13a is shown in Fig. 7-15b where it is assumed that the fretting oscillation is only in one direction indicated by the arrow. This diagram also points out that maximum of fretting/fatigue damage parameter exist in the slip region. With reciprocating motion, the contour diagram is given as shown in Fig. 7-15c. A maximum alternating tangential shear strain energy,  $U_{\max}$ , exists at the places illustrated in Fig. 7-15c. These places correspond to the crack initiation points in Fig. 7-13a. As described in Chapter 7-4-3-1, it is, therefore, obvious that

fracture induced by fretting wear (or fretting fatigue) is significantly governed by the tangential shear strain energy,  $U$ , and the crack initiates at the maximum alternating tangential shear strain energy,  $U_{max}$ .

#### 7-4-3-3. FRETTING WEAR AND FRETTING FATIGUE

In previous Chapters, the mechanisms of both fretting wear and fretting fatigue were discussed. It was proposed that the main driving force of fretting wear was the total tangential shear strain,  $e$ , and that of fretting fatigue was the maximum alternating tangential shear strain energy,  $U_{max}$ . It was also found that fretting fatigue cracks initiated with a inclination in the subsurface, and propagated perpendicularly to the surface in the body of the component. On the other hand, Goto and Waterhouse [121] have reported that delamination is found at the edge of the fretting wear scar when the specimen is subjected to high normal load and tangential load. Hence, it is apparent that crack initiation and propagation mechanisms are different between fretting wear and fretting fatigue. The cracks in fretting wear seem to initiate at the surface where is subjected the highest tangential shear strain,  $e_{max}$ , to propagate parallel to the surface and to lead to a delamination-like-wear. The different behaviour of the cracks between fretting wear and fretting fatigue can be explained by the aforementioned driving forces (i.e. the total tangential shear strain,  $e$ , and the maximum alternating tangential shear strain energy,  $U_{max}$ ).

## 7-5. CONCLUSIONS

The following conclusions are drawn from the investigations of fretting wear and fracture induced by fretting wear in high carbon chromium bearing steel.

(1) The development of the fretting scar depends upon the numerical relationship between  $T$  and  $\mu P$ . When  $T < \mu P$ , the annular slip region grows towards the centre of the annulus. In contrast, when  $T > \mu P$ , the fretting scar grows outwards, and further metal-to-metal contact takes place at the outer edge of the scar during fretting oscillation.

(2) A critical slip amplitude in fracture induced by fretting wear was found. The coefficient of friction assumes a very high value at the critical slip amplitude. The critical slip amplitude was  $35\mu\text{m}$  in this study.

(3) The oxide film produced at  $200^\circ\text{C}$  leads to a very low coefficient of friction. In addition, no specimen was fractured in the tests at  $200^\circ\text{C}$ . It is, therefore, obvious that the coefficient of friction is one of the most important factors in fracture induced by fretting wear. It has been generally suggested that the critical slip amplitude in fretting fatigue is nullified by the presence of oxide films.

(4) High normal loads have little effect on crack propagation in fretting fatigue or fracture induced by fretting wear, but do influence crack initiation due to fretting oscillation by increasing the tangential stress and strain. The

effect of high normal load on crack initiation may be larger than that on crack propagation in fretting fatigue.

(5) Compressive residual stresses in the subsurface of the fretted specimen have little influence on crack initiation, but have a large influence on crack propagation rate.

(6) The driving force of fracture induced by fretting wear can be explained by the distributions of the stresses, strains and energy during fretting oscillation.

(7) The crack in fracture induced by fretting wear (or fretting fatigue) initiates at the points of maximum alternating tangential shear strain energy,  $U_{max}$ . The position of the crack initiation is independent of the numerical relationship between  $T$  and  $\mu P$ .

(8) In fretting wear, the total tangential shear strain,  $e$ , is the most effective factor. On the other hand, the maximum alternating tangential shear strain energy,  $U_{max}$ , is the most effective factor in fracture induced by fretting wear (or fretting fatigue). It is true that the cracks in fretting fatigue propagate perpendicularly to the surface of the component. In contrast, the cracks in fretting wear seems to initiate at the surface where is subjected to the highest total tangential strain,  $e_{max}$ , to propagate parallel to the surface and to lead to a delamination-like-wear.

(9) It is very important to obtain the numerical relationships between crack propagation rate and

fretting wear rate and between the depth of the fretting crack initiation and the depth of the fretting wear scar when fracture induced by fretting wear (or fretting fatigue) is discussed. If the wear rate exceeds the propagation rate, the cracks are wiped out before they are able to propagate into the body of the material. In summary, fretting wear is dominated by the total tangential shear strain,  $e$ , whereas crack initiation in fracture induced by fretting wear (or fretting fatigue) is dominated by the maximum alternating tangential shear strain energy,  $U_{max}$ . Therefore, the numerical relationship between  $e$  and  $U_{max}$  is important as indicated in Fig. 2-18.

(10) Consequently, coefficient of friction is the most effective factor in both fretting wear and fretting fatigue as it is a parameter contributing to the total tangential stress,  $T$ , which significantly affects both the total tangential shear strain,  $e$ , and tangential shear strain energy,  $U$ .

## 8. PRACTICAL APPLICATION OF FRETTING DAMAGE PREVENTION FOR ROLLING BEARINGS

Throughout this study, the following aspects are drawn as a practical application of fretting damage prevention for rolling bearings.

### 8-1. HIGH CARBON CHROMIUM BEARING STEEL

(1) High carbon chromium bearing steel shows a low wear volume against  $Al_2O_3$  and WC-Co. High hardness is one of the most effective mechanical characteristics to prevent severe fretting wear as there is a relationship between fretting wear volume and  $P_{max.}/VHN$ .

(2) Generally, high carbon chromium bearing steel tempered at less than  $350^\circ C$  leads to low coefficient of friction due to a glaze type oxide film. Hence, the oxide film formed before fretting wear action overrides the effect of hardness on fretting wear volume.

(3) WC-Co shows a good lubricating performance as the cobalt bonding agent and tungstic oxide have a lubricating effect. On the other hand, high torque results if WC-Co is used as a material for rolling bearings, because the density of WC-Co is much higher than that of steel.

## 8-2. FRETTING WEAR AND FRETTING FATIGUE IN ROLLING BEARINGS

(1) The most effective physical factors on fretting wear volume are frictional energy and frequency of metal-to-metal contact during fretting oscillation. Therefore, raceways of rolling bearings may be subjected to larger frictional energy than rolling elements. Therefore, the raceways of the bearings in which lubrication is not easily controlled, such as miniature bearings, may be likely to be damaged.

(2) Fretting wear damage is dominated by fretting contact arrangement, material combination and oscillatory direction, because the behaviour of debris significantly affects fretting contact conditions (i.e. metal-to-metal contact).

(3) High normal load leads to increase of the tangential shear stress and strain. It is well known that angular contact ball bearings are usually subjected to a preload where the maximum Hertzian Contact stress ( $P_{max}$ ) is approximately 700 - 900MPa. Therefore, if such bearings are subjected to a certain hoop stress together with vibration in the absence of a lubricant film, they may be significantly damaged by fretting wear.

(4) Compressive residual stress has a great influence on fretting crack propagation, but has little effect on crack initiation. Hence, treatments which introduce compressive residual stress and increase surface hardness, such as carburising, nitriding and shotpeening are very useful methods for preventing severe fretting

wear. However, fretting damage to a case hardened steel is greater the thicker the case [122].

(5) There is a critical slip amplitude in fracture induced by fretting wear. In this test, the critical slip amplitude is  $35\mu\text{m}$ . The coefficient of friction at this slip amplitude is much higher than those at other slip amplitudes. Therefore, the displacement between components (i.e. between rolling elements and raceways, housing and outer ring and shaft and inner ring) must be avoided from the value of the critical slip amplitude when rolling bearings are designed.

(6) Fretting wear is dominated by the total tangential shear strain,  $e$ . In contrast, crack initiation in fracture induced by fretting wear (or fretting fatigue) is governed by the maximum alternating tangential shear strain energy,  $U_{\text{max}}$ . It is obvious that the cracks in fretting fatigue propagate perpendicularly to the surface of the component. On the other hand, the cracks in fretting wear seem to initiate at the surface where is subjected to the highest total tangential shear strain,  $e_{\text{max}}$ , and propagate parallel to the surface and lead to a delamination-like- wear.

(7) For rolling bearings, particularly raceways of the bearings, both fretting wear and fretting fatigue must be prevented, because they both lead to bearing failure. Both the total tangential shear strain,  $e$ , and the tangential shear strain energy,  $U$ , are significantly affected by coefficient of friction. It is, therefore, obvious that the most profitable countermeasure to prevent both fretting wear and fracture induced by

fretting (or fretting fatigue) is to obtain low coefficient of friction.

## ACKNOWLEDGEMENTS

The author would like to express his appreciation to Dr. R.B. Waterhouse for all his supervision and encouragement throughout the time to complete this thesis.

The author would like to thank the NTN Toyo Bearing Co. Ltd., Osaka, Japan, for their financial support and extraordinary opportunity for him to be able to study at the University of Nottingham.

Thanks are due to Professor J.S.L. Leach for the provision of research facilities in the Department; Dr. P.A. Brook for his computing advice; Dr. J.R. Moon for his advice in the field of physical metallurgy; all staff and research students of the Department for their advice and encouragement, particularly Mr. K. Dinsdale and Dr. B.R. Pearson; the technical staff in the Department for the contribution in building the testing machine, making the specimens and preparation for research facilities.

The author is grateful to acknowledge Professor J. Sato in Tokyo University of Mercantile Marine for his special encouragement and arrangement.

Dr. D.A. Hills and Mr. D. Nowell in the Department of Engineering Science, University of Oxford, are also gratefully acknowledged for their help and advice.

Many thanks are also due to Professor K. Okabayashi and Professor M. Kawamoto in the University of Osaka Prefecture, and Professor S. Komatsu in Kansai University, Japan.

The author particularly wishes to thank the following people, Dr. H. Muro, Mr. A. Wada, Mr. S. Itoh, Dr. N. Tsushima, Mr. A. Ishii, Mr. K. Nakamura, Mr. H. Inoue, Mr. K. Kodera, all members of the Material Research Laboratory in the NTN Toyo Bearing Co. Ltd, David, Adrian, Gerrard, Nicholas, Steven, Jonathan, Andrew, and L.C.J. Finally, the author will never forget his parents' encouragement.

## REFERENCES

- [1] Tsushima N., NTN Technical Manual - fracture - NTN Toyo Bearing Co., Ltd. (1986) p.7
  
- [2] Scarlett N.A., Greases to Prevent Fretting Corrosion, Engineering, 25 March (1960) pp.424
  
- [3] Aoki S., Fujiwara T. and Furukawa I., Fretting of Bearing Steel by Rolling Contact, Bull. JSPE 2, 3 (1967) pp. 238
  
- [4] Ito S., Fretting Wear of Bearing Steel, NTN Bearing Engineer, 9, 1 (1960) pp.1127
  
- [5] Waterhouse R.B., Fretting Corrosion, Pergamon Press, Oxford, (1972) p.2
  
- [6] Waterhouse R.B., Fretting Corrosion, Pergamon Press, Oxford, (1972) p.232
  
- [7] Waterhouse R.B., Fretting Corrosion, Pergamon Press, Oxford, (1972) p.4
  
- [8] Aldham D. and Warburton J., The Unlubricated Fretting Wear of Mild Steel in Air, Wear 106 (1985) pp.177
  
- [9] Buckley D.H., Effect of Various Material Properties on the Adhesive Stage of Fretting, AGARD Conf. Proc. No. 161, Specialists Meeting on Fretting Aircraft Systems
  
- [10] Bethune B. and Waterhouse R.B., Adhesion between Fretting Steel Surfaces, Wear 8 (1965) pp. 22

- [11] Feng I.M. and Rightmire B.G., An Experimental Study of Fretting, Proc. Inst. Mech. Engrs. 170 (1956) pp. 1056
- [12] Goodzeit C.L., Friction and Wear, Elsevier (1959) p.67
- [13] Uhlig H.H., Mechanism of Fretting Corrosion, J. Appl. Mech. 21 (1954) pp. 401
- [14] Suh N.P., The delamination theory of wear, Wear 25 (1973) pp. 111
- [15] Suh N.P., An overview of the delamination theory of wear, Wear 44 (1977) pp. 1
- [16] Lundberg G. and Palmgren A., Dynamic Capacity of Rolling Bearings, Ingeniörsvetenskapsakademiens Handlingar, 196 (1947) p.6
- [17] Waterhouse R.B. and Taylor D.E., Fretting Debris and the Delamination Theory of Wear, Wear 29 (1974) pp. 337
- [18] Waterhouse R.B., The Role of Adhesion and Delamination in the Fretting Wear of Metallic Materials, Wear 45 (1977) pp. 335
- [19] Mindlin R.D., Compliance of Elastic Bodies in Contact, J. Appl. Mech. 16 (1949) pp. 259
- [20] Johnson K.L., Contact Mechanics, Cambridge University Press (1985) p. 213
- [21] Halling J., Principles of Tribology, The Macmillan Press (1975) p. 53

- [22] Nishioka K. and Hirakawa K., Fundamental Investigations of Fretting Fatigue (Part5), Bull. JSME, 12, 52 (1969) pp. 692
- [23] Sato J. and Shima M., Studies of Fretting (Part2), JSLE 28, 6 (1983) pp.442
- [24] Waterhouse R.B., Fretting Wear, Wear 100 (1984) pp. 107
- [25] Sato J., Shima M., Igarashi J., Tanaka M. and Waterhouse R.B., Studies of Fretting (Part1), JSLE 26, 8 (1981) pp.555
- [26] Sato J. and Sugawara T., A Fundamental Study of Fretting Damage to Glass using an Improved Apparatus, Wear 106 (1986) pp. 53
- [27] Stowers I.F. and Rabinowicz E., The Mechanism of Fretting Wear, J. Lub. Tech. 95, 1 (1973) pp. 65
- [28] Ohmae N. and Tsukizoe T., The Effect of Slip Amplitude on Fretting, Wear 27 (1974) pp.281
- [29] Sato J., Recent Trend in Studies of Fretting Wear, JSLE, 30, 12 (1985) pp. 853
- [30] Waterhouse R.B., Fretting Wear, Proc. Int. Conf. on Wear of Materials (1981) ASME, pp. 17
- [31] Sato J., Recent Studies on Fretting, JSLE 22, 10 (1977) pp.622
- [32] Sato J., Shima M. and Sugawara T., A Fundamental Study of fretting Damage to Glass

using an Improved Apparatus, Wear 106 (1985) pp. 53

[33] Sato J. and Shima M., Studies of Fretting (Part2), JSLE 28, 6 (1983) pp.442

[34] Graham W.A., MSc Thesis, University of Oklahoma (1963)

[35] Waterhouse R.B., Fretting Corrosion, Pergamon Press, Oxford, (1972) p. 120

[36] Waterhouse R.B., Fretting Corrosion, Pergamon Press, Oxford, (1972) p. 119

[37] Sato J., Yamamoto H., Mochizuki Z. and Kawaguchi, Fretting Wear of Wear-Resistance Materials, JSLE 29, 10 (1984) pp.775

[38] Kayaba T. and Iwabuchi A., Influence of hardness on fretting wear, proc. Int. Conf. on Wear of materials, ASME (1981) pp. 371

[39] Sato J. and Takeuchi M., Effect of Hardness and Environment on Fretting Wear of Steel, JSLE Annu Conf. Preprint (1986)

[40] eg. Sander H., Multitechnique Studies on Fretting Fatigue : Influence of Surface Treatment - Final Technical Report -, United States Army European Research Office of The U.S. Army, London, Contract Number DAJA 45-83-C-0019, November (1986), Bundesanstalt für Materialprüfung Berlin (BAM)

[41] Kuno M., NTN Test Report (1984), NTN Toyo Bearing Co., Ltd.

[42] Hurricks P.L. and Ashford K.S., Proc. Instn. Mech. Engrs., 184, PtL, pp.165

[43] Waterhouse R.B., Influence of Local Temperature increase on the Fretting Corrosion of Mild Steel, J. Iron Steel Inst. 197 (1961) pp. 301

[44] Wright K.H., Corr. Preventn. and Contl., 1 (1954) pp. 465

[45] Godfrey D., Investigation of Fretting Corrosion by Microscopic Observation, NACA Report No. 1009 (1951)

[46] Iwabuchi A., Kayaba T. and Kato K., Effect of Atmospheric pressure on Friction and Wear of 0.45%C steel in Fretting, Wear 91 (1983) pp. 289

[47] Wright K.H., Fretting Wear debris, Proc. Inst. Mech. Engrs., IB (1952/3) pp. 556

[48] Fenner A.J., Wright K.H.R. and Mann J.Y., Fretting Corrosion and its Influence on Fatigue Failure, Int. Conf. Fatigue of Metals, Inst. Mech. Engr (1956) pp. 11

[49] Halliday J.S. and Hirst W., The Fretting Corrosion of Mild Steel, Proc. Roy. Soc., Ser. A, 236 (1956) pp. 411

[50] Shima M. and Sato J., Studies of Fretting (Part3), JSLE, 30, 3 (1985) pp. 201

[51] Rowe G.W., The Chemistry of Tribology, Roy. Inst. Chem., 12 (1968) pp. 135

[52] Harris S.J., Overs M.P. and Gould A.J., The Use of Coatings to control Fretting Wear at Ambient and elevated Temperature, Wear, 106 (1985) pp. 35

[53] Bowden F.P. and Tabor D., The Friction and Lubrication of Solids, The Clarendon Press (1958) p.151

[54] Bowden F.P. and Tabor D., The Friction and Lubrication of Solids, The Clarendon Press (1958) p. 294

[55] Waterhouse R.B., Fretting Corrosion, Pergamon Press, Oxford, (1972) p.117

[56] Hurricks P.L., The Fretting Wear of Mild Steel from Room Temperature to 200°C, wear, 19 (1972) pp. 207

[57] Hurrick P.L., The Fretting Wear of Mild Steel from 200°C to 500°C, Wear, 30 (1974) pp. 189

[58] Waterhouse R.B., Fretting at High Temperatures, Trib. Interntl, Aug. 1981, pp. 203

[59] Waterhouse R.B. and Iwabuchi A., High Temperature Fretting Wear of Four Titanium Alloys, Wear, 106 (1985) pp. 303

[60] Waterhouse R.B., The Fretting Wear of Nitrogen-Bearing Austenitic Stainless Steel at

Temperatures to 600°C, J. of Tribology, 108 (1986)  
pp. 359

[61] Bill R.C., Fretting Wear of Iron, Nickel and  
Titanium under varied Environmental Conditions,  
Proc. Int. Conf. on Wear of Materials (1979) pp.  
356

[62] Sato J., Shima M. and Takeuchi M., Fretting  
Wear in Seawater, Wear, 110 (1986) pp. 227

[63] Pearson B.R., Brook P.A. and Waterhouse R.B.,  
Fretting in Aqueous Media, particularly of Roping  
Steels in Seawater, Wear, 106 (1985) pp. 225

[64] Iwabuchi A., Kato K. and Kayaba T., Fretting  
Properties of SUS 304 Stainless Steel in Vacuum  
Environment, Wear, 110 (1986) pp. 205

[65] Antler M., Electrical Effects of Fretting  
Connector Contact Materials : A Review, Wear, 106  
(1985) pp.5

[66] Pendlebury R.E., Unlubricated Fretting Wear  
of Mild Steel Surfaces in Air at Room Temperature  
: II Electrical Contact Resistance Measurements  
and The Effect on Wear of Intermittent Loading,  
Wear, 118 (1987) pp.341

[67] Pendlebury R.E., Unlubricated Fretting and  
Sliding Wear of Steel in Air, Inst. Mech Engrs.,  
Proc. Interntl Conf. (1987) pp.267

[68] Tsushima N. and Nakashima H., NTN Test  
Report, NTN Toyo Bearing Co., Ltd.

[69] Callity B.D., Elements of X-ray Diffraction, Addison-Wesley Publishing Company Inc. (1978) p.292

[70] Sato K., Fujii H. and Kodama S., Effect of Stress Ratio and Fretting Fatigue Cycles on the Formation of Fretting Fatigue Damage of Carbon Steel S45C, Bulletin of JSME, 29, 255, September (1986)

[71] Sato J., Igarashi J., Shima M. and Waterhouse R.B., Fretting of Glass, wear, 65 (1980) pp.55

[72] Switek W., Early Stage Crack Propagation in Fretting Fatigue, Mechanics of Materials, 3 (1984) pp.257

[73] Mutoh Y., Tanaka K. and Kondoh M., Fretting Fatigue in S45C Steel under Two-Step Block Loading, JSME 478, A (1986) pp.1477

[74] Nowell D. and Hills D.A., An Analysis of Fretting Fatigue, Inst. Mech Engrs., Proc. Interntl Conf. (1987) pp. 965

[75] Sato K. and Fujii H., Crack Propagation Behaviour in Fretting Fatigue, Wear, 107 (1986) pp.245

[76] Aronov V. and Mesyef T., Wear in Ceramic/Ceramic and Ceramic/Metal Reciprocating Sliding Contact. Part I, J ourl of Tribology, Jan, 108 (1986) pp.16

- [77] Habeeb J.J., Blahey A.G. and Rogers W.N., Wear and Lubrication of Ceramics, Inst Mech Engr., Proc. Interntl Conf. (1987) pp.555
- [78] Buckley D.H. and Miyoshi K., Friction and Wear of Ceramics, Wear 100 (1984) pp.333
- [79] Fukuhara M., Fukazawa K. and Fukawa A., Physical Properties and Cutting Performance of Silicon Nitride Ceramic, Wear, 102 (1985) pp.195
- [80] Ishigaki H., Friction of ceramics, JSLE 30, 9 (1985) pp.627
- [81] Klaffke D., Fretting Wear of Ceramic-Steel : The Importance of Wear Ranking Criteria, Wear, 104 (1985) pp.337
- [82] Klaffke D. and Habig K.H., Fretting Wear Tests of Silicon Carbide, ASME, Proc. of Internl Conf., Wear of Materials, (1987), pp.361
- [83] Waterhouse R.B., Fretting Corrosion, Pergamon Press, Oxford, (1972) p.37
- [84] Eschmann, Hasbargen and Weigand, Ball and Roller Bearings, John Weiley and Sons Ltd. (1985) p. 349
- [85] NTN Handbook (1982), NTN Toyo Bearing Co., Ltd.
- [86] Clauss F.J., Solid Lubricants and Self-Lubricating Solids, Academic Press (1972) p.7

[87] Culp D.V., Fretting Corrosion in Wheel Bearings for Automobiles, Lubrication Engineering, 27, 10 (1971) pp.350

[88] Johnson K.L., Contact Mechanics, Cambridge University Press, (1985) p.397

[89] Hamdy M.M, Overs M.P. and Waterhouse R.B., A New High-Temperature Fretting Wear Test Rig, J. Phys. E. Sci. Instrum, 14 (1981) pp. 889

[90] Kayaba T. and Iwabuchi A., The fretting wear of 0.45% C Steel and Austenitic Stainless Steel from 20 to 650°C in Air, Wear, 74 (1981-1982) pp.229

[91] Betteridge W., Cobalt and its Alloys, Ellis Horwood Ltd. (1982) p. 26

[92] Buckley D.H., Adhesion Friction and Wear of Cobalt and Cobalt-base Alloys, Cobalt, 38 (1968) pp. 13

[93] Hamdy M.M. and Waterhouse R.B., The Fretting Wear of Ti-6Al-4V and aged Inconel 718 at Elevated Temperatures, Wear, 71 (1981) pp. 237

[94] Johnson K.L. and O'Connor J.J., The Role of Surface Asperities in Transmitting Tangential force between Metals, Wear, 6 (1963) pp. 118

[95] Waterhouse R.B., Fretting Corrosion, Pergamon Press, Oxford, (1972) p.119

[96] Uhlig H.H., Corrosion and Corrosion Control - an introduction to corrosion science and

engineering - Second Edition, John Wiley & Sons Inc., (1971) p.160, 404

[97] Halling J., Principles of Tribology, The Macmillan Press, (1975) p.65

[98] Johnson K.L., Contact Mechanics, Cambridge University Press, (1985) p.416

[99] Hannink R.H.J., Murray M.J. and Scott H.G., Friction and Wear of Partially Stabilised Zirconia : Basic Science and Practical Applications, Wear, 100 (1984) pp.355

[100] Kayaba T. and Iwabuchi A., The Effect of Temperature on Fretting Wear, JSLE, 27, 1 (1982), pp.31

[101] Kubaschewski O. and Hopkins B.E., Oxidation of Metals and Alloys, Butterworth Scientific Publications (1953) p.105

[102] Kuno M., Waterhouse R.B. and Pearson B.R., Fretting Wear in Sintered Alumina- and Tungsten carbide Cermet- Metal couples, Proc. of Wear of Materials 1987, ASME, vol.1 (1987) pp.371

[103] Ruiz C., Boddington P.H.B. and Chen K.C., An Investigation of Fatigue and Fretting in a Dovetail Joint, Experimental Mechanics, Sept. (1984) pp.208

[104] Ruiz C. and Chen K.C., Life Assessment of Dovetail Joints between Blades and Discs in Aero-Engines, Proc. of IMechE, Fatigue of Engineering Materials and Structures (1986) pp. 187

- [105] Halling J., Principles of Tribology, The Macmillan Press (1975) p.55
- [106] Nishioka K. and Hirakawa K., Fundamental Investigations of Fretting Fatigue (Part 2), Bull. of JSME, 12, 50 (1969) pp.180
- [107] Nishioka K. and Hirakawa K., Fundamental Investigations of Fretting Fatigue (Part 4), Bull. of JSME, 12, 51 (1969) pp.408
- [108] Nishioka K. and Hirakawa K., Fundamental Investigations of Fretting Fatigue (Part 6), Bull. of JSME, 15, 80 (1972) pp.135
- [109] Kudva S.M. and Duquette D.J., Effect of Surface Residual Stress on the Fretting Fatigue of a 4130 Steel, Residual stress effects in fatigue (ASTM), (1982) pp.195
- [110] eg. Berns H. and Weber L, Fatigue Crack Growth in the Presence of Residual Stresses, Residual Stresses in Science and Technology, Informationsgesellschaft, Deutsche Gesellschaft für Metallkunde, Verlag (1987) pp.751
- [111] eg. Desvignes M, Gentil B and Castex L., Fatigue Progressing of Shot Peened Steel, Residual Stresses in Science and Technology, Informationsgesellschaft, DGM, Verlag (1987) pp.441
- [112] Gray H., Wagner L. and Lütjering G., Influence of Residual Stresses on Fatigue Crack Propagation of Small Surface Cracks, Residual stresses in Science and Technology, DGM, Verlag (1987) pp.815

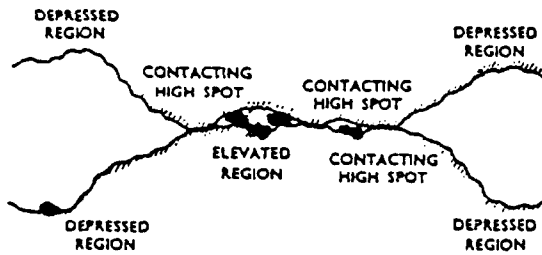
- [113] Labedz J., Experimental Research on the Influence of Uniaxial Residual Stresses on Contact Fatigue Strength, will be published on the Advances in Surface Treatment vol. 6, Pergamon, Oxford (1988)
- [114] Waterhouse R.B., Fretting Corrosion, Pergamon Press, Oxford, (1972) p.242
- [115] Kaneta M., Murakami Y. and Okazaki T., Growth Mechanism of Subsurface Crack due to Hertzian Contact, J. of Tribology, ASME, vol. 108, January 1986, pp.134
- [116] Broszeit E., Heß F.J. and Kloos K.H., Werkstoffanstrengung bei oszillierender Gleitbewegung, Z. Werkstofftech., 8 (1977) pp.425
- [117] Edwards P.R., The Application of Fracture Mechanics to Predicting Fretting Fatigue, Fretting fatigue edited by Waterhouse R.B., Applied Science Publishers, London (1981) p.67
- [118] Rooke D.P. and Jones D.A., Stress Intensity Factors in Fretting Fatigue, J. Strain Analysis, 14, 1 (1979) pp.1
- [119] Hamilton G.M., Explicit Equations for the Stresses beneath a Sliding Spherical Contact, Proc. of IMechE series C, 197 (1983) pp.53
- [120] Johnson K.L., Contact Mechanics, Cambridge University Press, Cambridge, p. 219, (Eq. 7.41a)
- [121] Goto S. and Waterhouse R.B., Fretting and Fretting Fatigue of Titanium Alloys under

Conditions of High Normal Load, Proc. of the 4th  
Intnatl. conf. on Titanium Titanium '80 Science  
and Technology vol. 3, pp.1837

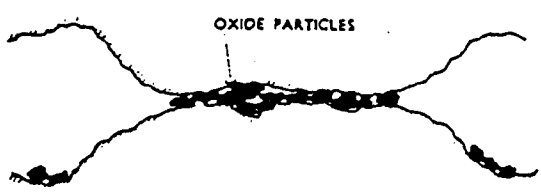
[122] Waterhouse R.B., Fretting Corrosion,  
Pergamon Press, Oxford, (1972) p.122

[123] Fair G.H., Effect of Shot-Peening on Fatigue  
and Fretting Fatigue of Aluminium Alloys, Ph.D  
thesis (1988), University of Nottingham

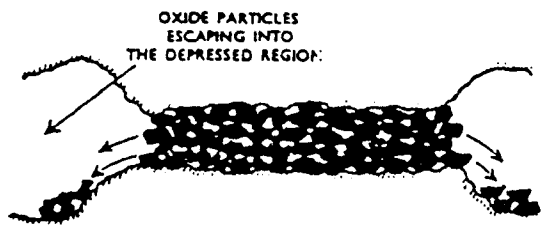
[124] Mutch Y., Fair G.H., Noble B. and Waterhouse  
R.B., The Effect of Residual Stresses induced by  
Shot-Peening on Fatigue Crack Propagation in Two  
High Strength Aluminium Alloys, Fatigue Fract.  
Engng Mater. Struct., 10, 4 (1987) pp.261



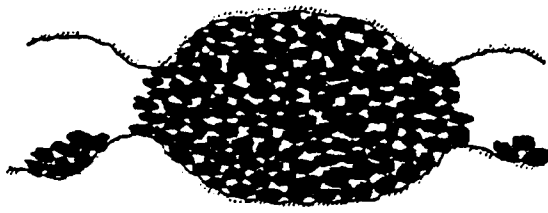
a Accumulation of trapped particles in the space among the high spots.



b Integration of a company of contacting areas into a united area.



c Spilling of particles into the adjoining depressed regions.



d Curved shape of the large pit as the result of stronger abrasive action acting in the central region.

Fig. 2-1 *Sketches Illustrating the Initiation of Fretting and the Formation of Large and Deep Pits*

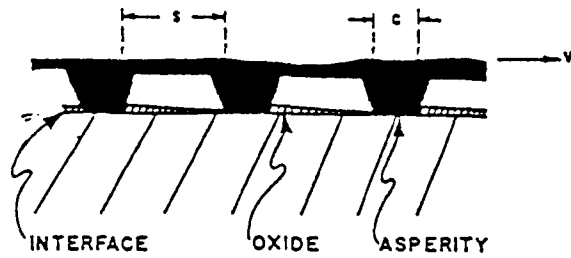


Fig. 2-2 IDEALIZED MODEL OF FRETTING AT A METALLIC SURFACE  
(Asperities of upper surface move over plane under surface.)

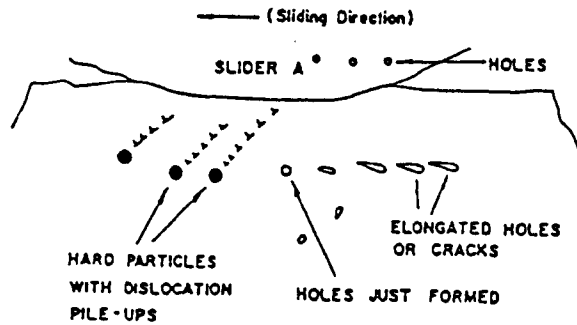
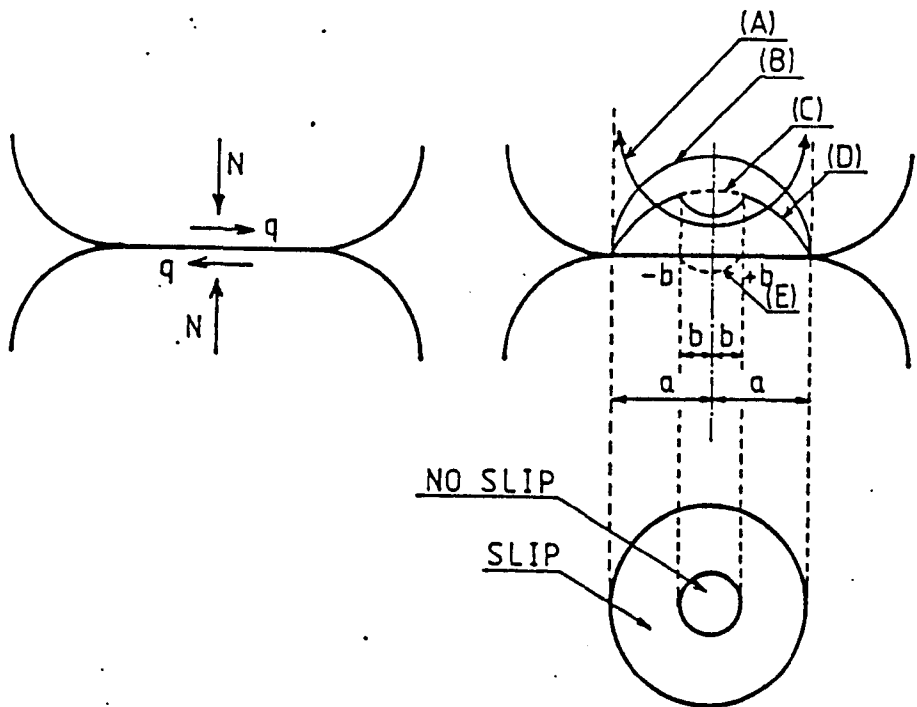


Fig. 2-3 The process of wear particle formation by the shear deformation of voids.



- (A) tangential force
- (B) Hertzian contact stress
- (C) frictional force ( $q' = \mu P$ ) ( $+b \rightarrow -b$ )
- (D) tangential shear stress ( $q = q' + q''$ )
- (E) frictional force ( $q'' = -\frac{b}{a} \mu P$ ) ( $-b \rightarrow +b$ )

Fig. 2-4 The distributions of stresses during fretting according to the Mindlin's theory

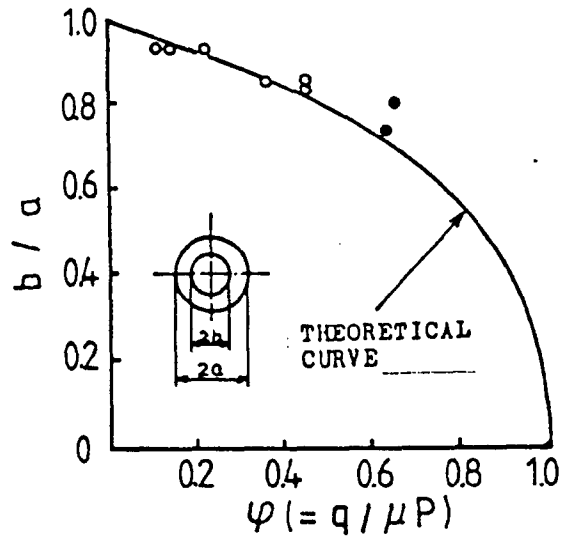


Fig. 2-5 The relationship between  $b/a$  and the tangential force coefficient in contact between a sphere and a flat plate

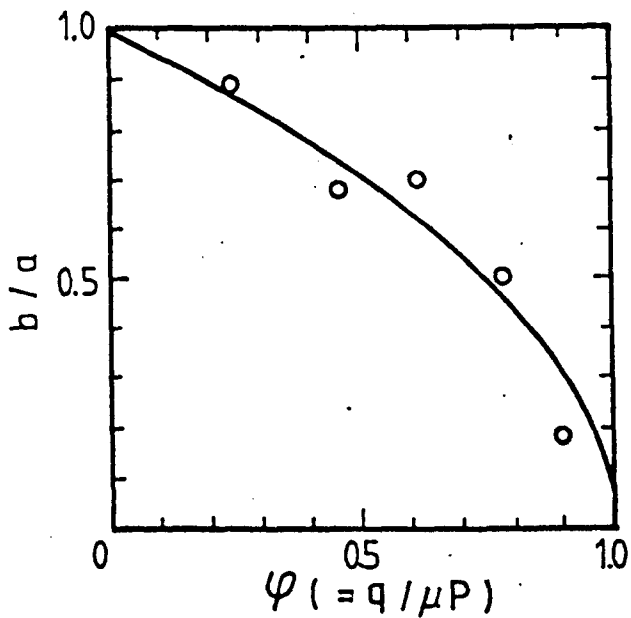


Fig. 2-6 The relationship between  $b/a$  and the tangential force coefficient in contact between a cylindrical shoe and a flat plate

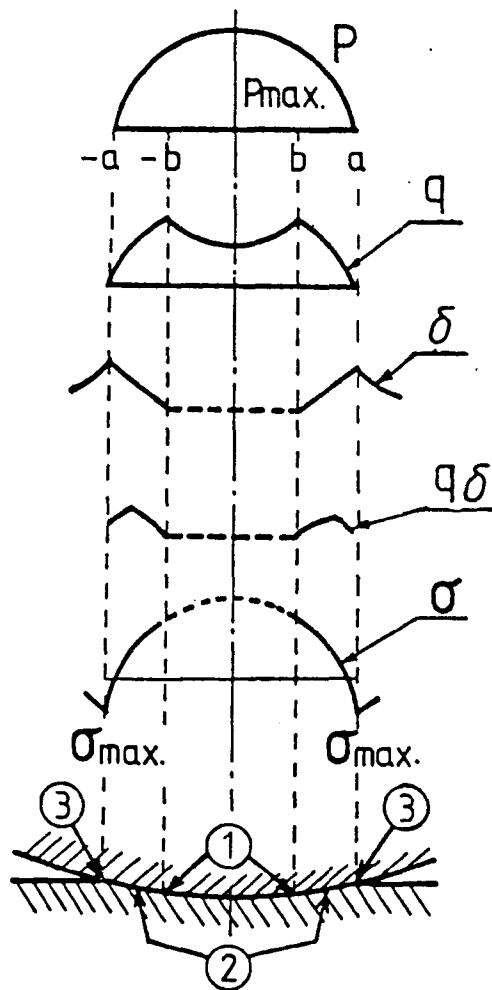


Fig. 2-7

The distributions of stresses and strains in contact surface

- $P$  : normal stress,                       $q$  : tangential stress
- $\delta$  : tangential strain,                       $\sigma$  : principal stress
- 1 : damage produced at the point of  $q_{max}$
- 2 : damage produced at the point of  $(q\delta)_{max}$
- 3 : damage produced at the point of  $\sigma_{max}$

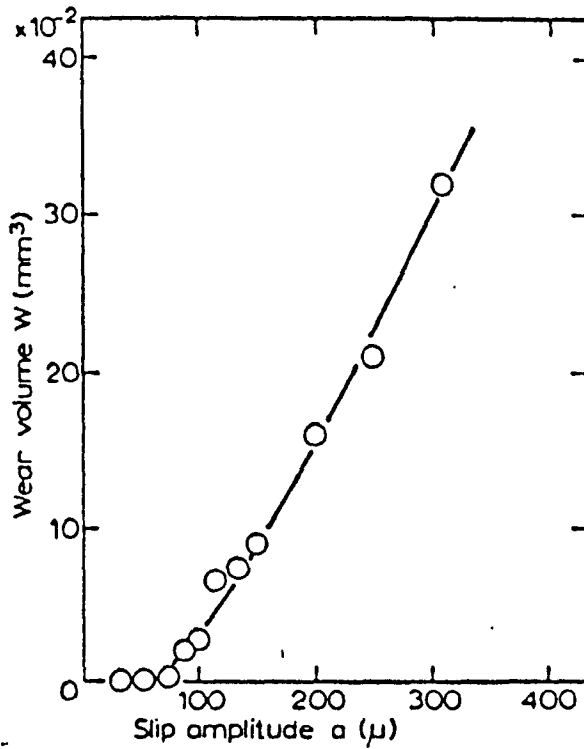


Fig. 2-8 Wear volume against slip amplitude after 100,000 cycles.

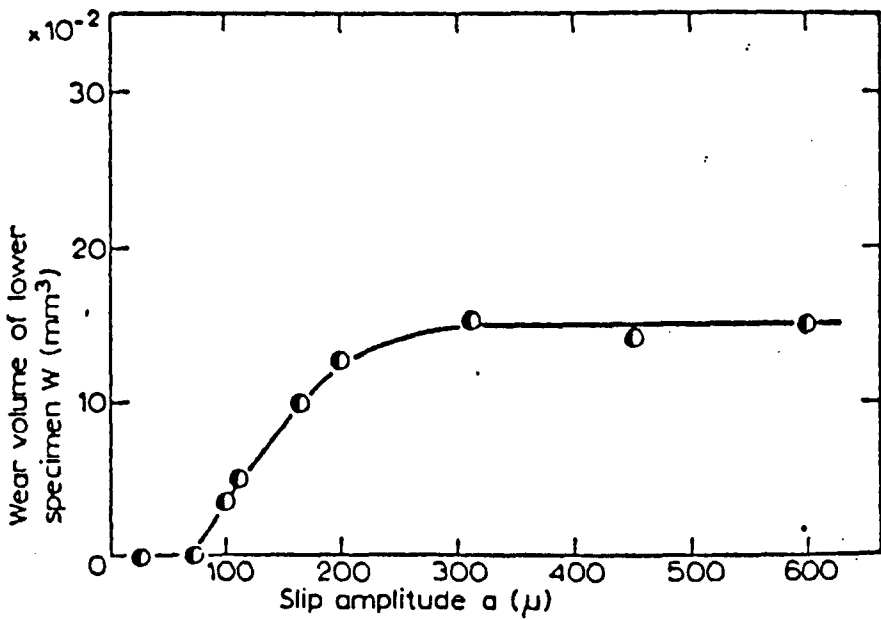


Fig. 2-9 Wear volume of lower specimen against slip amplitude at a sliding distance of 36 m.

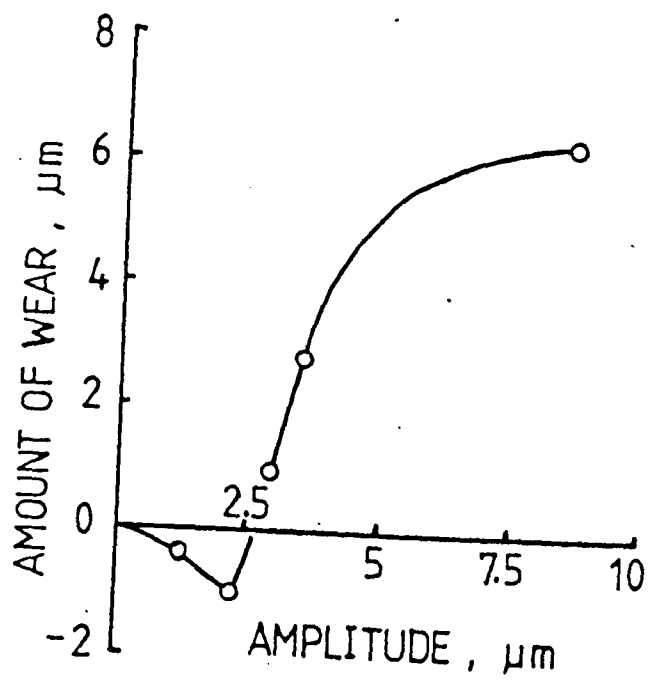


Fig. 2-10 The effect of amplitude on fretting wear (after  $5 \times 10^4$  cycles)

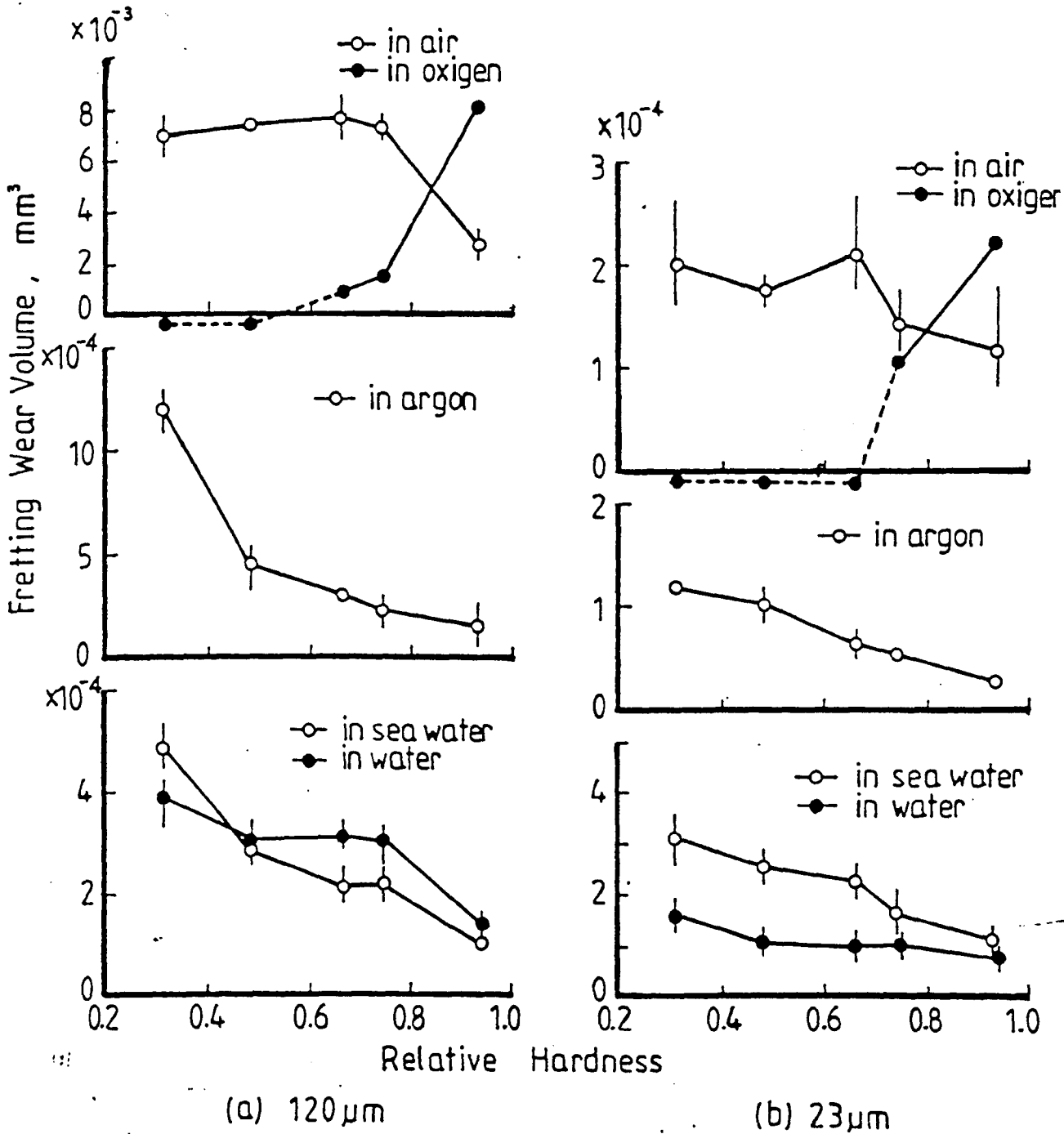


Fig. 2-11 The effects of hardness on fretting wear (wear volume of the flat plate specimens)

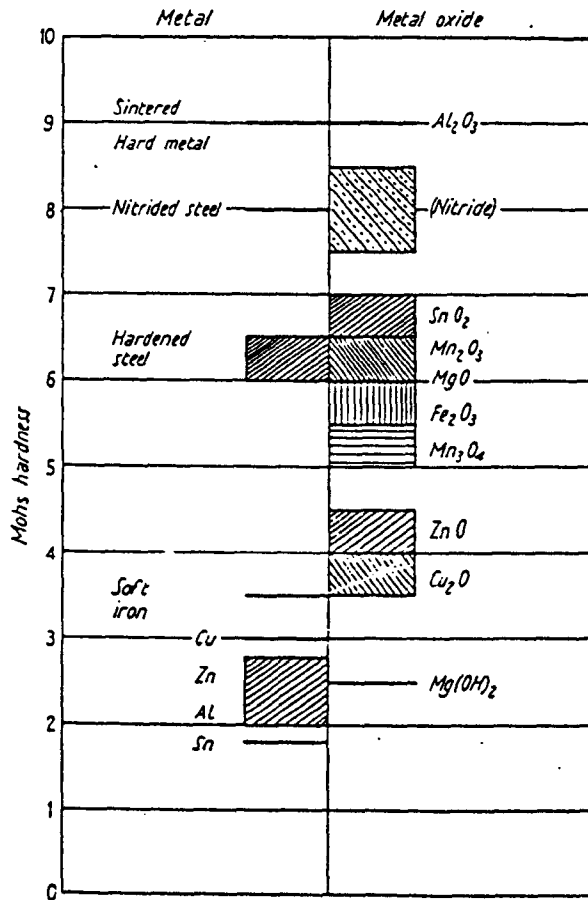
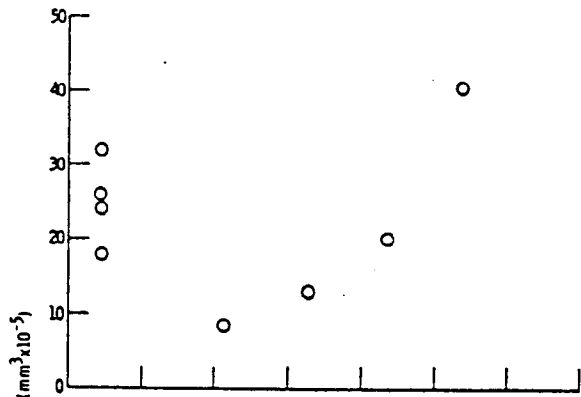
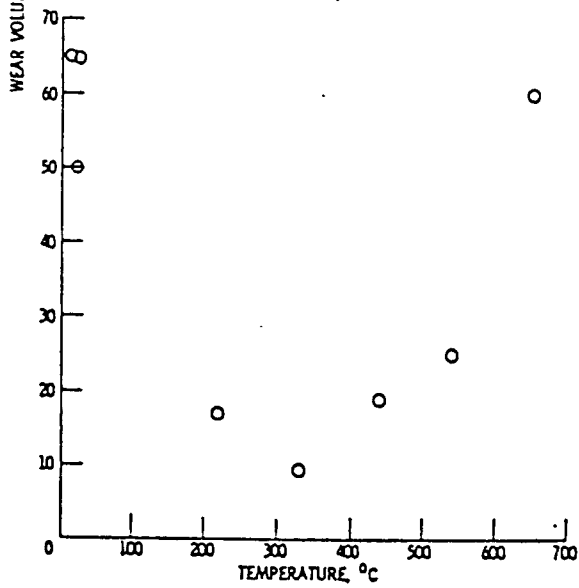


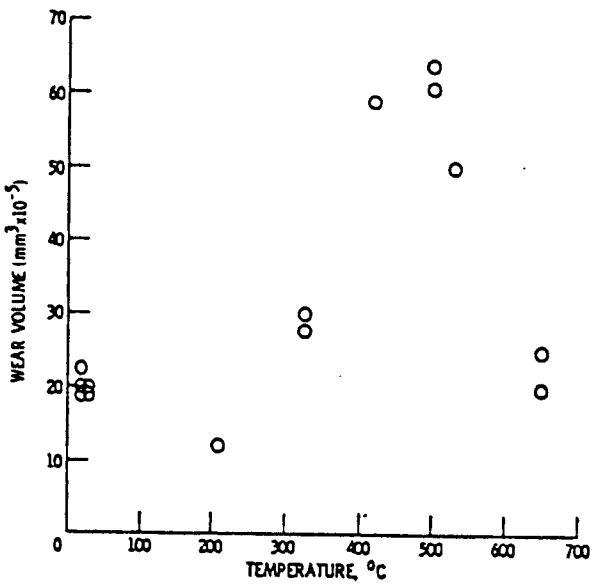
Fig. 2-12 Mohs hardness scale of metals and metal oxides (from Dies's paper). Under conditions favouring surface oxidation the wear of sliding metals may be determined primarily by the hardness of the corresponding metal oxide. Thus a soft metal such as tin may produce heavier wear of a hard chromium steel than a hard steel slider rubbing on the same chromium steel.



(a) IRON.



(b) NICKEL.



(c) TITANIUM.

Fig. 2-13 - Fretting wear volume as a function of temperature for high purity iron, nickel, and titanium, after  $3 \times 10^5$  fretting cycles in dry air.

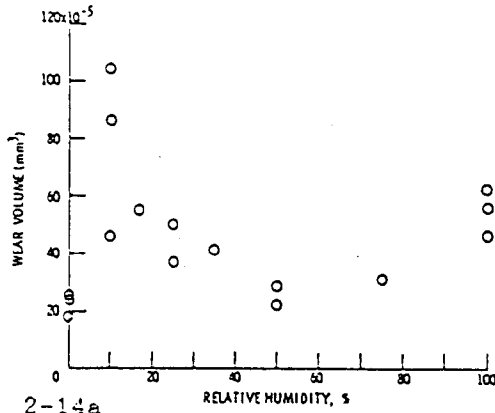


Fig. 2-14a - Fretting wear volume as a function of relative humidity for 99.95 iron.

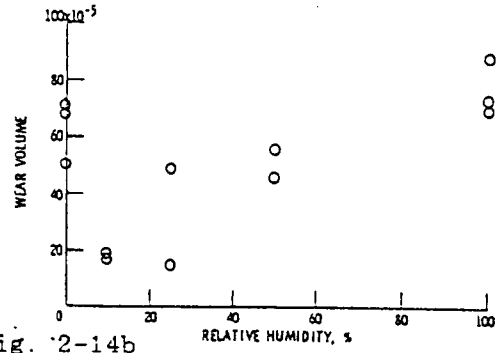


Fig. 2-14b - Fretting wear volume as a function of relative humidity for high purity nickel.

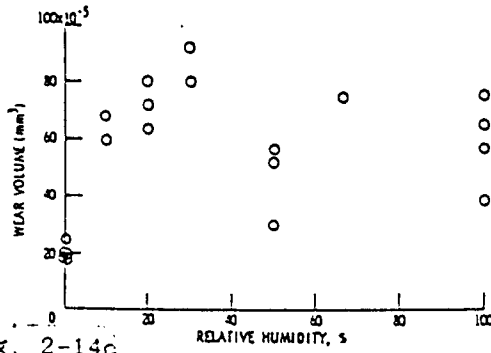


Fig. 2-14c - Fretting wear volume as a function of relative humidity for 99.95 titanium.

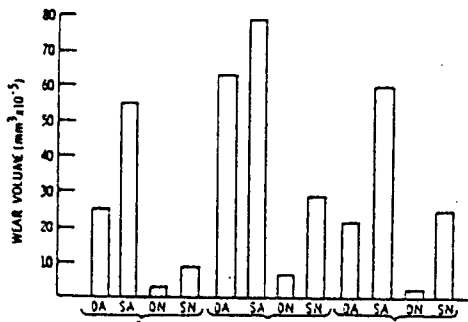


Fig. 2-14d - Fretting wear volume for high purity Fe, Ni, and Ti after  $3 \times 10^5$  fretting cycles in dry air (DA), saturated air (SA), dry nitrogen (DN), and saturated nitrogen (SN).

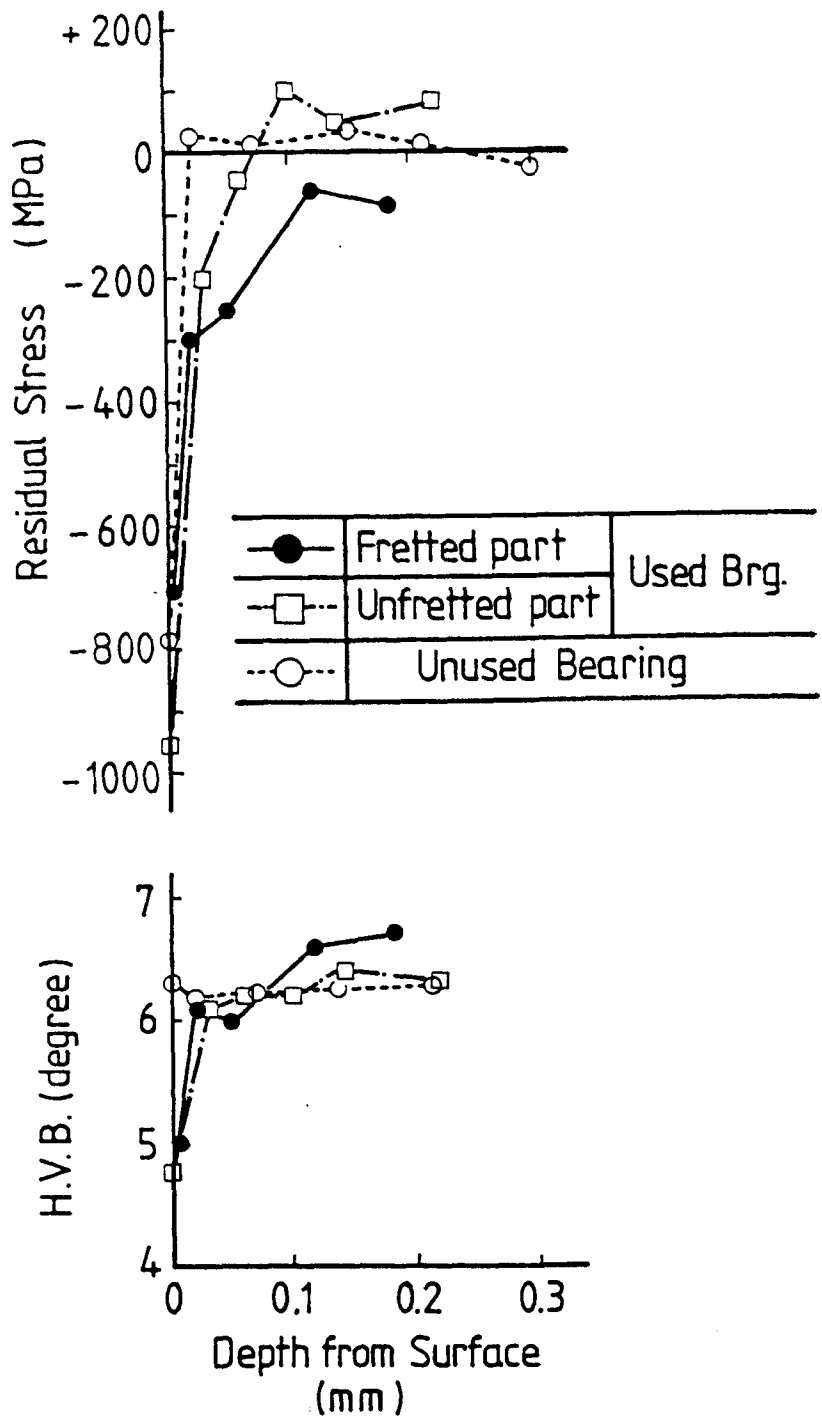
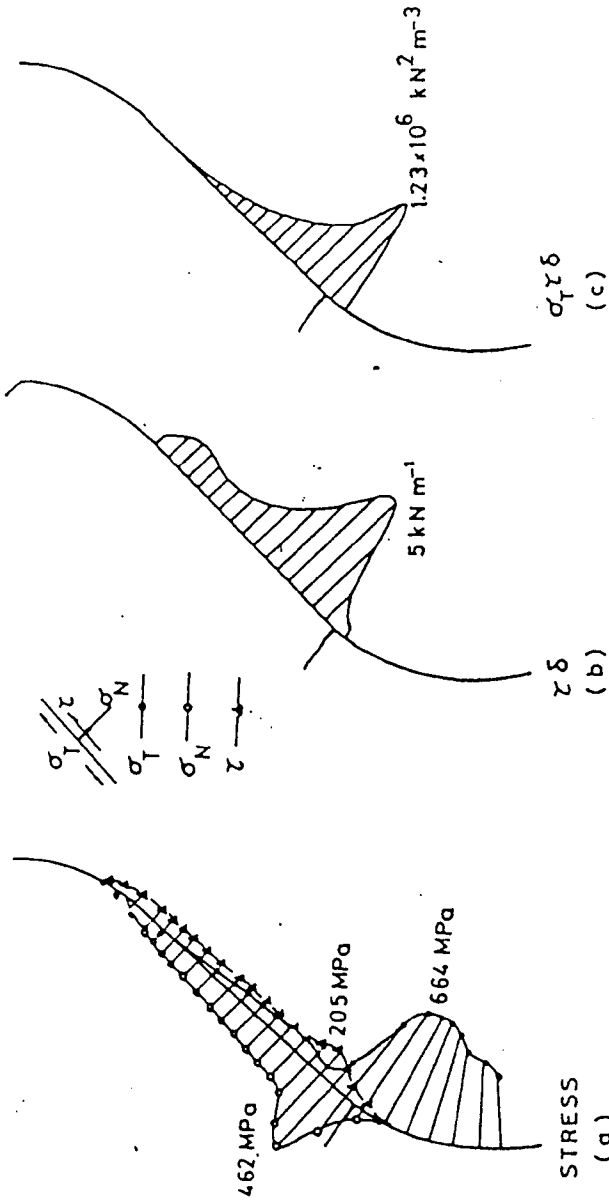
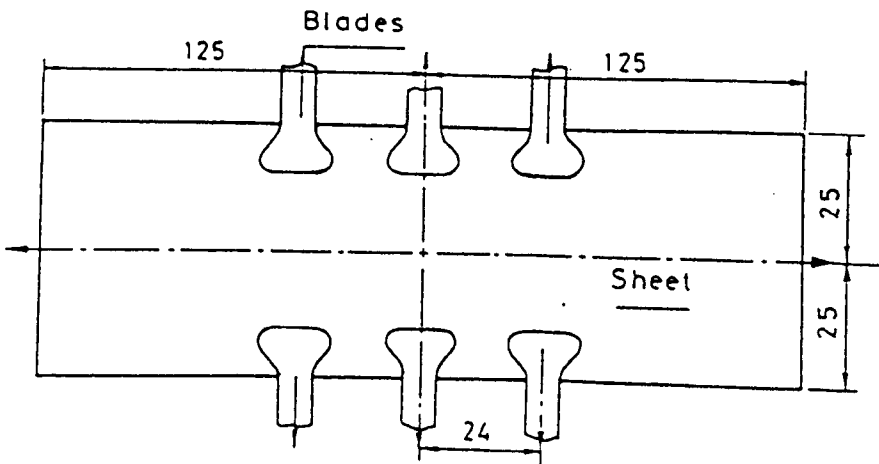


Fig. 2-15 Distributions of the residual stresses and the half value breadths of rolling bearings (by X-ray diffraction)



Dovetail joint at room temperature under 40 kN biaxial load ( $R=1$ )  
 (a) stresses  
 (b) fretting damage parameter  
 (c) combined fatigue/fretting damage parameter

Fig. 2-16 Test specimen used by Ruiz et al (left) and distributions of stresses and parameters

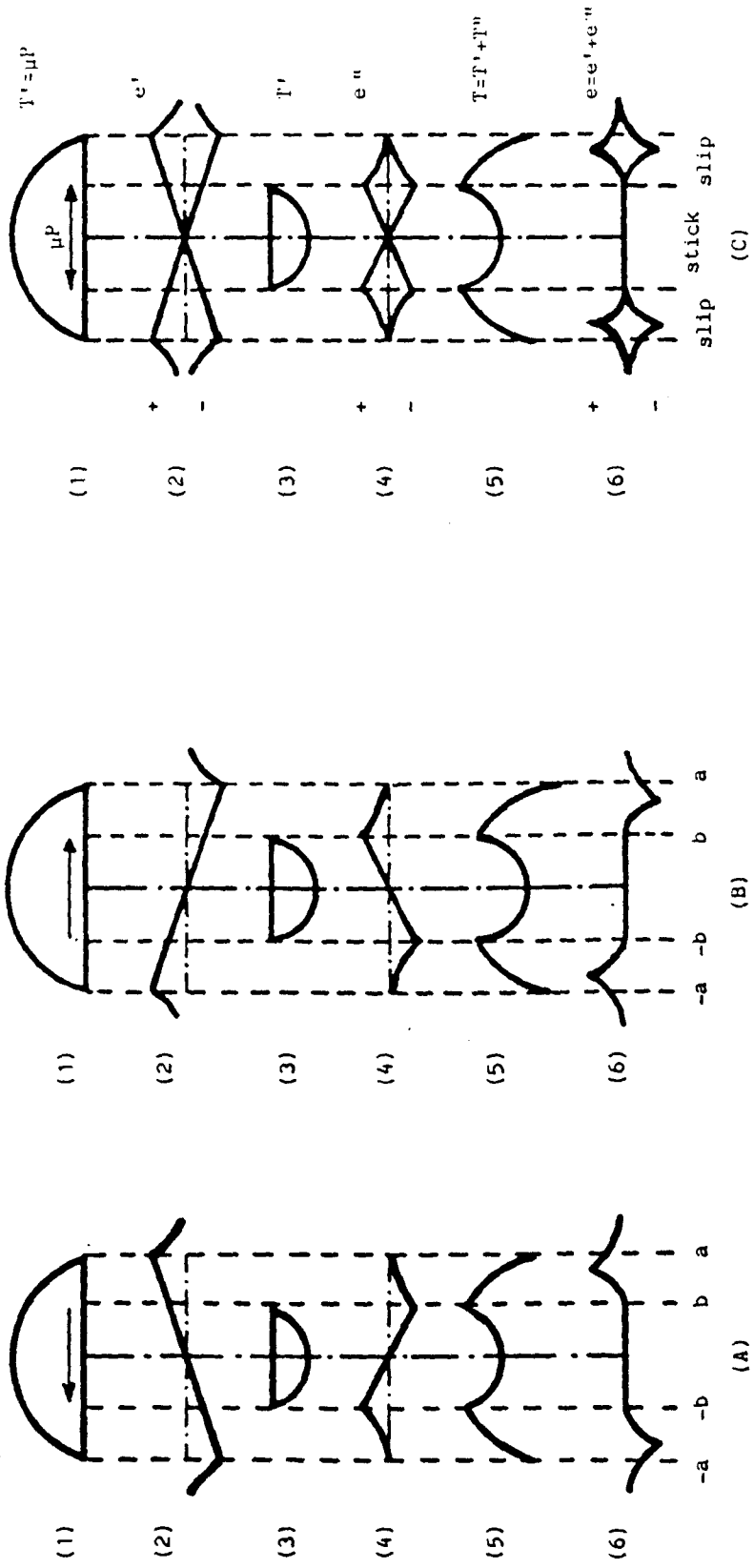
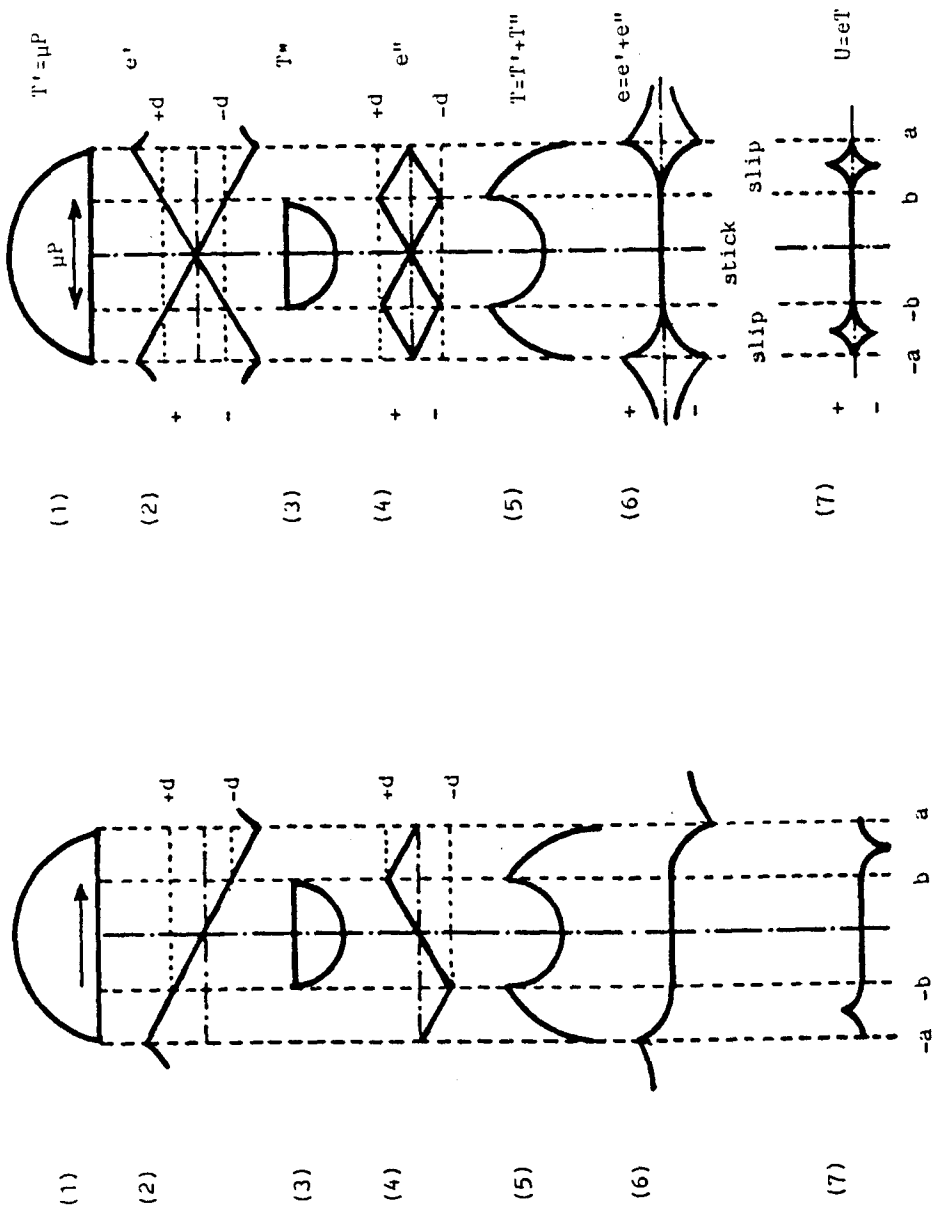


Fig. 2-17 The distributions of the stresses and strains during fretting oscillation



(A)

(B)

Fig. 2-18 The distributions of the stresses, the strains and the tangential shear strain energy

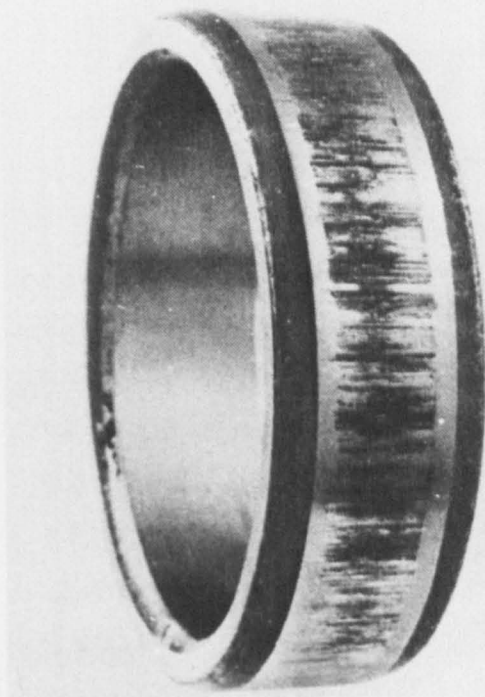
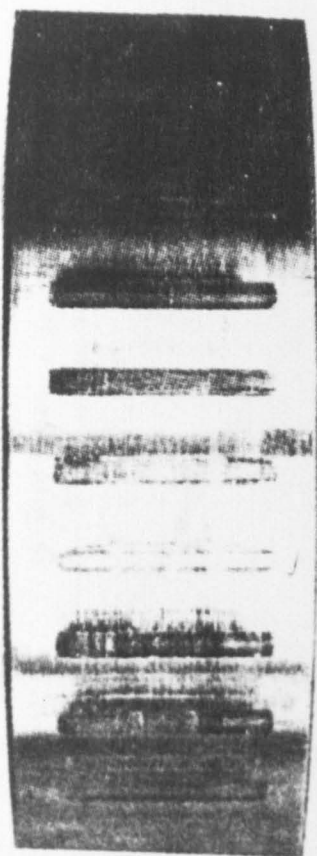


Fig. 2-20 Examples of fretting wear on roller bearings

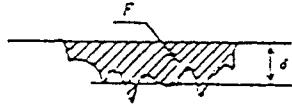


Fig. 2-21a Record of damage

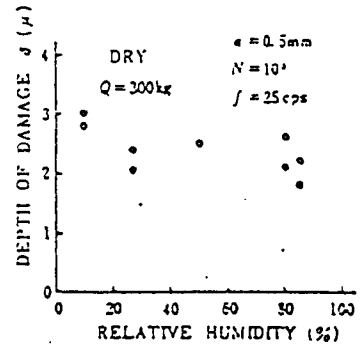


Fig. 2-21b Influence of humidity

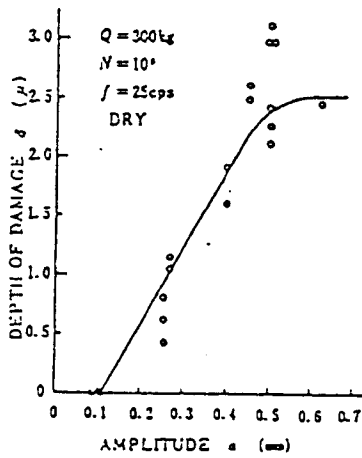


Fig. 2-21c Influence of amplitude

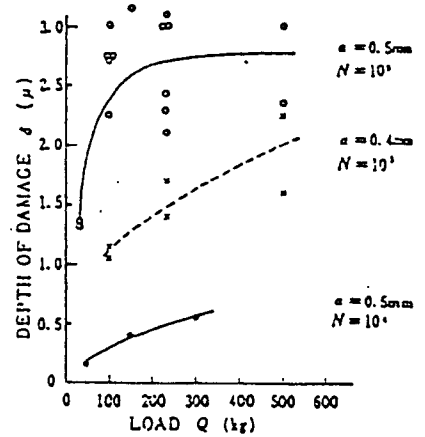


Fig. 2-21d Influence of load (DRY)

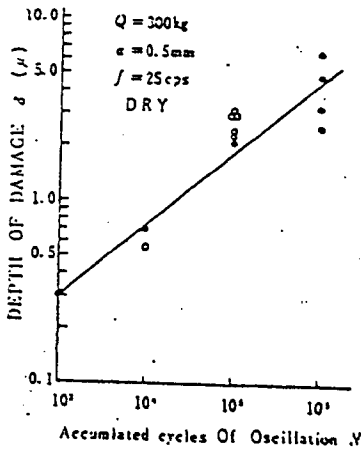


Fig. 2-21e Influence of accumulated cycles of oscillation

Table 3-1 Chemical Composition of the Steels and Titanium Alloy (wt.%)

MATERIALS	C	Si	Mn	P	S	Cr	Ni	Mo
0.64%C Steel	0.64	0.19	0.63	0.019	0.017	-	-	-
1.5%Mn Steel	0.18-0.25	<0.60	1.20-1.60	<0.050	<0.050	-	-	-
316 Stainless Steel	<0.080	<1.00	<2.00	-	-	16.0-18.0	10.0-14.0	2.00-3.00
JIS SUJ2 Steel	0.95-1.10	0.15-0.35	<0.50	<0.025	<0.025	1.30-1.60	-	-

MATERIAL	Ti	Al	V	Fe	O	H	C	N
Ti-6Al-4V	Bal.	6.35	4.24	0.08	0.17	0.003	0.012	0.006

Table 3-2 Mechanical Properties of the Materials Used

MATERIALS	CRYSTAL STRUCTURE	E (GN/m <sup>2</sup> )	VIHN	UTS (MN/m <sup>2</sup> )	PS (YS) (MN/m <sup>2</sup> )	ε (%)
99.5% Al <sub>2</sub> O <sub>3</sub>	HCP	366	-	5000	5000	-
WC-6%Co	HCP	530	-	6000	6000	-
Pure Fe	BCC	196	104	334	254	45
Pure Al	FCC	69	17.0	77.5	43.0	50
Pure Cu	FCC	124	102	358	342	22
Pure Zn	HCP	94	32.6	280	200	-
Ti-6Al-4V	HCP/BCC	105	415	1336	1273	12
0.64%C steel	BCC	180	412	1300	900	-
1.5%Mn steel	BCC	200	253	780	600	-
316 stainless steel	FCC	200	189	640	600	42
JIS SUJ2 steel	BCT	220	730	-	-	-

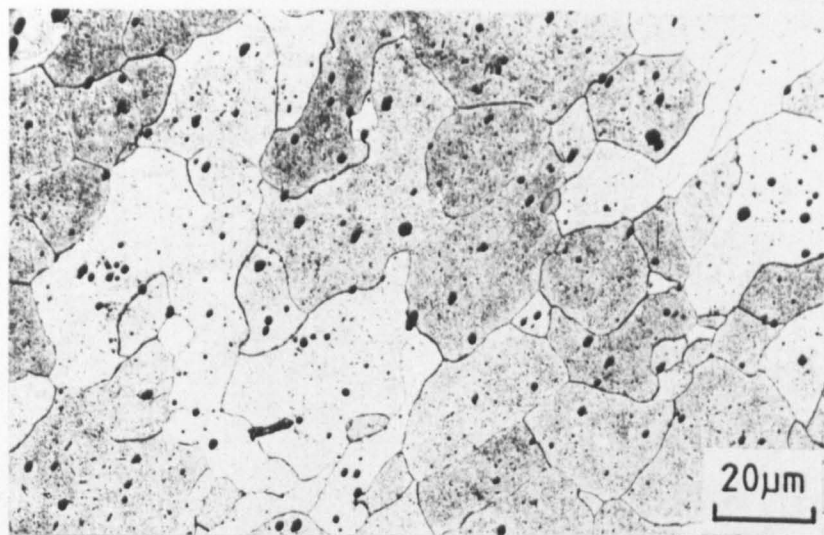


Fig. 3-1a Microstructure of the pure Fe used

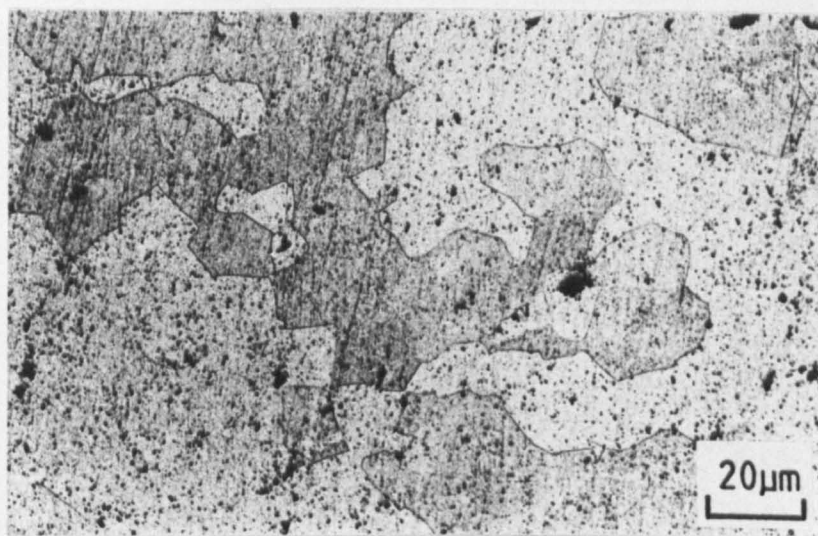


Fig. 3-1b Microstructure of the pure Al used

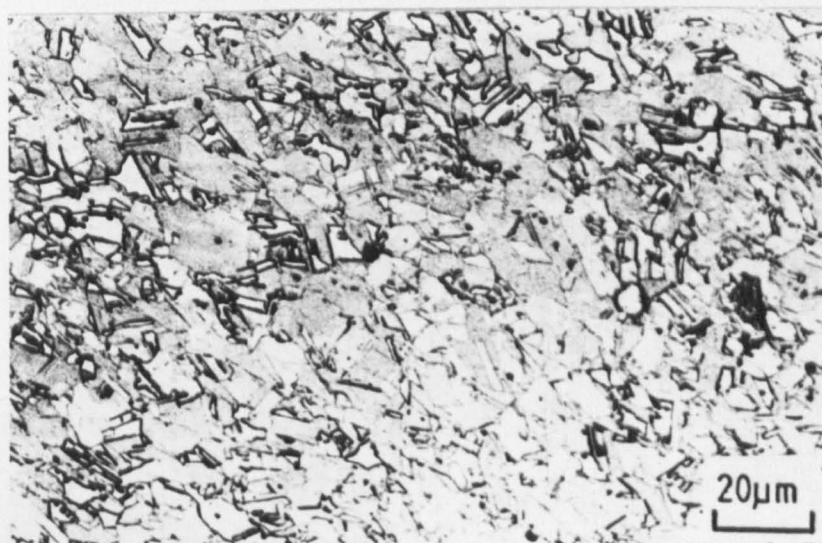


Fig. 3-1c Microstructure of the pure Cu used



Fig. 3-1d Microstructure of the pure Zn used

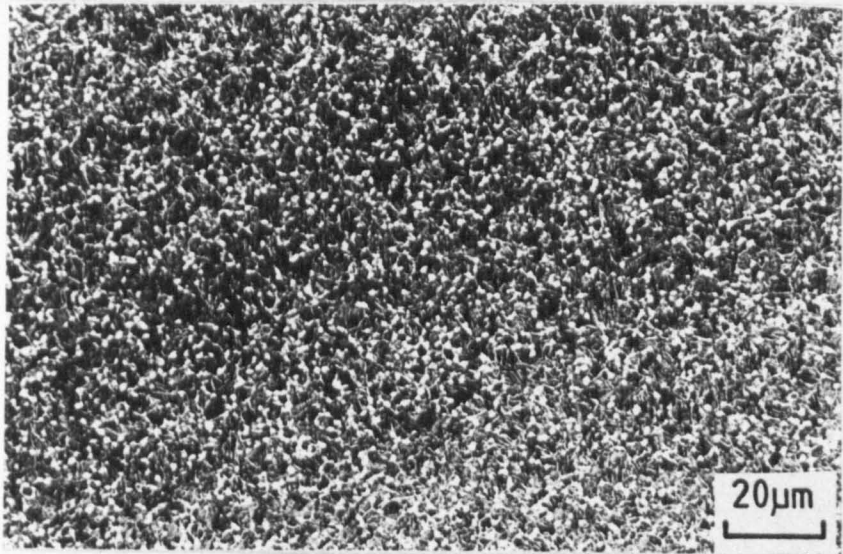


Fig. 3-1e Microstructure of the Ti 318 used

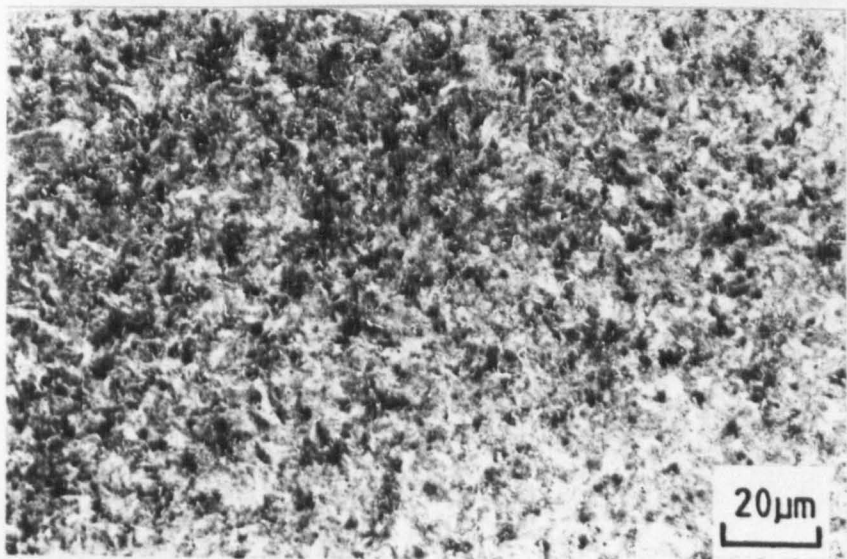


Fig. 3-1f Microstructure of the 0.64%C steel used

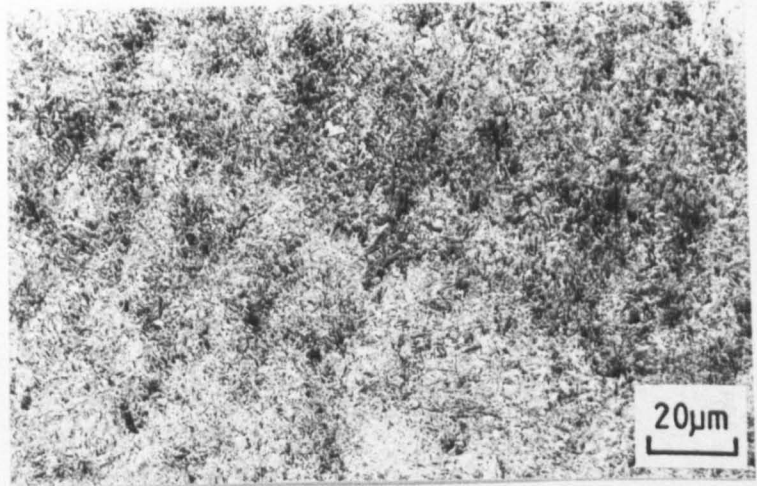


Fig. 3-1g Microstructure of the 1.5%Mn steel used

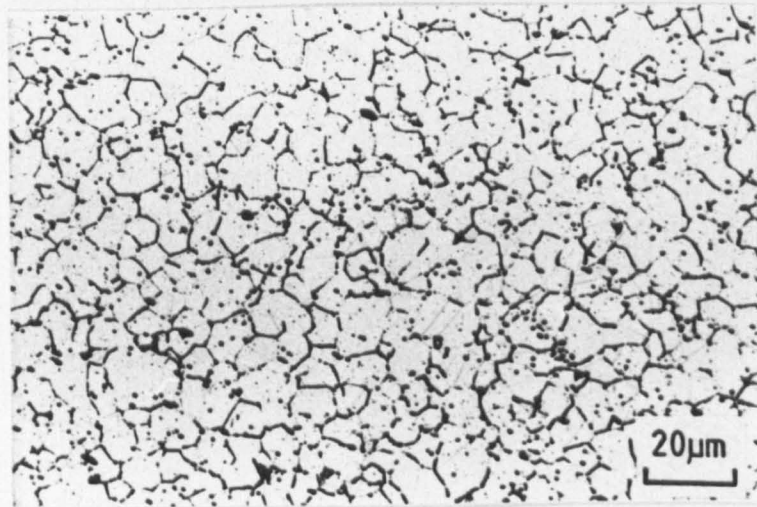


Fig. 3-1h Microstructure of the 316 stainless steel used

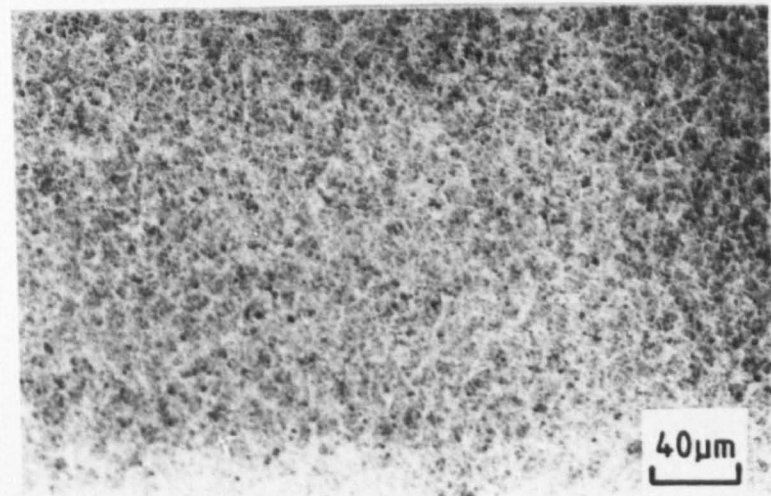


Fig. 3-1i Microstructure of the JIS SUJ2 steel used (TNO)

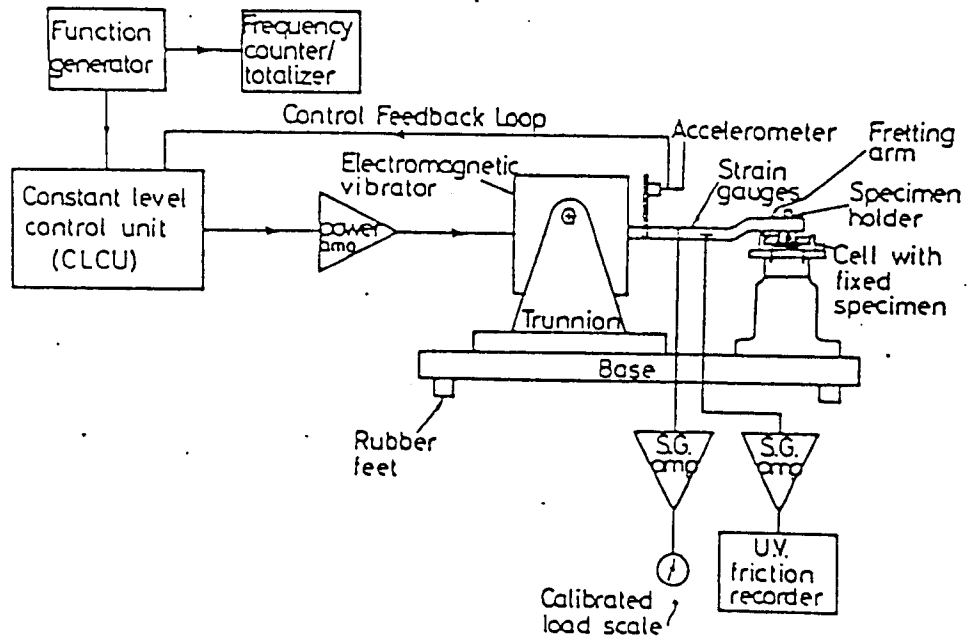


Fig. 3-2. Schematic diagram of electromagnetic fretting rig.

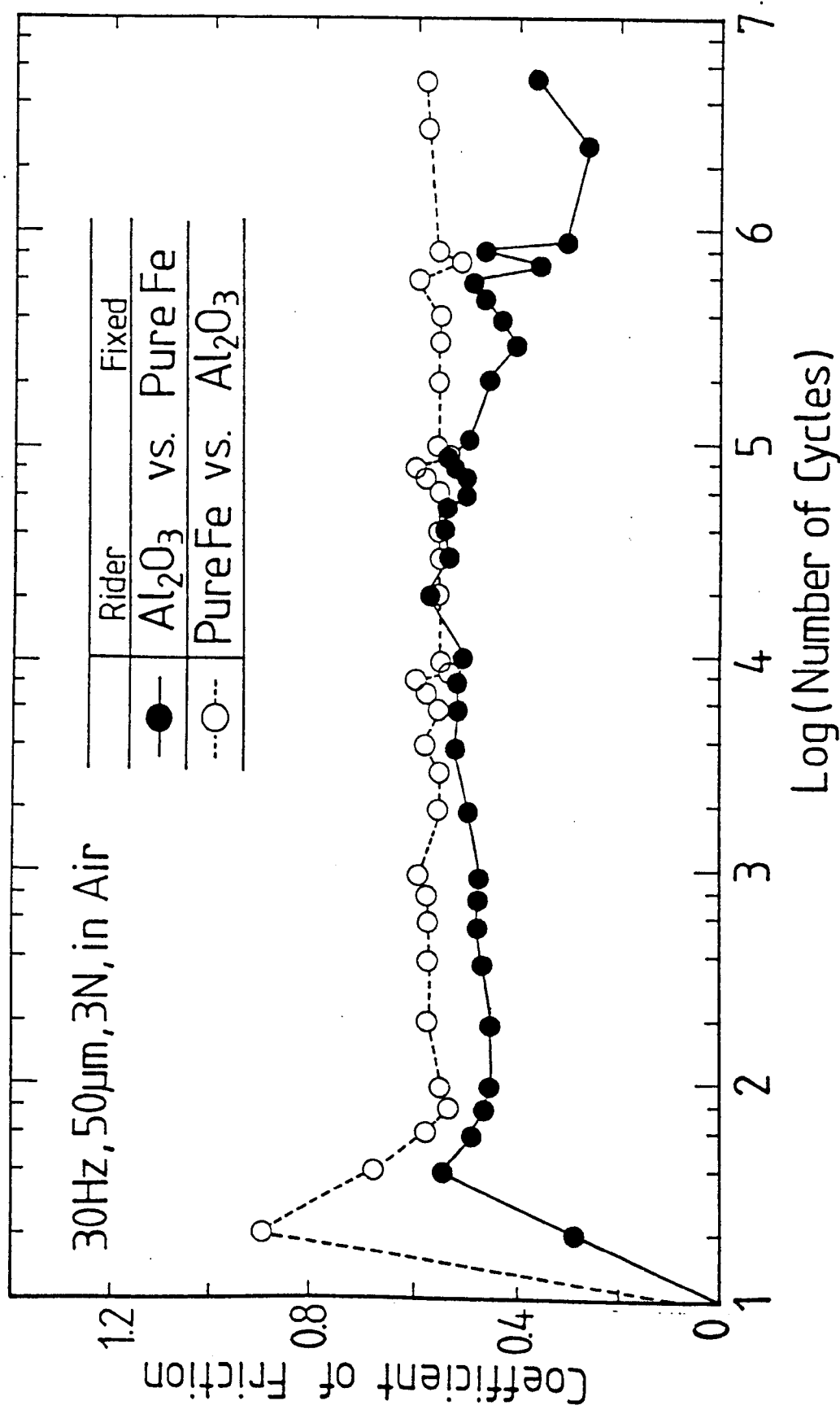


Fig. 3-3a Coefficient of friction vs. log(Number of cycles)

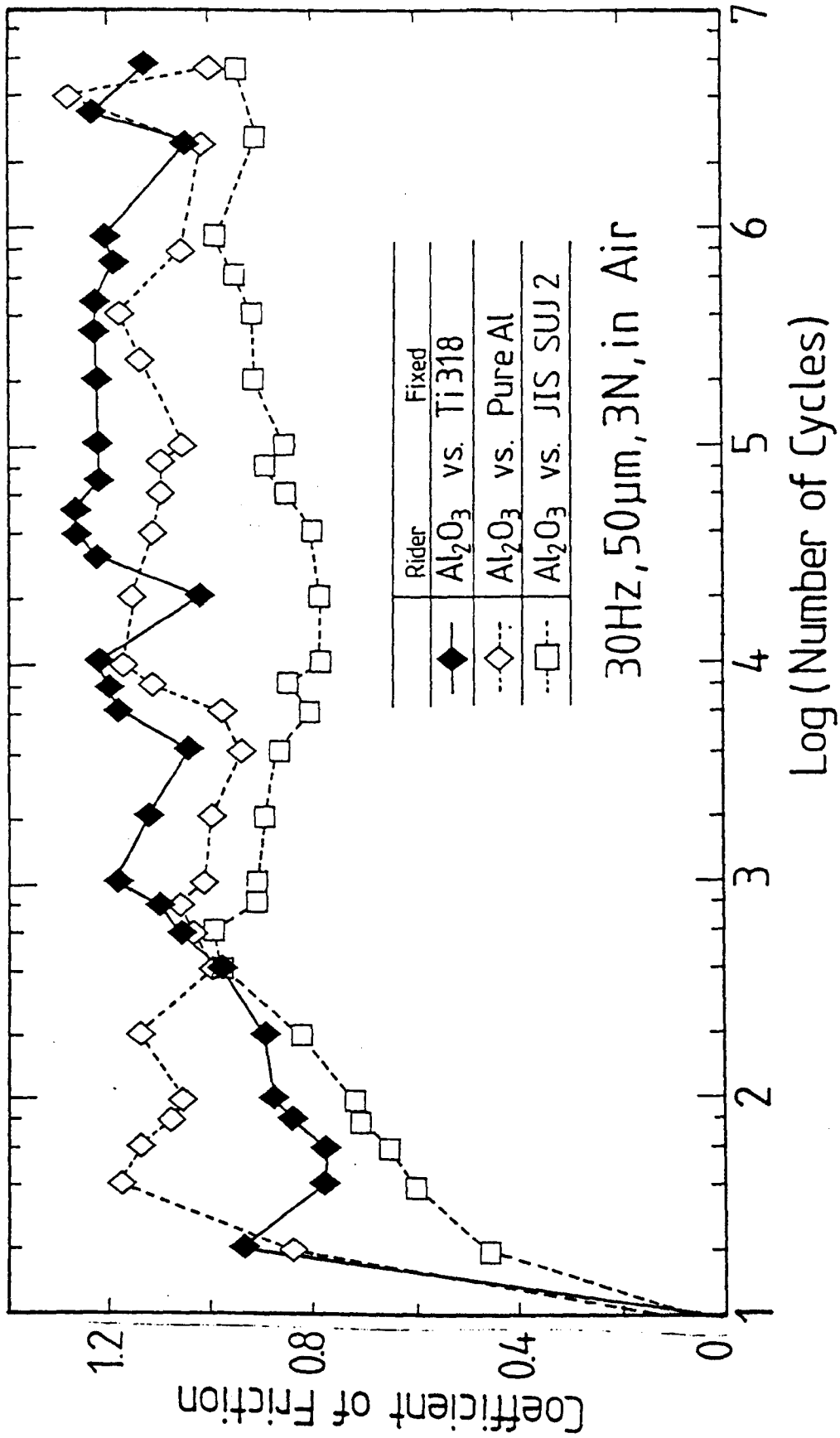
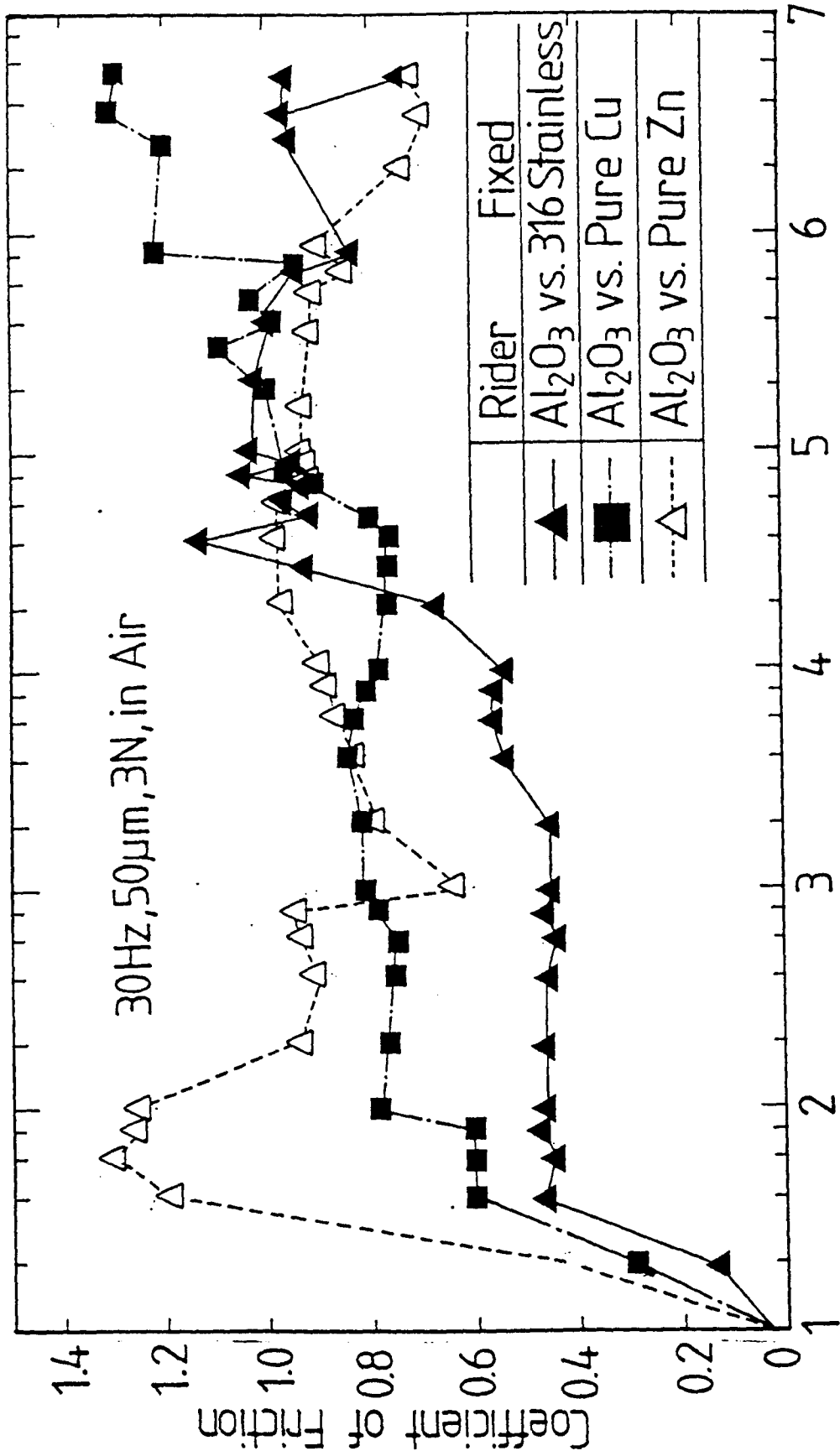


Fig. 3-3b Coefficient of friction vs. log(number of cycles)



Log(Number of Cycles)

Fig. 3-3c Coefficient of friction vs. log(number of cycles)

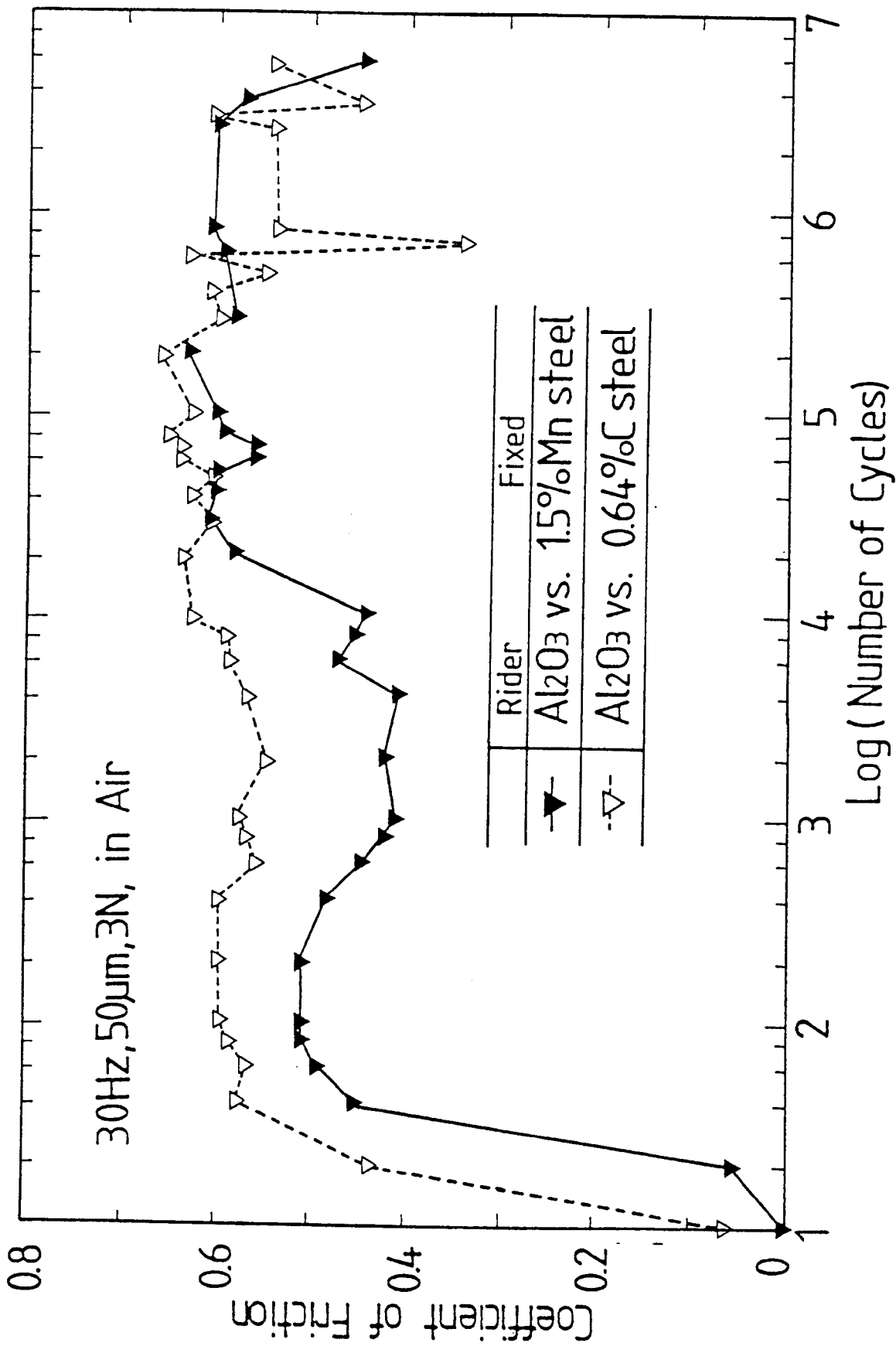


Fig. 3-3d Coefficient of friction vs. log(number of cycles)

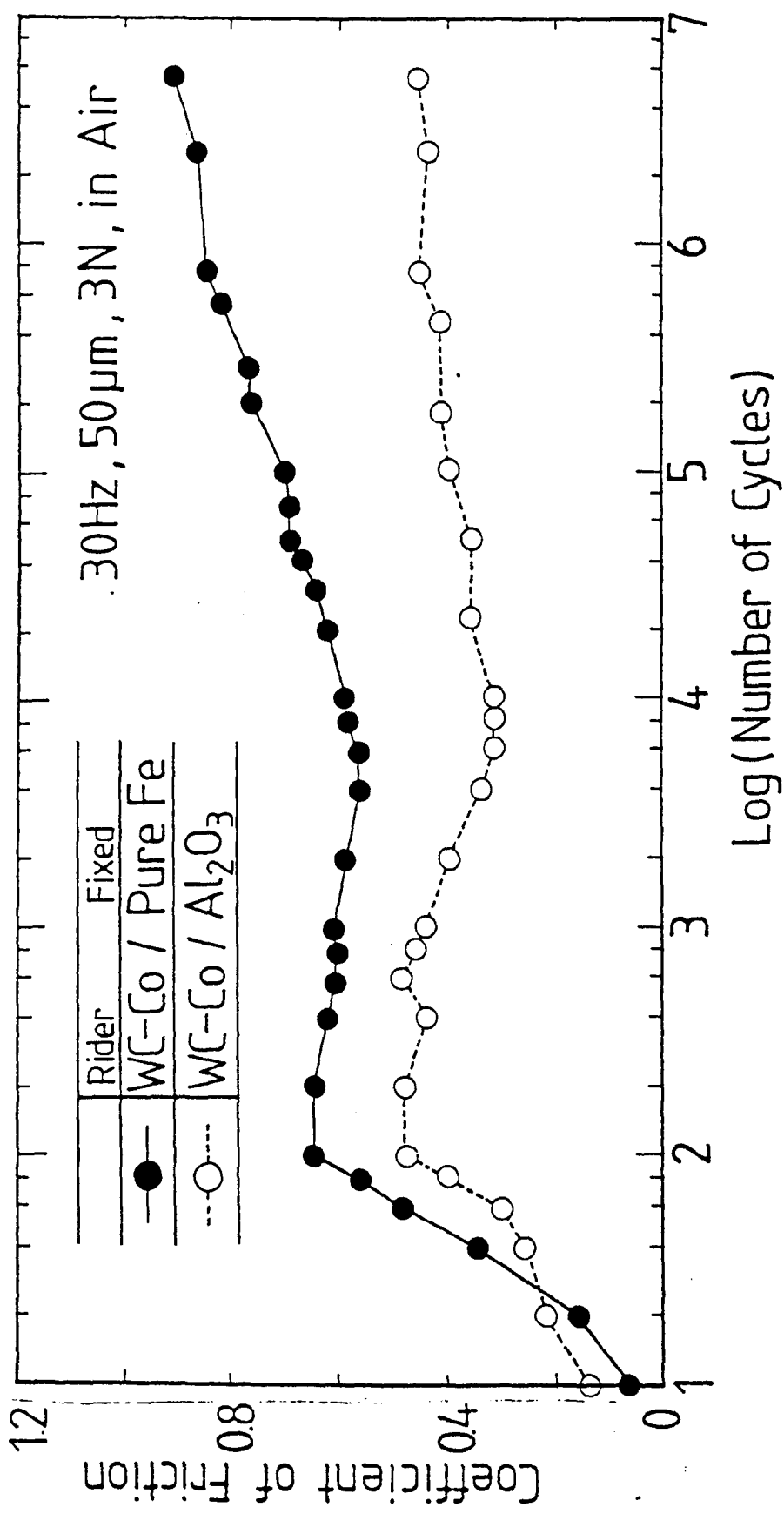


Fig. 3-3e Coefficient of friction vs. log(number of cycles)

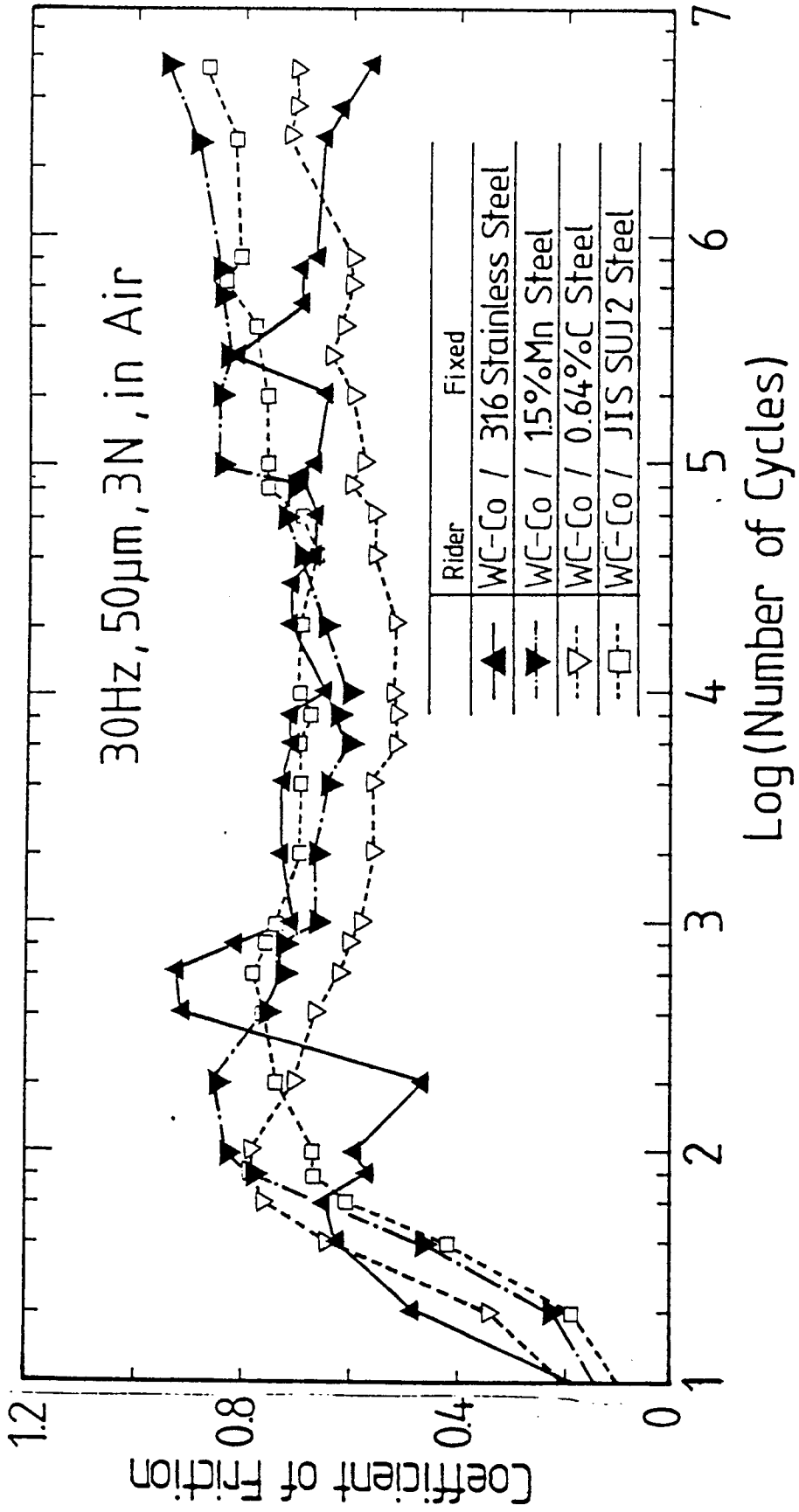


Fig. 3-3f Coefficient of friction vs. log(number of cycles)

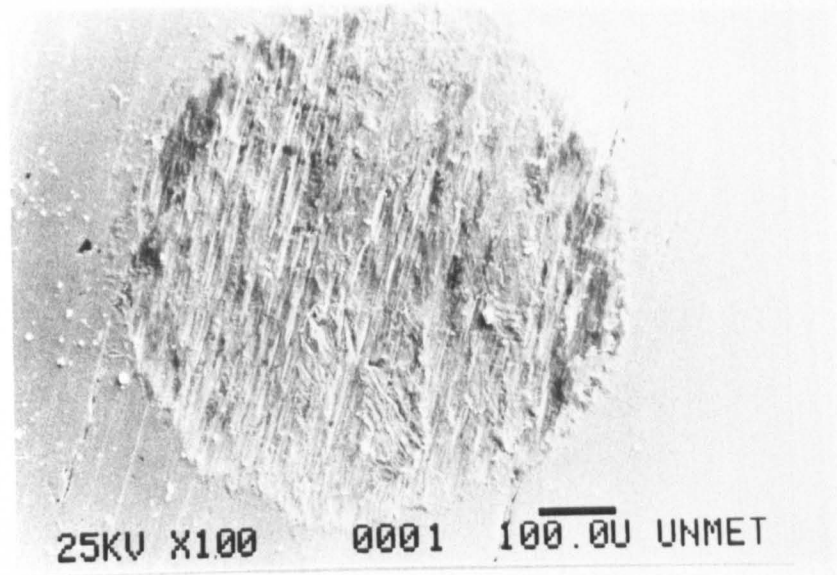


Fig. 3-4a The scar of the 0.64%C steel

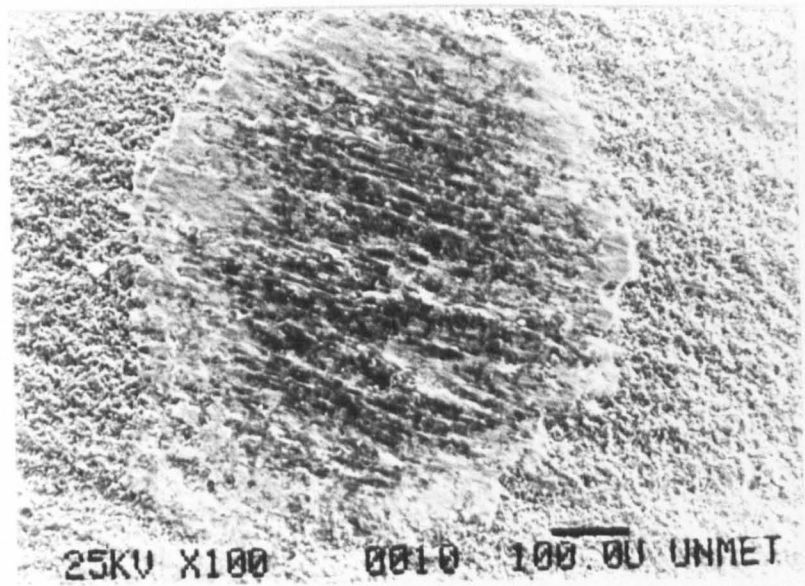


Fig. 3-4b The scar of the  $Al_2O_3$

Fig. 3-4 The scars of the  $Al_2O_3$  / 0.64%C steel couple

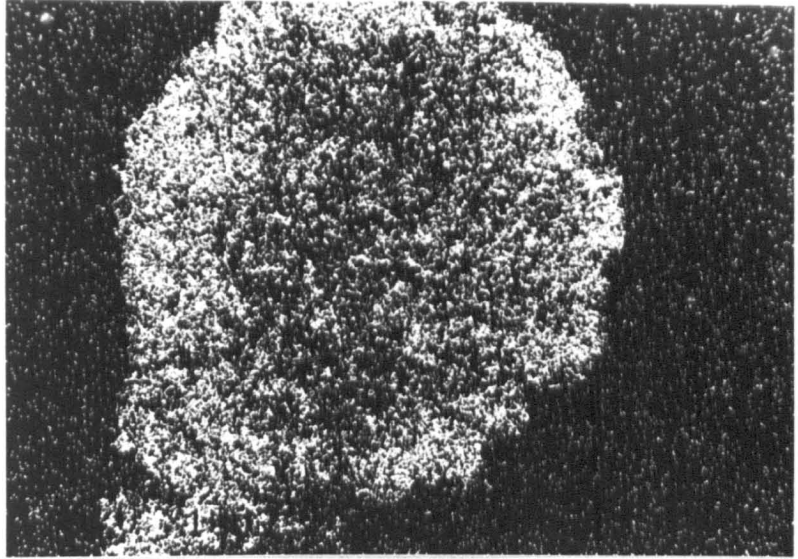


Fig. 3-4c The distribution of Fe on the scar of the  $\text{Al}_2\text{O}_3$

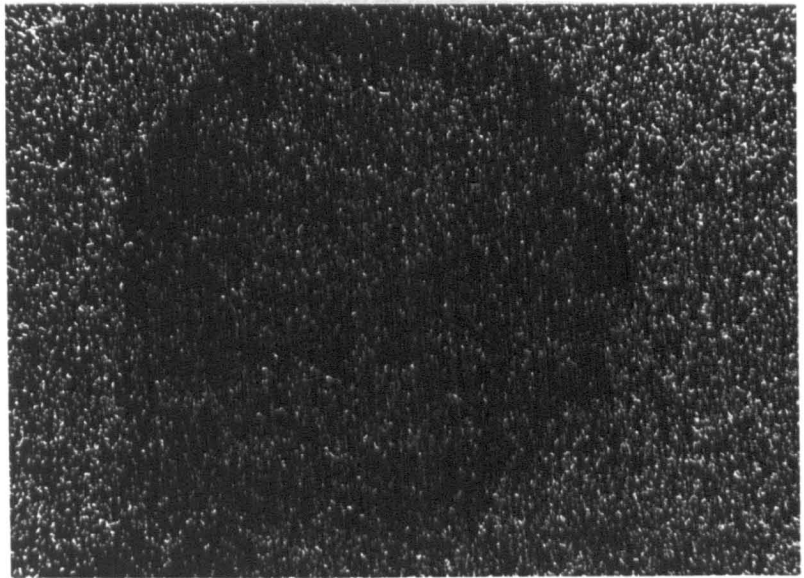


Fig. 3-4d The distribution of Al on the scar of the  $\text{Al}_2\text{O}_3$

Fig. 3-4 The scars of the  $\text{Al}_2\text{O}_3$  / 0.64%C steel couple

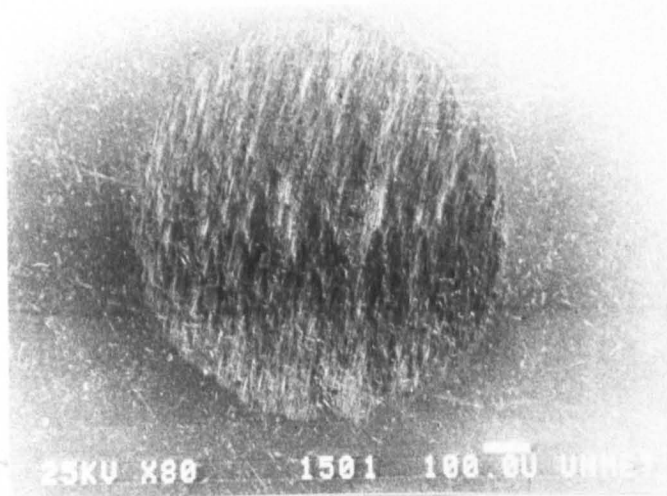


Fig. 3-5a The scar of the JIS SUJ2 steel

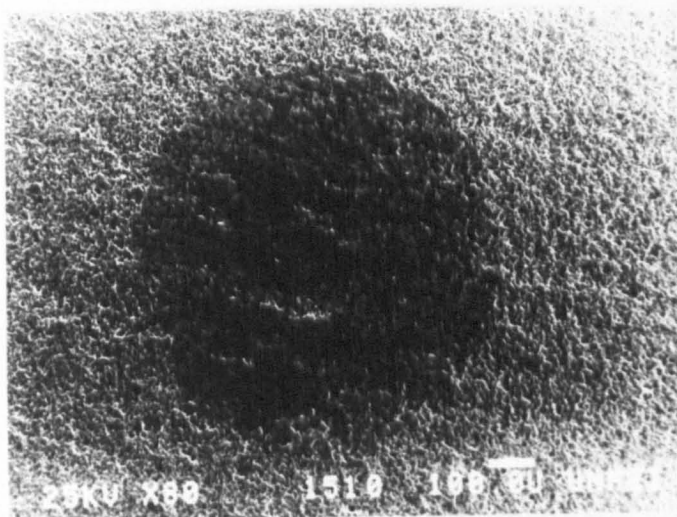


Fig. 3-5b The scar of the  $Al_2O_3$

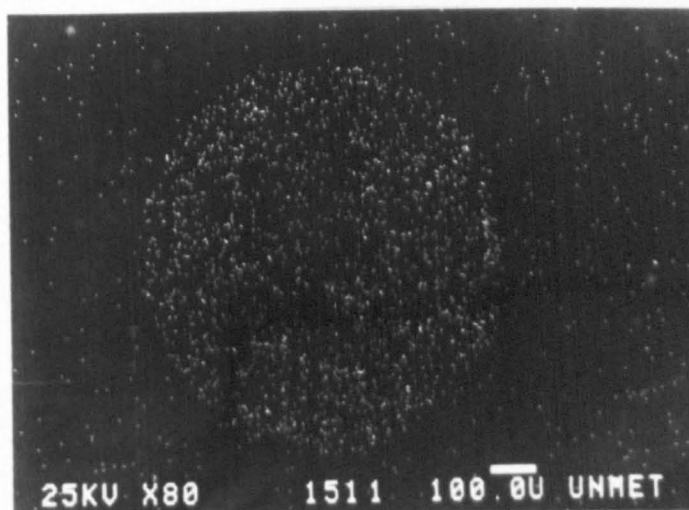


Fig. 3-5c The distribution of Fe on the scar of the  $Al_2O_3$

Fig. 3-5 The scars of the  $Al_2O_3$  / JIS SUJ2 steel couple

Table 3-3

The Values of Both the Volume of Scar and Hertzian Contact Stress (Pmax) in all the Couples

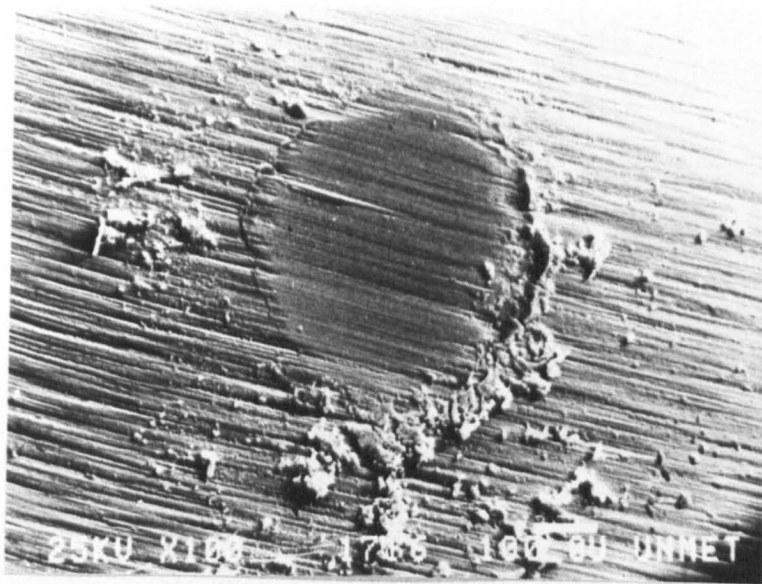
TEST NO.	MATERIALS		Pmax. (MN/m <sup>2</sup> )	VOLUME OF SCAR (x 10 <sup>-3</sup> mm <sup>3</sup> )
	UPPER	LOWER		
1	99.5% Al <sub>2</sub> O <sub>3</sub>	pure Fe	1224.3	1.77
2		pure Al	726.8	----*
3		pure Cu	990.5	6.92
4		pure Zn	859.7	----*
5		Ti 318	910.7	3.38
6		0.64%C steel	1179.6	2.87
7		1.5%Mn steel	1226.7	3.58
8		316 stainless steel	1226.7	6.08
9		JIS SUJ2 steel	1276.8	3.56
10		pure Fe	99.5% Al <sub>2</sub> O <sub>3</sub>	1224.3
11	WC-6%Co	pure Fe	1310.9	0.10
12		0.64%C steel	1257.7	0.06
13		1.5%Mn steel	1323.6	0.11
14		316 stainless steel	1323.6	0.21
15		JIS SUJ2 steel	1384.5	0.09
16		99.5% Al <sub>2</sub> O <sub>3</sub>	1697.6	----**

\*Scar depth greater than maximum measurable depth of profilometer.

\*\*Scar depth smaller than minimum measurable depth of profilometer.

Table 3-4. Symbols used to indicate the components of fretting couples

FRETTING WEAR TEST COUPLES		
	UPPER	LOWER STATIONERY SPECIMENS
●	Al <sub>2</sub> O <sub>3</sub> or WC-Co	pure Fe
■		pure Cu
◆		Ti 318 alloy
▽		0.64%C steel
▼		1.5%Mn steel
▲		316 stainless steel
□		JIS SUJ2 steel
◎	pure Fe	Al <sub>2</sub> O <sub>3</sub>



(a) The scar of the WC

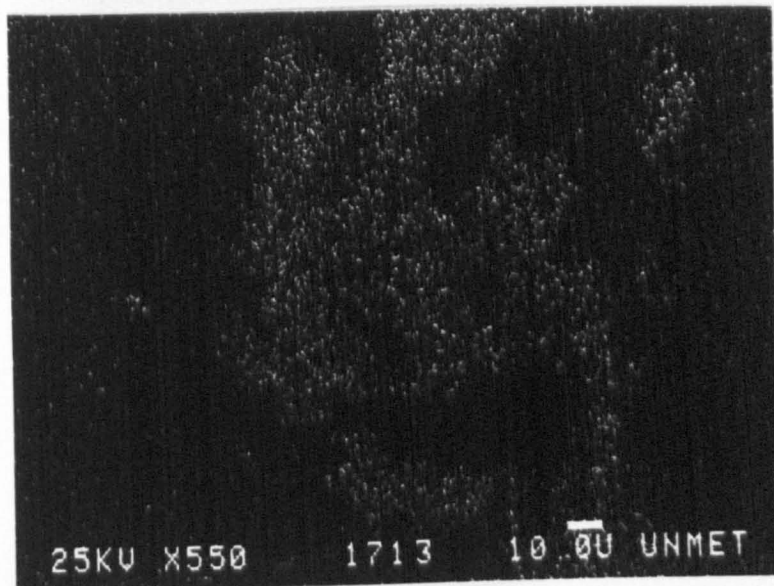


(b) The scar of the JIS SUJ2 steel

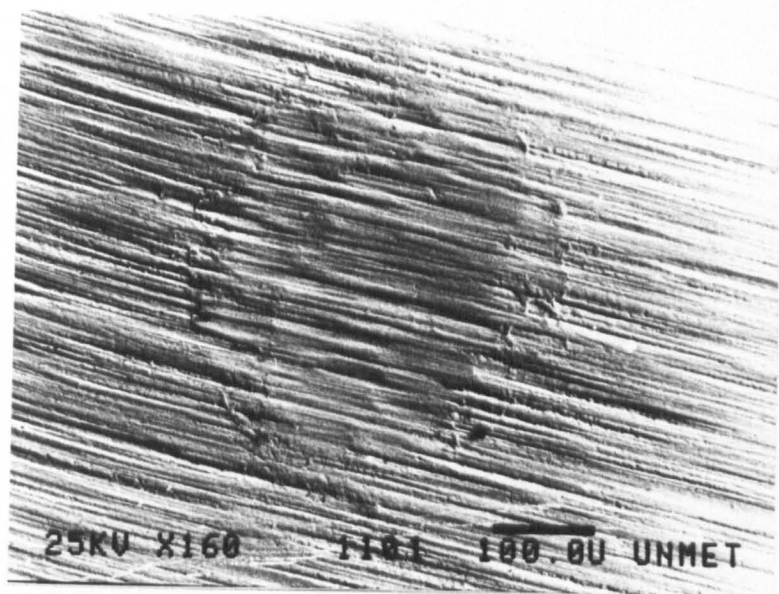
Fig. 3-6 The scars of the WC / JIS SUJ2 str



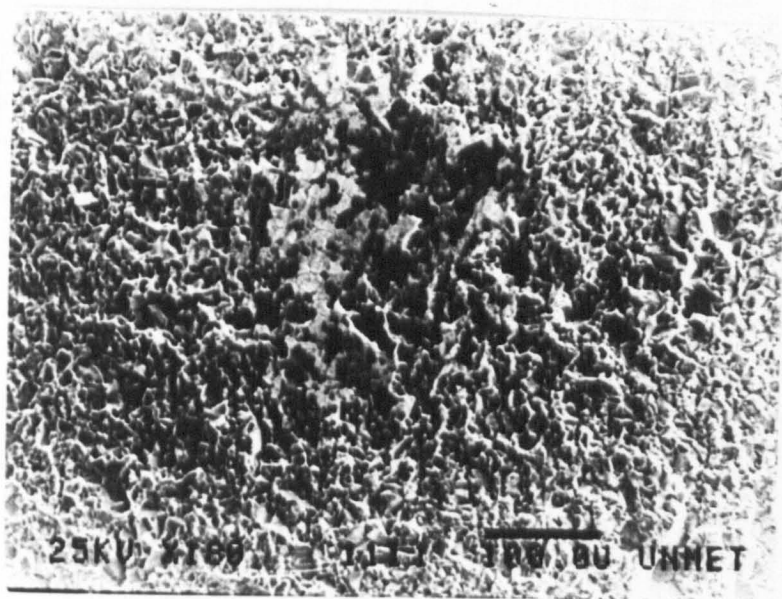
(c) The debris on the JIS SUJ2 steel



(d) The identification of the debris on the JIS SUJ2 steel by an X-ray microanalyser (the debris of W on the JIS SUJ2 steel)



(a) The scar of the WC



(b) The scar of the Al<sub>2</sub>O<sub>3</sub>

Fig. 3-7

The scars of the WC / Al<sub>2</sub>O<sub>3</sub> couple

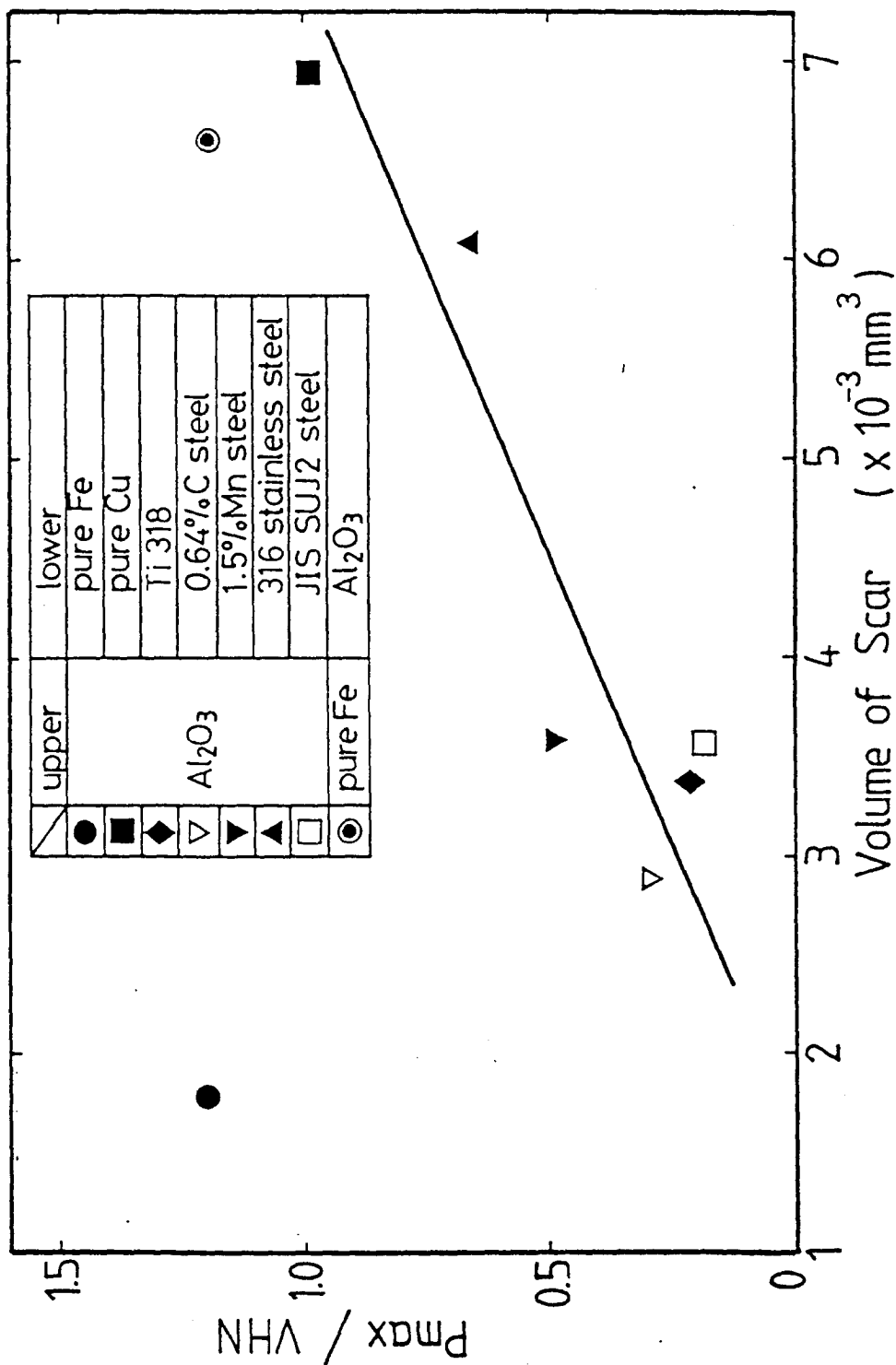


Fig. 3- 8a Relationship between P<sub>max</sub>/VHN and volume of scar

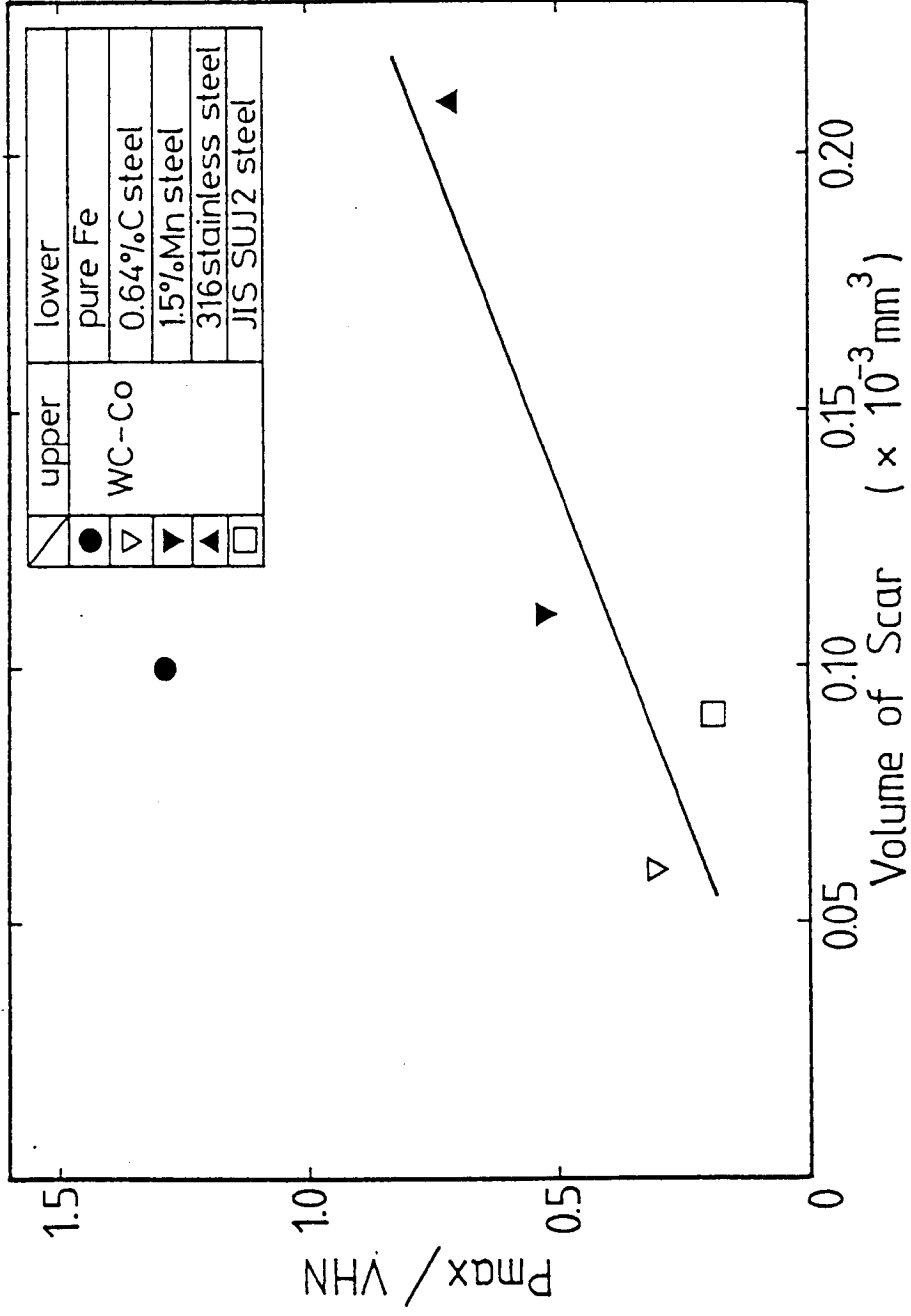


Fig. 3-8b Relationship between  $P_{max}/VHN$  and volume of scar

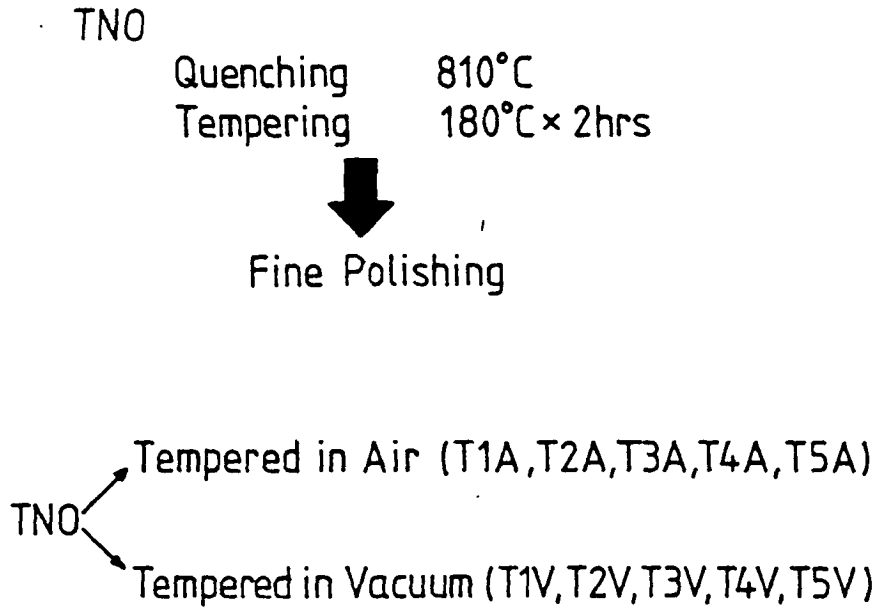


Fig. 4-1 Process used in the preparation of the high carbon chromium bearing steel specimens (JIS SUJ2)

Table 4-1 Tempering conditions and hardnesses of high carbon chromium steel (JIS SUJ2)

SPECIMENS	TEMPERING CONDITIONS		VHN
TNO	as received		715
T1V	200°C for 2hrs.	in Vacuum	673
T1A		in Air	
T2V	230°C for 2hrs.	in Vacuum	665
T2A		in Air	
T3V	260°C for 2hrs.	in Vacuum	642
T3A		in Air	
T4V	350°C for 2hrs.	in Vacuum	585
T4A		in Air	
T5V	400°C for 2hrs.	in Vacuum	498
T5A		in Air	

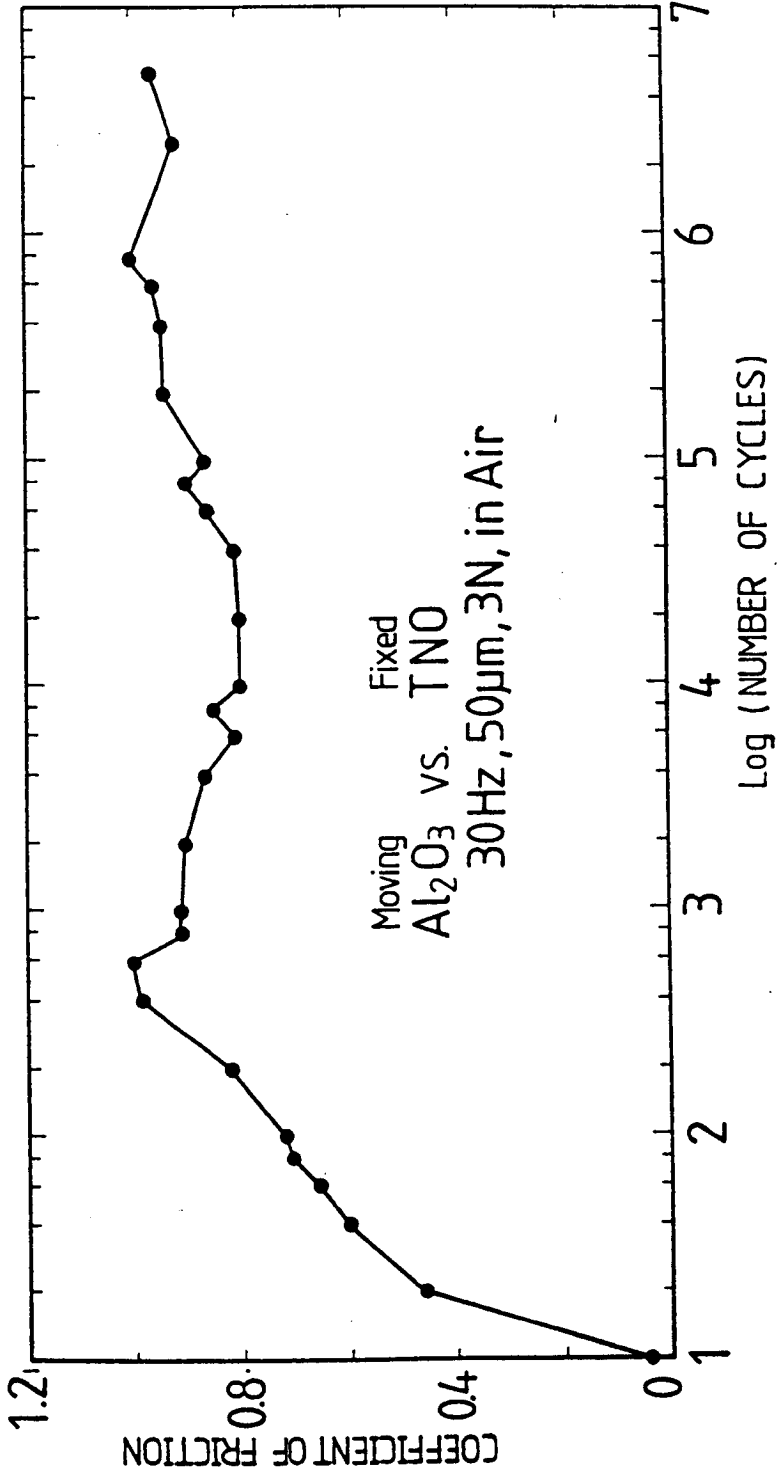


Fig. 4-2a Coefficient of friction vs. log(number of cycles)

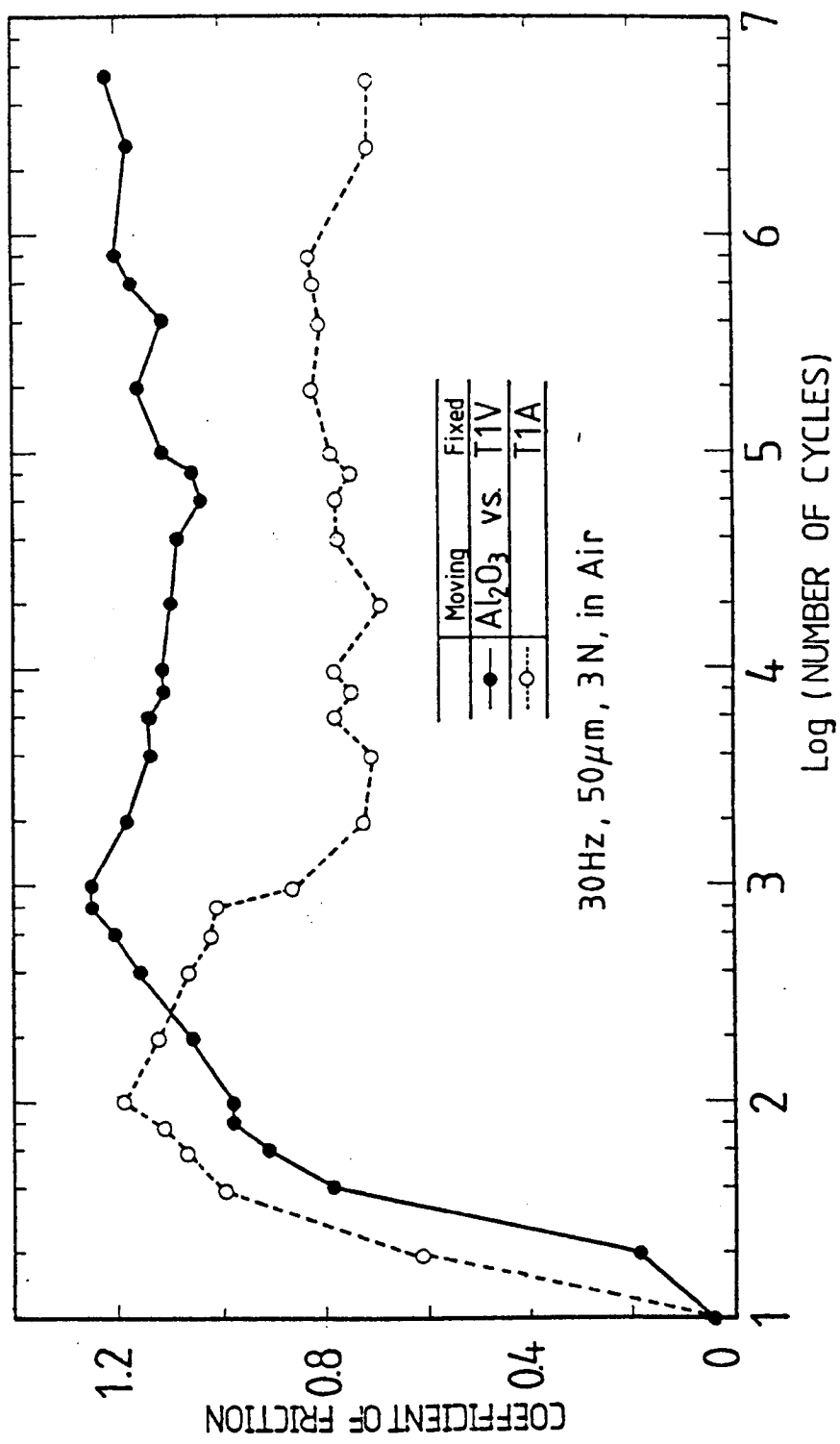


Fig. 4-2b Coefficient of friction vs log(number of cycles)

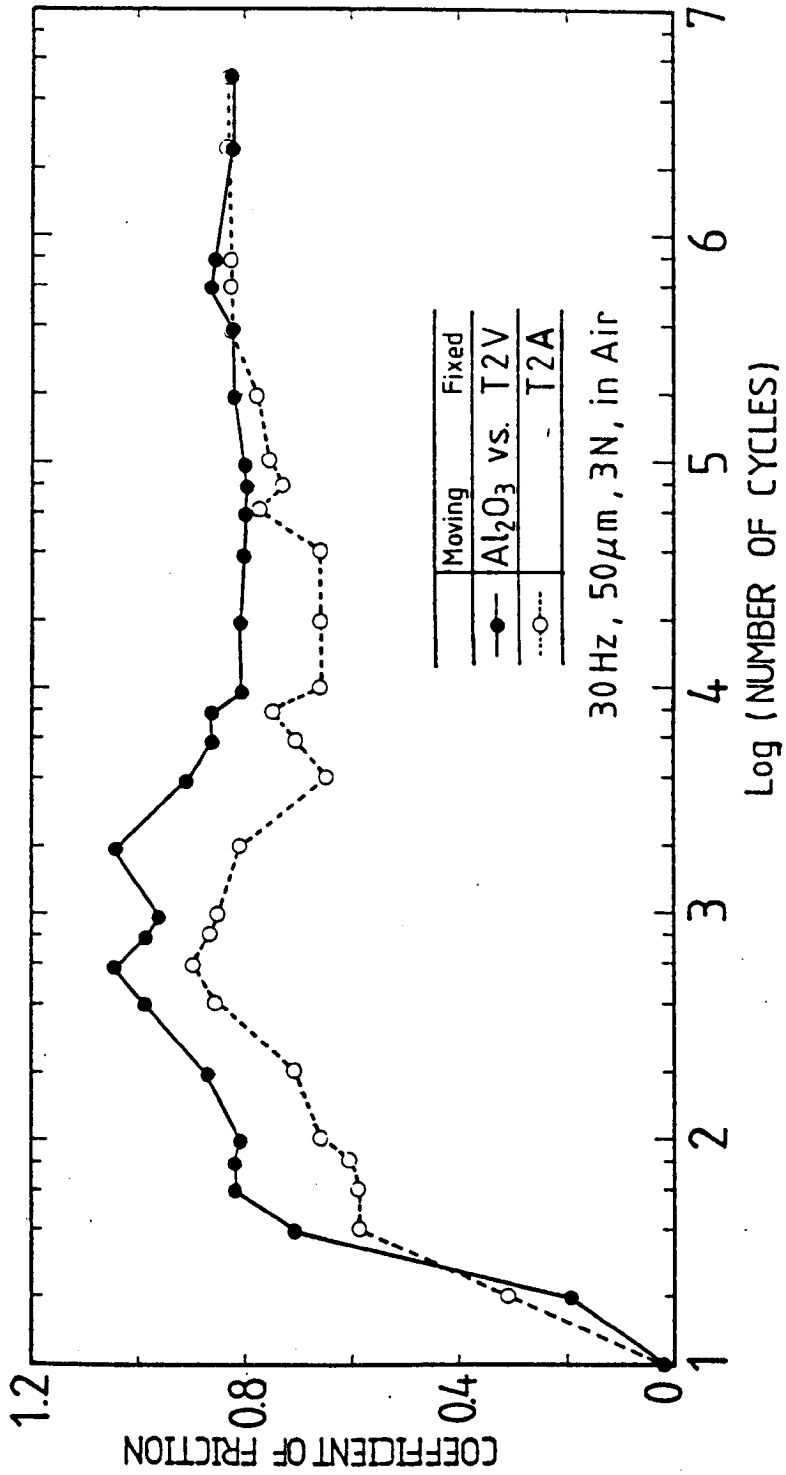


Fig. 4-2c Coefficient of friction vs. log(number of cycles)

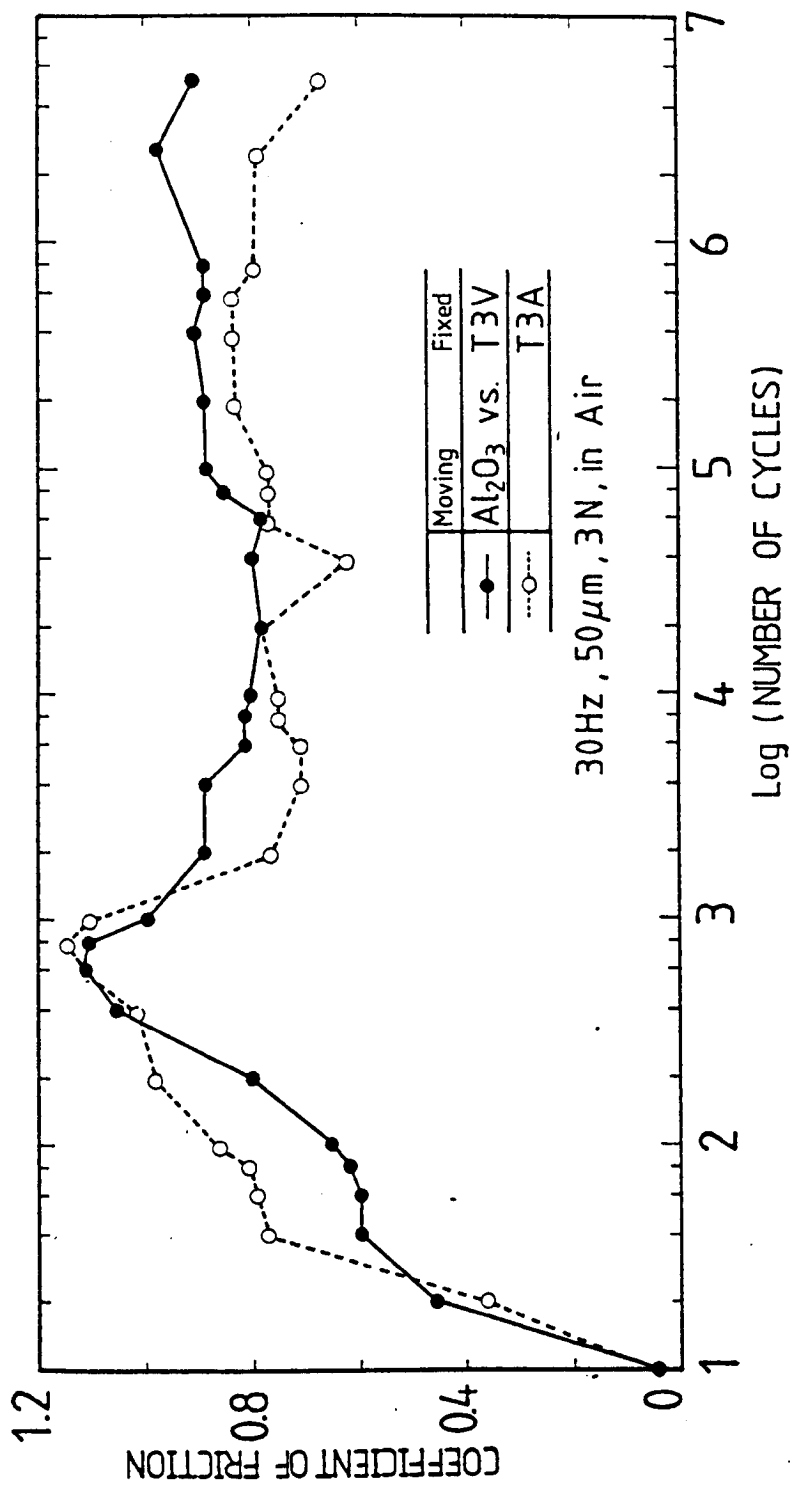


Fig. 4-2d Coefficient of friction vs. log(number of cycles)

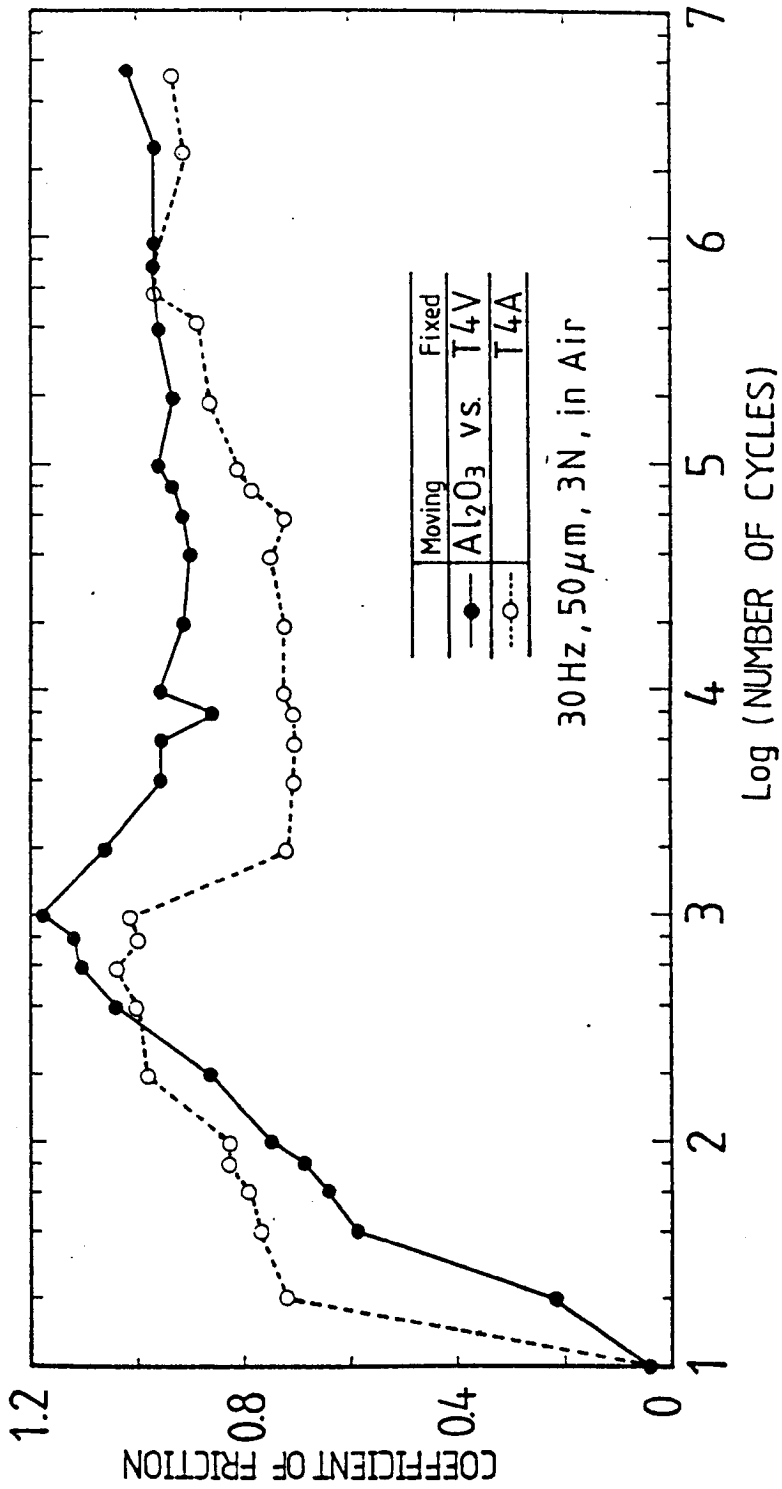


Fig. 4-2e Coefficient of friction vs. log(number of cycles)

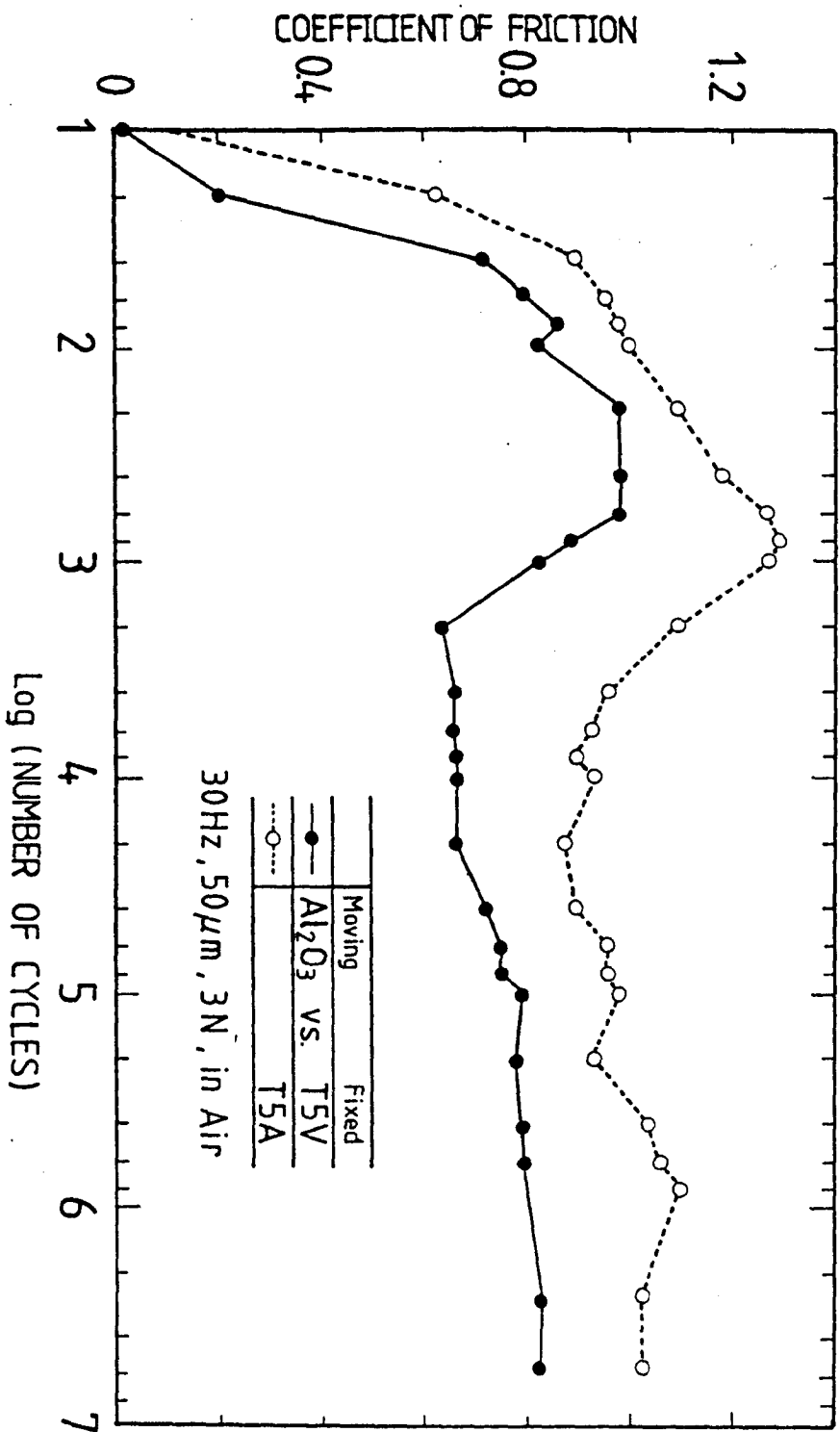


Fig. 4-2f

Coefficient of friction vs. log(number of cycles)

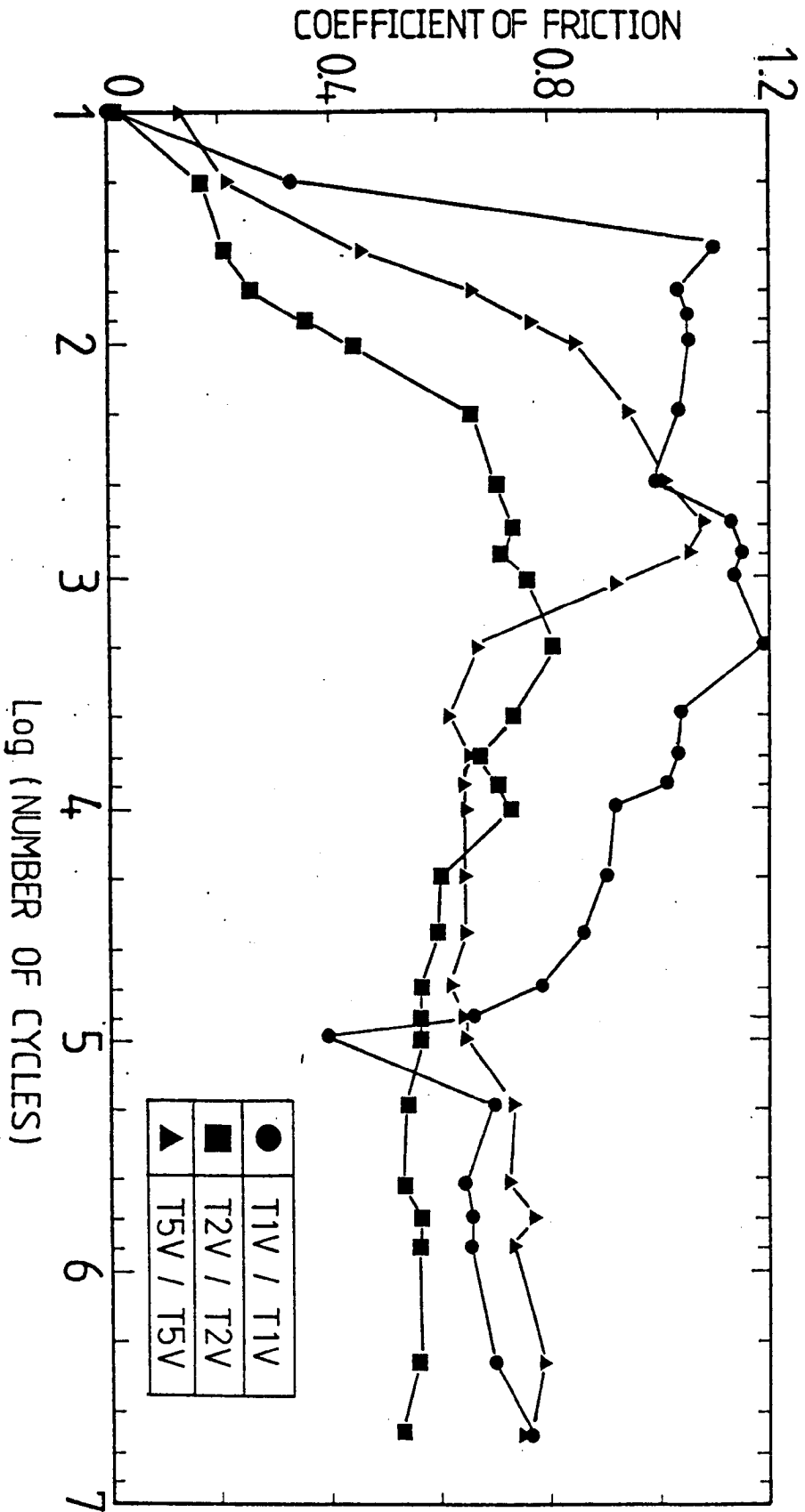


Fig. 4-3a Coefficient of friction vs. log(number of cycles)

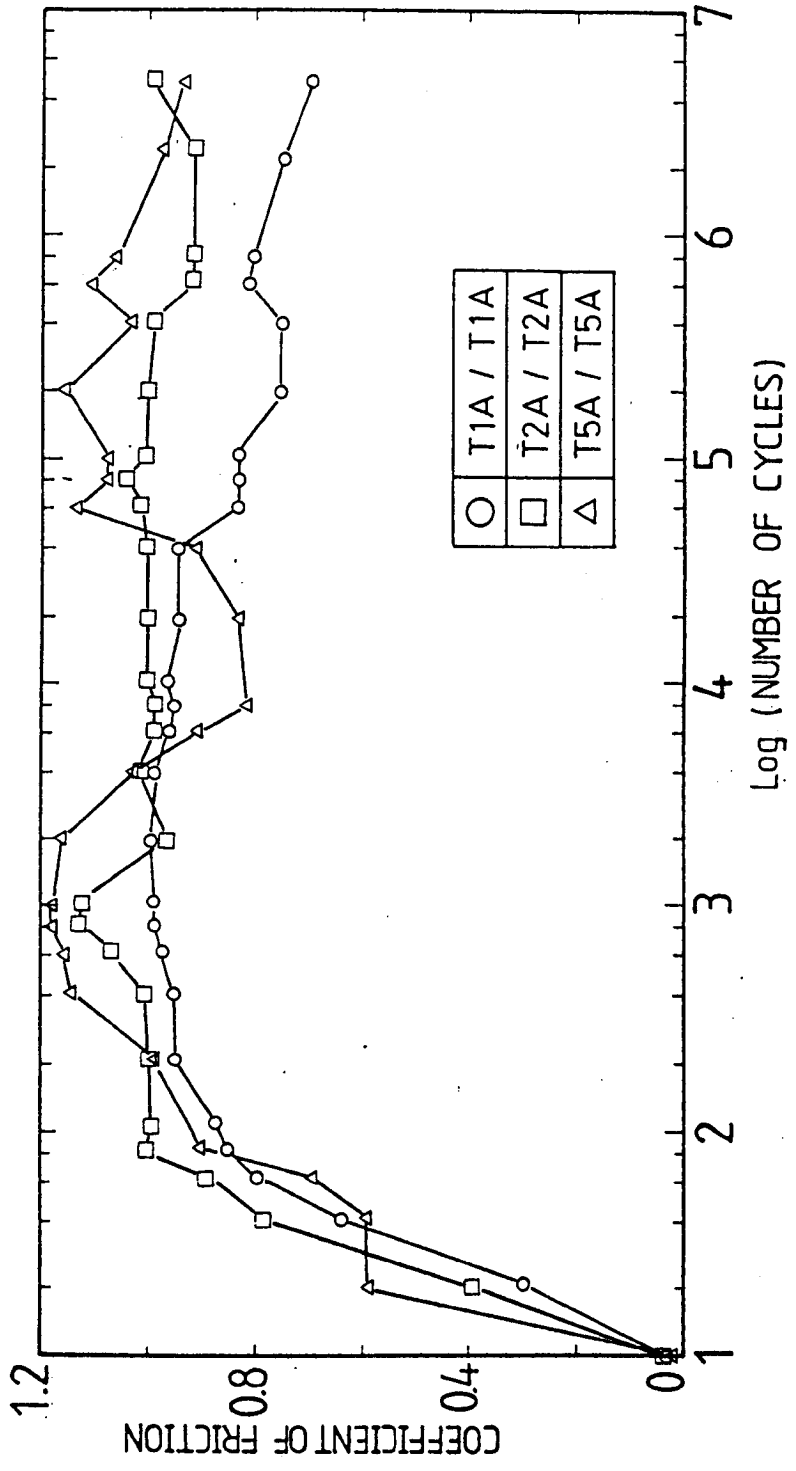


Fig. 4-3b Coefficient of friction vs. log(number of cycles)

Table 4-2 The results of the fretting wear tests between  $\text{Al}_2\text{O}_3$  and high carbon chromium bearing steel specimens tempered at various temperatures in a vacuum and in air

MATERIALS		SCARS ON FIXED SPECIMENS (JIS SUJ2)		
RIDER	FIXED	VOLUME ( $10^{-3}\text{mm}^3$ )	PROJ. AREA ( $\text{mm}^2$ )	MEAN DEPTH ( $\mu\text{m}$ )
$\text{Al}_2\text{O}_3$	TNO	3.56	0.46	7.68
	T1V	2.11	0.29	7.25
	T2V	2.75	0.34	8.16
	T3V	2.34	0.39	6.00
	T4V	3.22	0.35	9.18
	T5V	3.36	0.36	9.21
	T1A	3.23	0.35	9.20
	T2A	3.35	0.36	9.29
	T3A	3.71	0.38	9.78
	T4A	3.57	0.36	9.74
	T5A	3.38	0.36	9.49

Table 4-3 The results of the fretting wear tests between high carbon chromium bearing steel specimens tempered at various temperatures in a vacuum and in air

FRETTING COUPLE	AVE. VOLUME ( $\times 10^{-3} \text{mm}^3$ )			PROJ. AREA ( $\text{mm}^2$ )		MEAN DEPTH ( $\mu\text{m}$ )	
	UPPER	LOWER	SUM	UPPER	LOWER	UPPER	LOWER
T1V	4.02	0.77	4.79	0.35	0.32	11.54	2.42
T2V	3.82	1.37	5.19	0.39	0.42	9.72	3.24
T3V	3.19	1.39	4.58	0.35	0.39	9.09	3.52
T4V	3.02	1.41	4.43	0.36	0.41	8.39	3.44
T5V	1.60	1.81	3.41	0.28	0.34	5.74	5.20
T1A	5.46	2.68	8.14	0.50	0.51	10.85	5.26
T2A	4.17	2.65	6.82	0.53	0.56	7.91	4.69
T3A	3.28	3.19	6.47	0.37	0.47	8.96	6.75
T4A	3.78	2.37	6.15	0.38	0.39	9.99	6.08
T5A	2.86	----	(2.86)	0.29	----	9.93	----

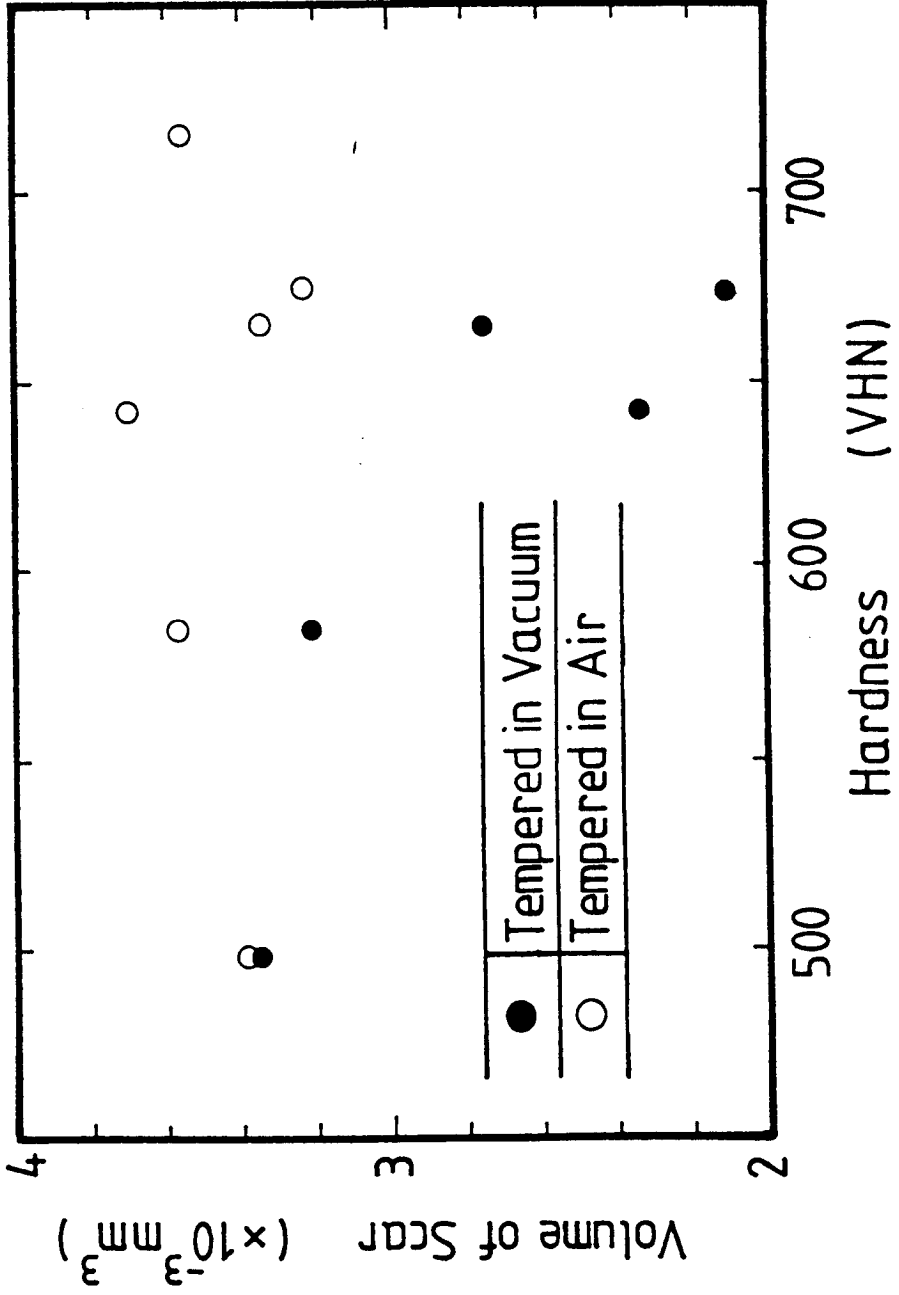


Fig. 4-4a Relationship between volume of scar and hardness of  $\text{Al}_2\text{O}_3$  / JIS SUJ2 couples

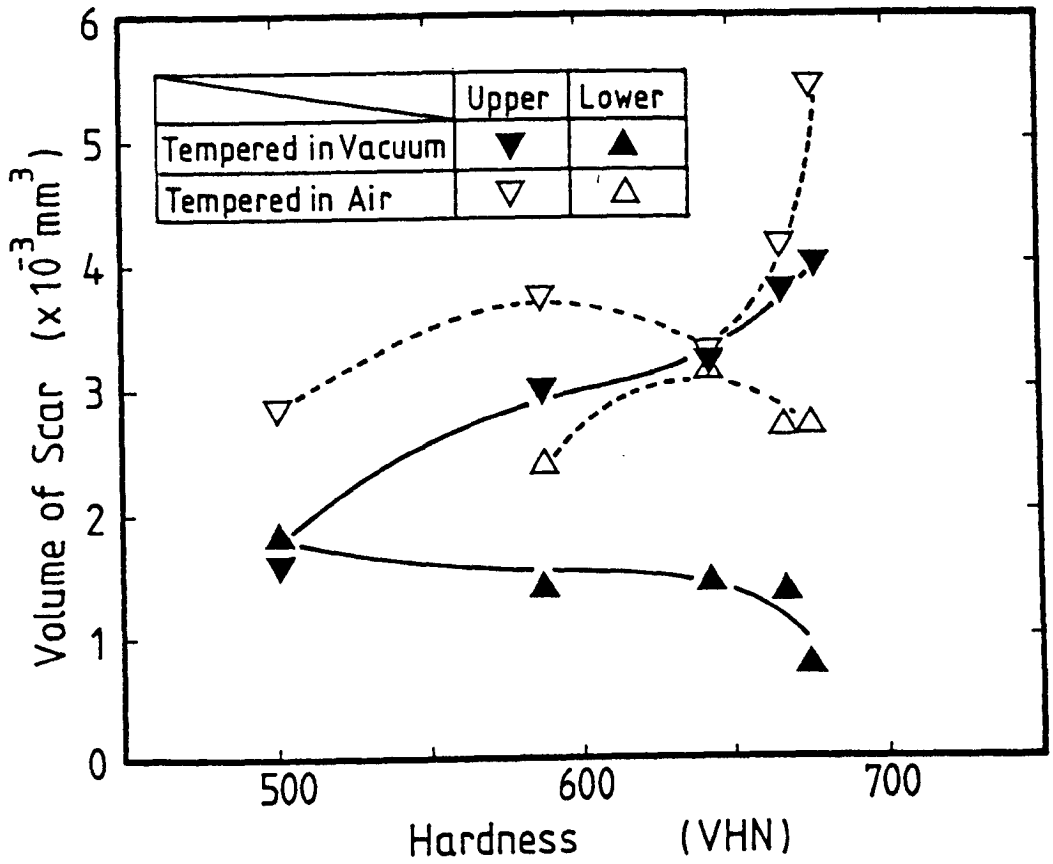
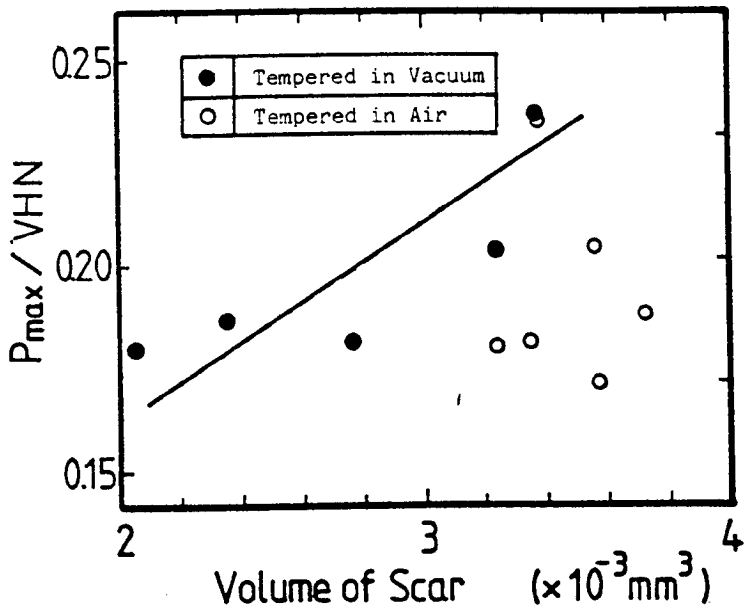
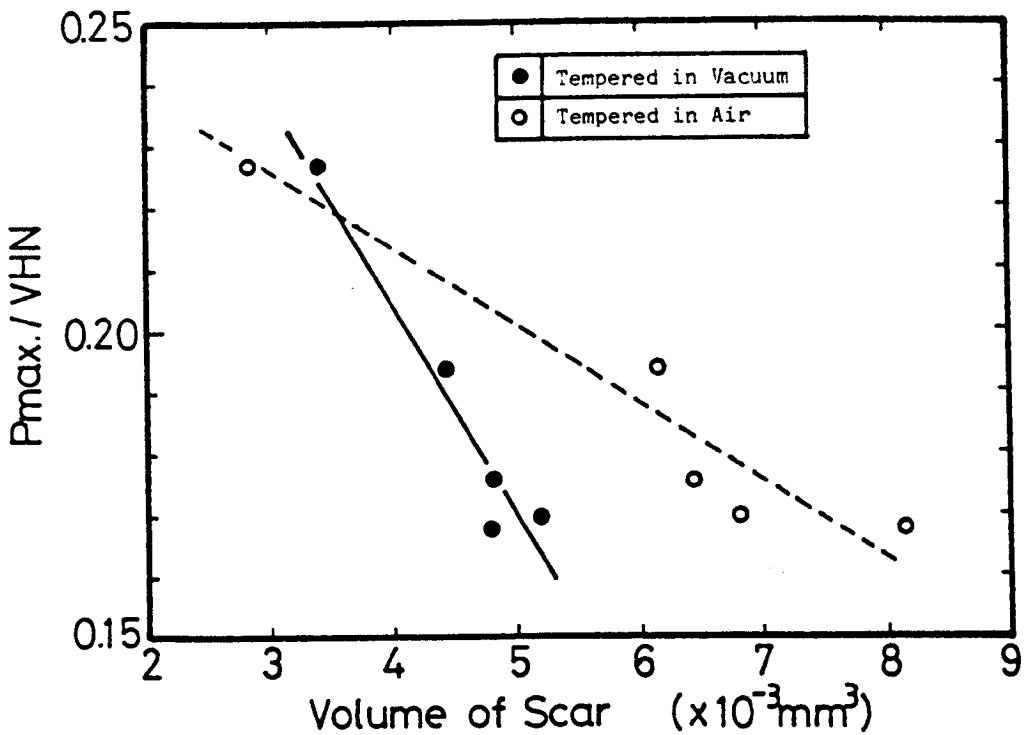


Fig. 4-4b Relationship between volume of scar and hardness of JIS SUJ2 / JIS SUJ2 couples



(a)  $\text{Al}_2\text{O}_3$  / JIS SUJ2 couples



(b) JIS SUJ2 / JIS SUJ2 couples

Fig. 4-5 Relationship between  $P_{\text{max}}/\text{VHN}$  and volume of scar

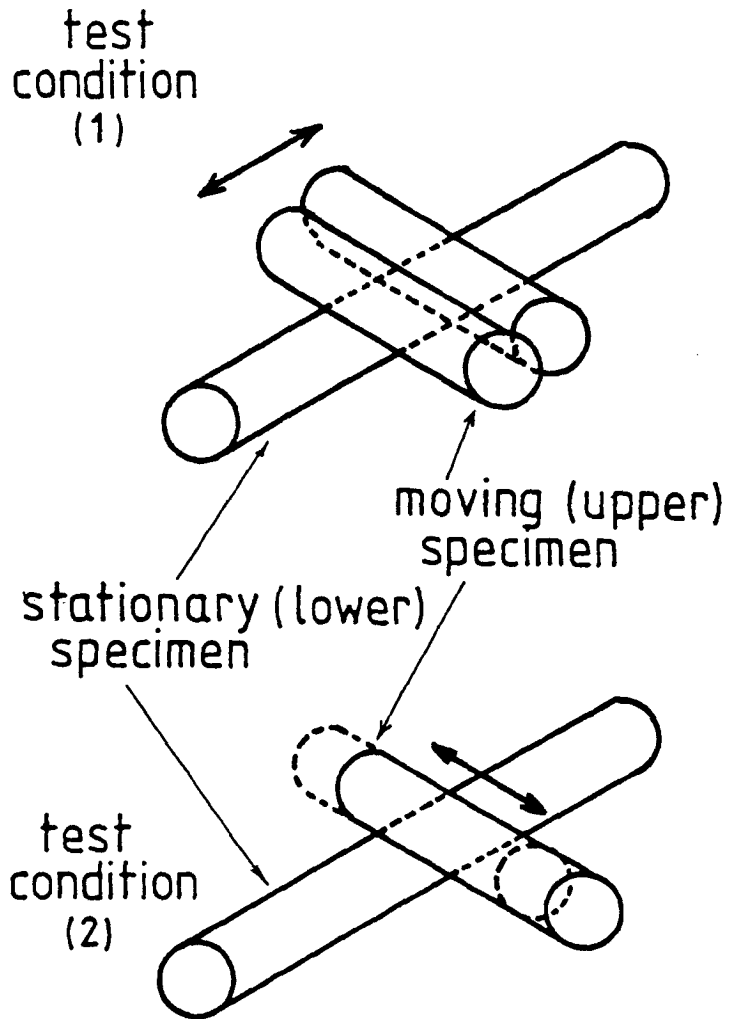


Fig. 5-1 Schematic diagrams of the fretting wear test conditions

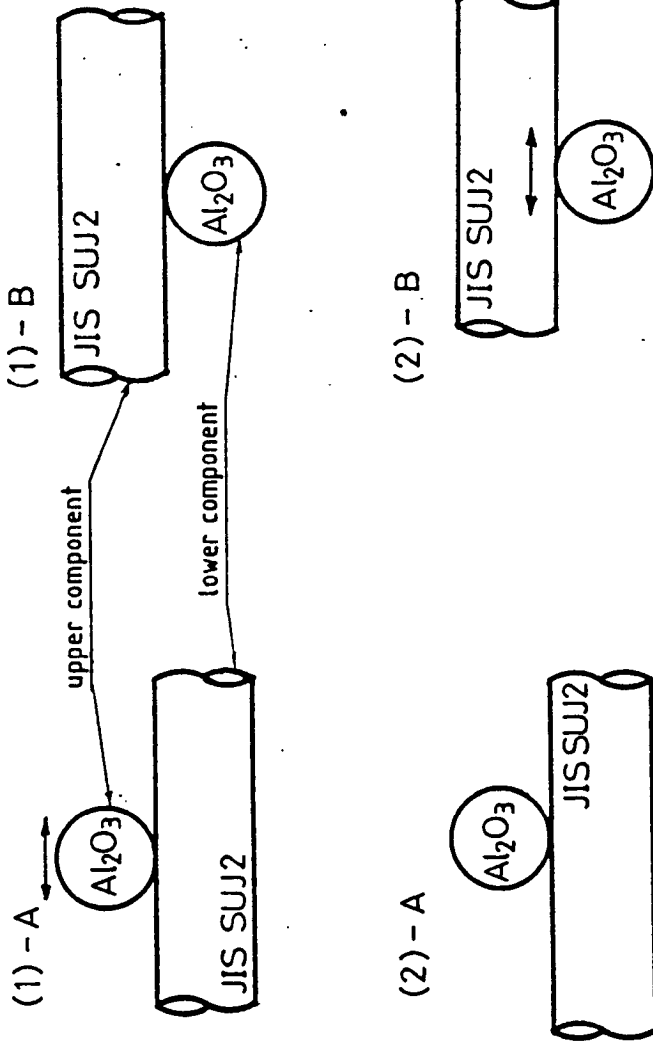


Fig. 5-2 Schematic diagrams of fretting wear mechanisms under test conditions

(1)-A and (2)-B : upper component oscillates in the direction by the arrows  
 (1)-B and (2)-A : upper component oscillates perpendicular to the plane of the page

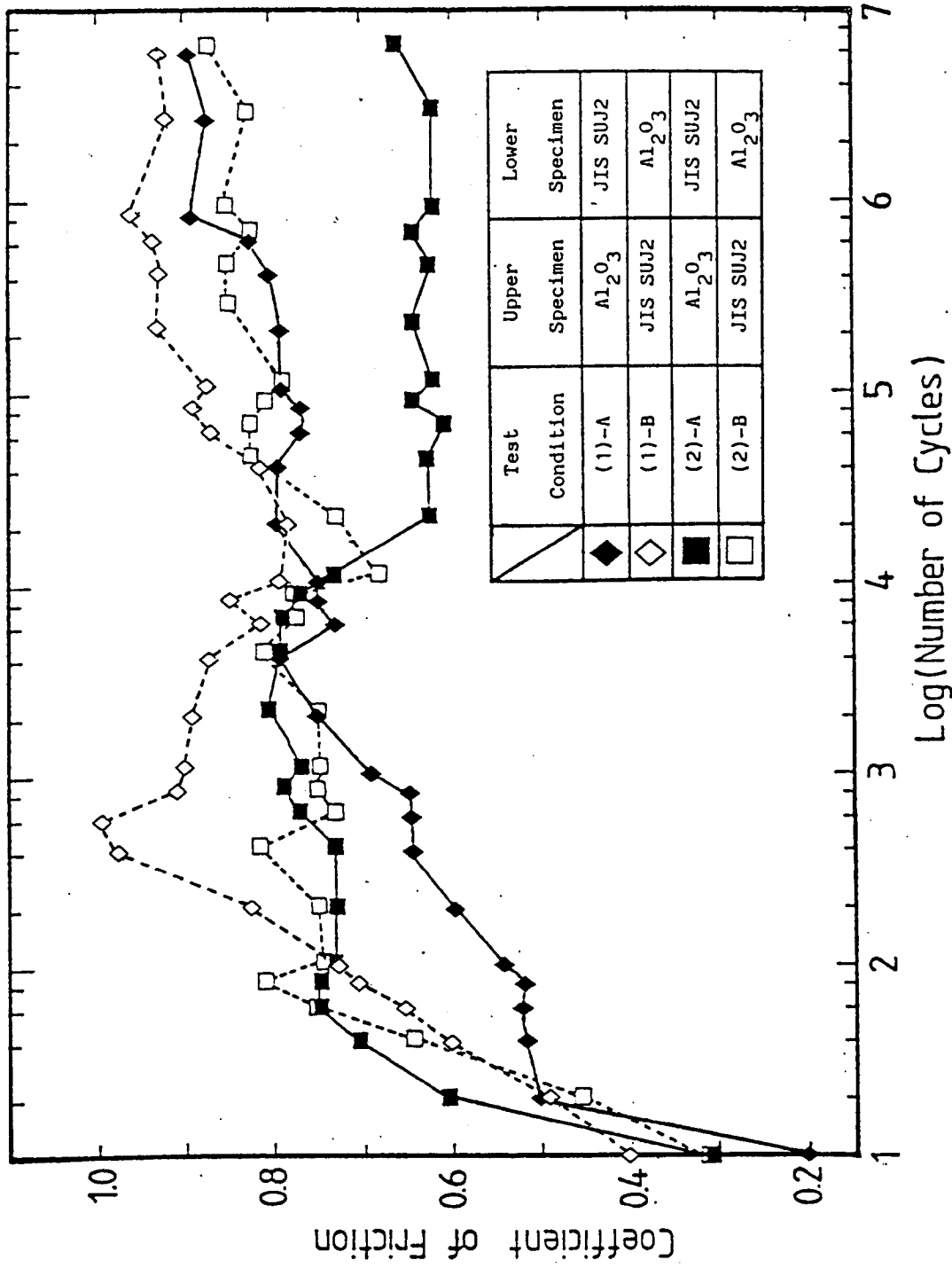


Fig. 5-3a Friction behaviour of the JIS SUJ2 / Al<sub>2</sub>O<sub>3</sub> couples under various test conditions

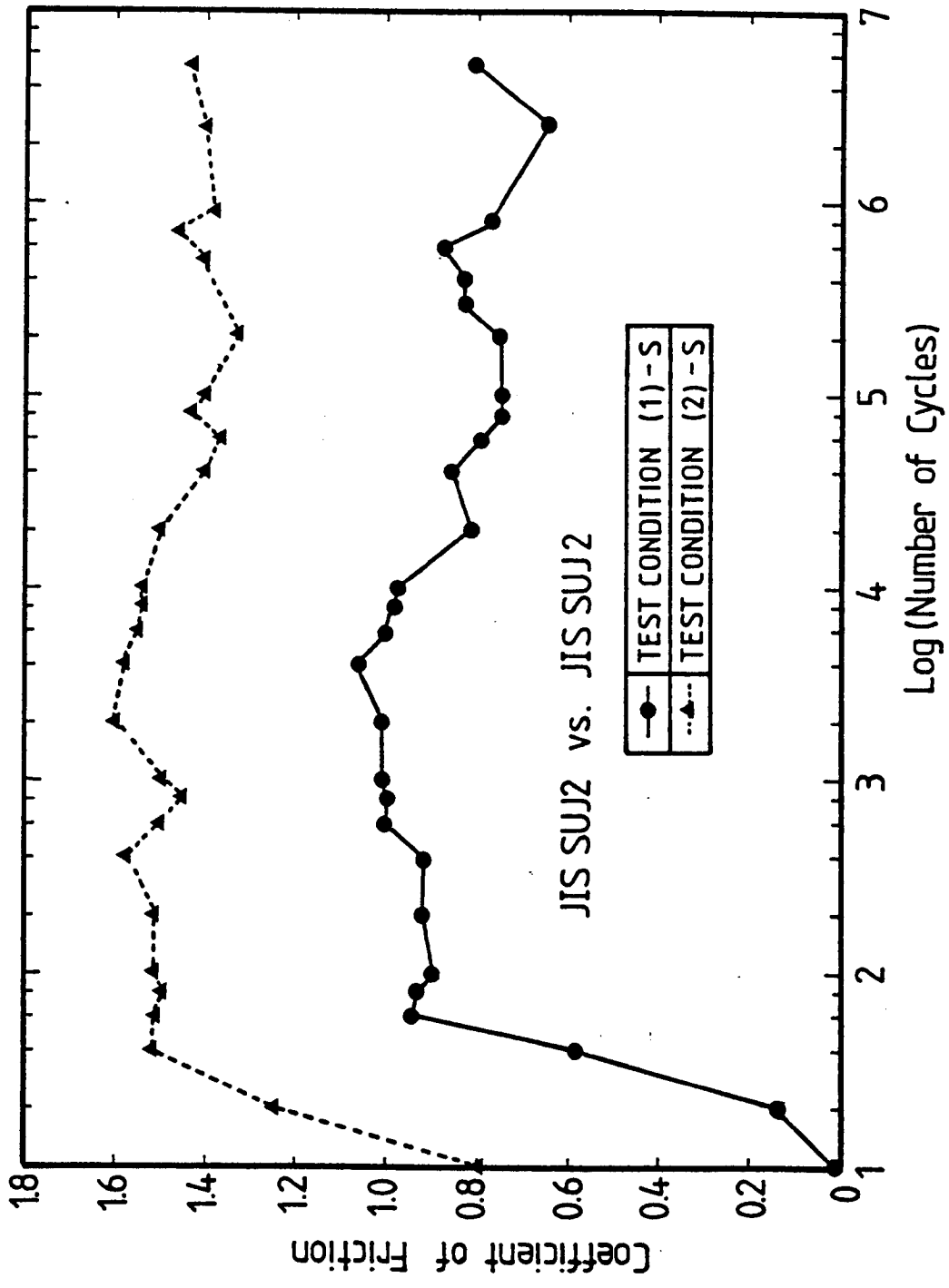


Fig. 5-3b Friction behaviour of the JIS SUJ2 / JIS SUJ2 couples under both test conditions (1) and (2)

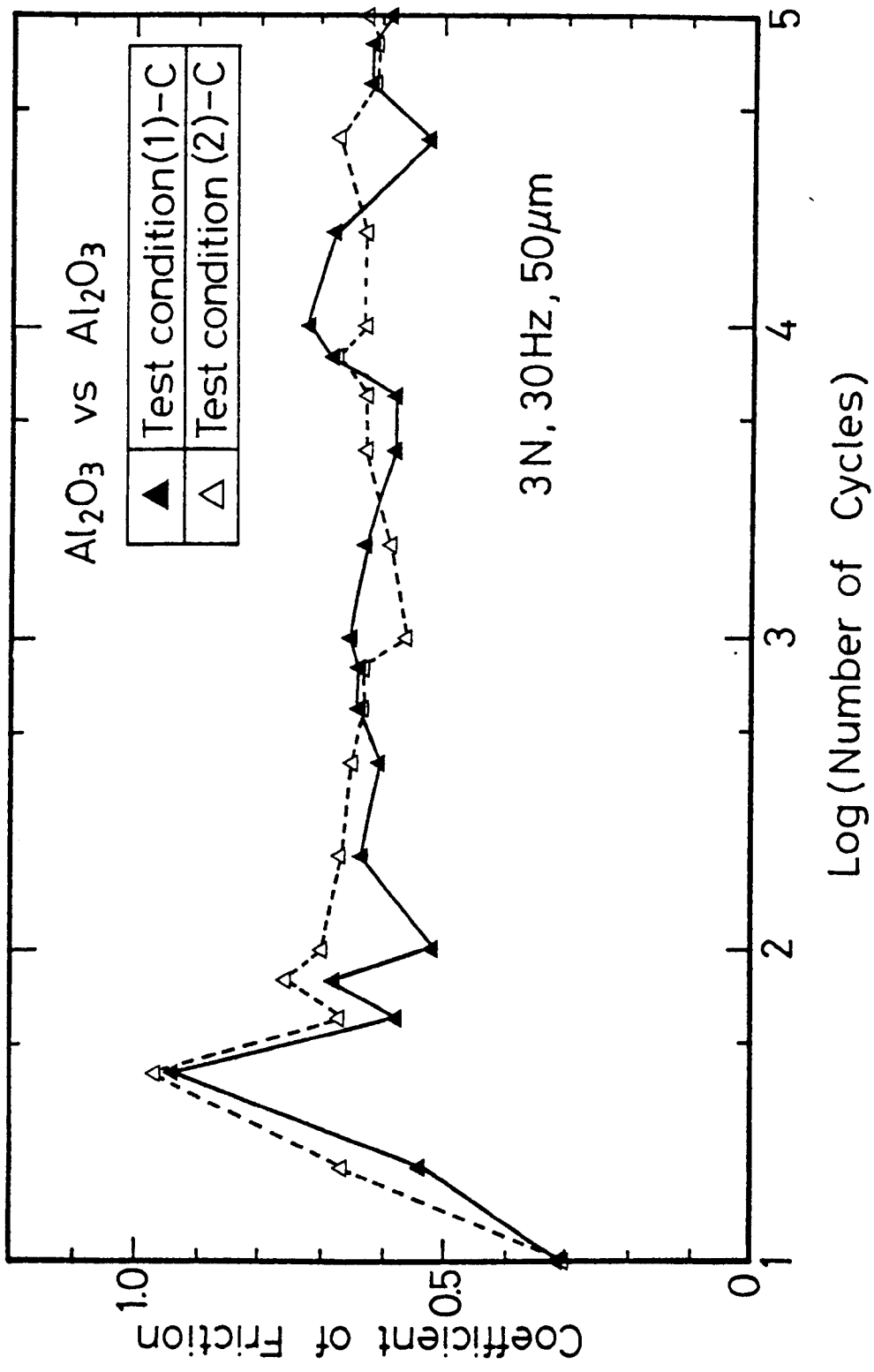


Fig. 5-3c Friction behaviour of the Alumina / Alumina couples under both test conditions (1) and (2)

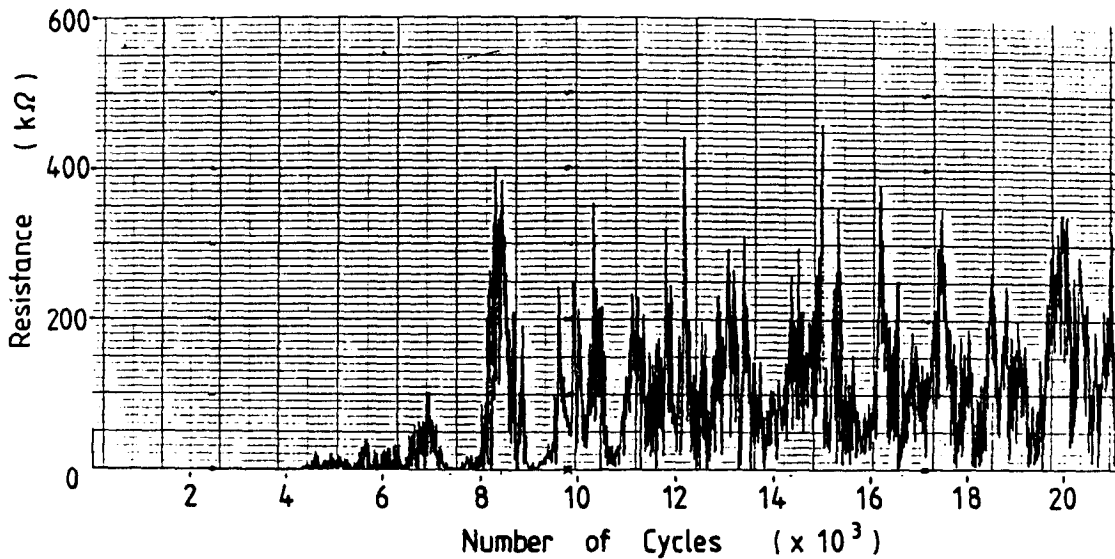


Fig. 5-4a VARIATION OF ELECTRICAL CONTACT RESISTANCE DURING FRETTING OSCILLATION UNDER TEST CONDITION (1)-S

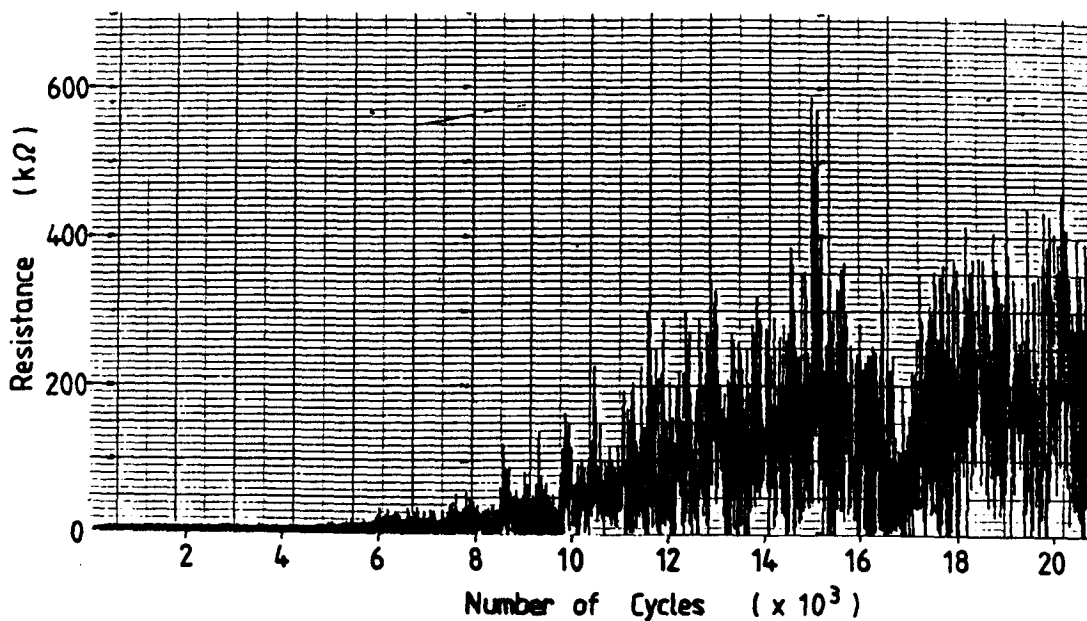


Fig. 5-4b VARIATION OF ELECTRICAL CONTACT RESISTANCE DURING FRETTING OSCILLATION UNDER TEST CONDITION (2)-S

Table 5-1 Average volumes, projected areas and mean depths of the scars on the JIS SUJ2 specimens

Test Condition	Upper Specimen	Lower Specimen	Scars on JIS SUJ2 specimens		
			Vol. (x 10 <sup>-3</sup> mm <sup>3</sup> )	Area (mm <sup>2</sup> )	Depth (μm)
(1)-A	Al <sub>2</sub> O <sub>3</sub>	JIS SUJ2	3.56	0.46	7.7
(1)-B	JIS SUJ2	Al <sub>2</sub> O <sub>3</sub>	8.86	0.55	16.1
(2)-A	Al <sub>2</sub> O <sub>3</sub>	JIS SUJ2	12.94	0.66	19.6
(2)-B	JIS SUJ2	Al <sub>2</sub> O <sub>3</sub>	6.88	0.52	13.2

Table 5-2 Average volumes, projected areas and mean depths of the scars under fretting between JIS SUJ2 specimens

FRETTING CONDITION	AVE. VOLUME ( $\times 10^{-3} \text{ mm}^3$ )			PROJ. AREA ( $\text{mm}^2$ )		MEAN DEPTH ( $\mu\text{m}$ )	
	UPPER	LOWER	SUM	UPPER	LOWER	UPPER	LOWER
(1)-S	3.57	2.42	5.99	0.41	0.44	8.73	5.44
(2)-S	4.35	16.10	20.45	0.91	0.79	4.78	20.34

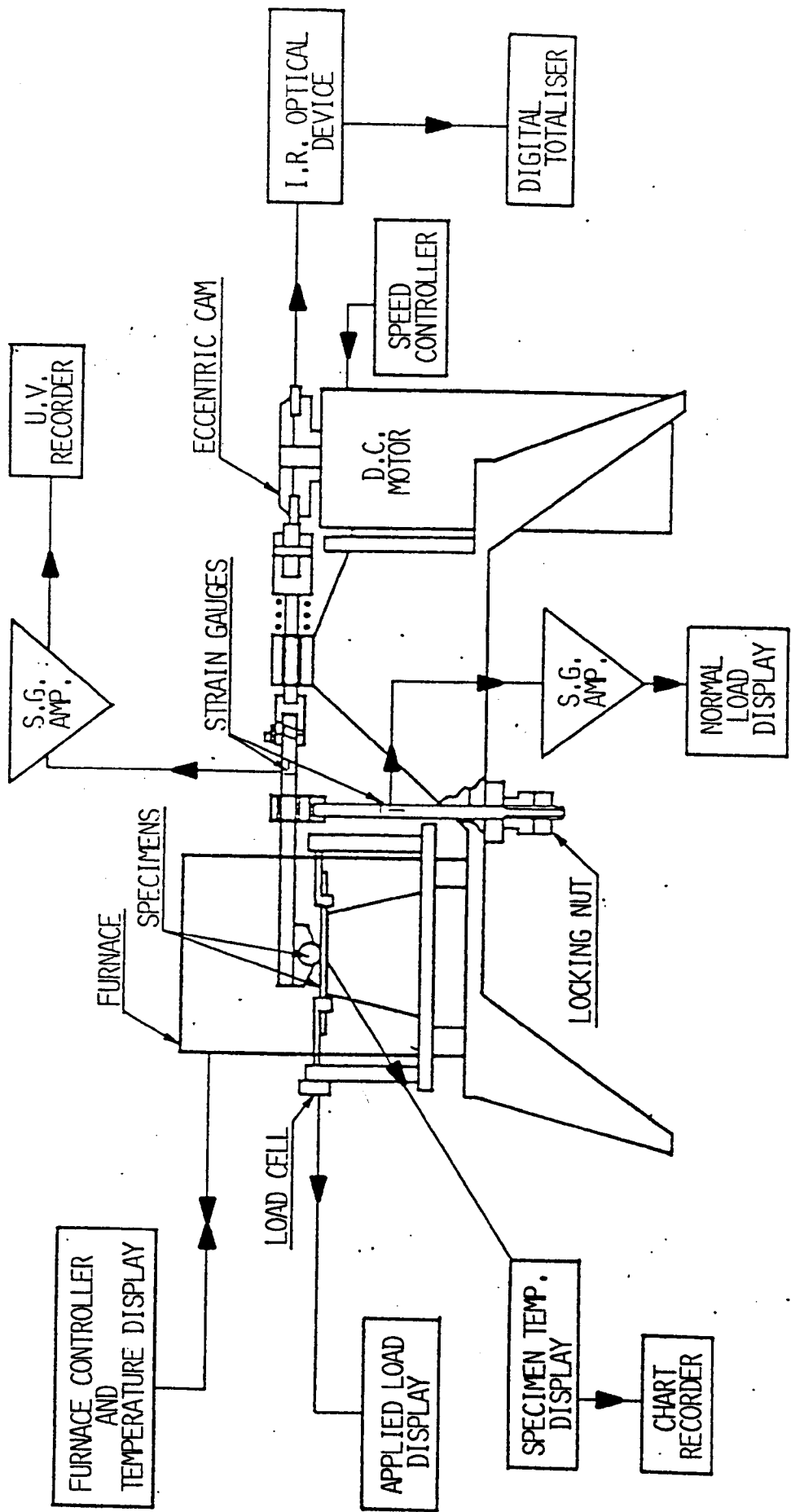


Fig. 6-1 A schematic diagram of the fretting wear apparatus

Fig. 6-1

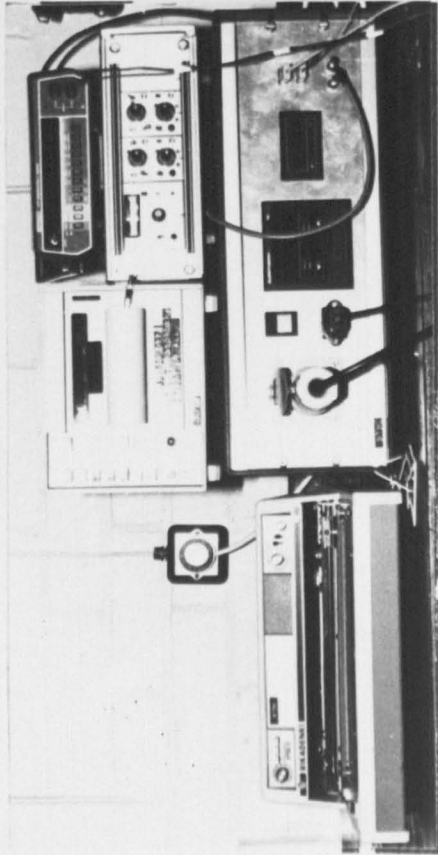
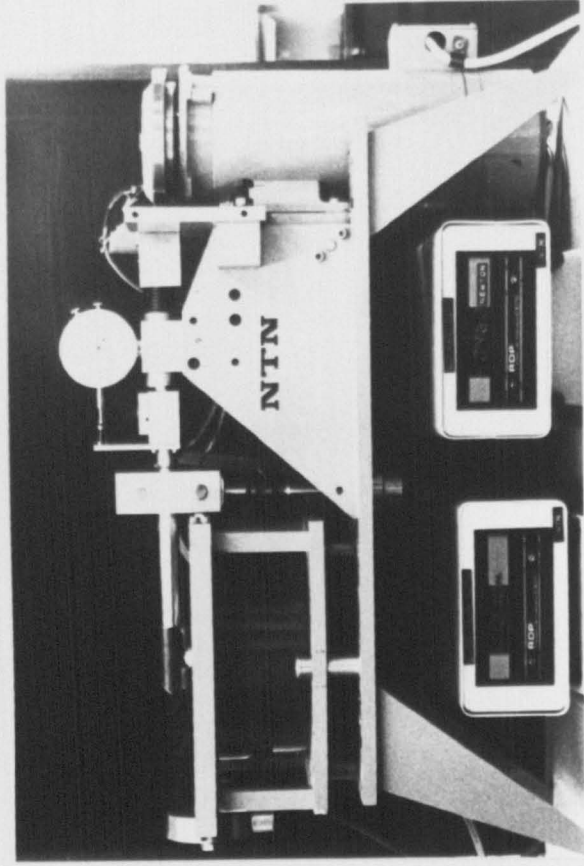


Fig. 6-2 The fretting wear apparatus

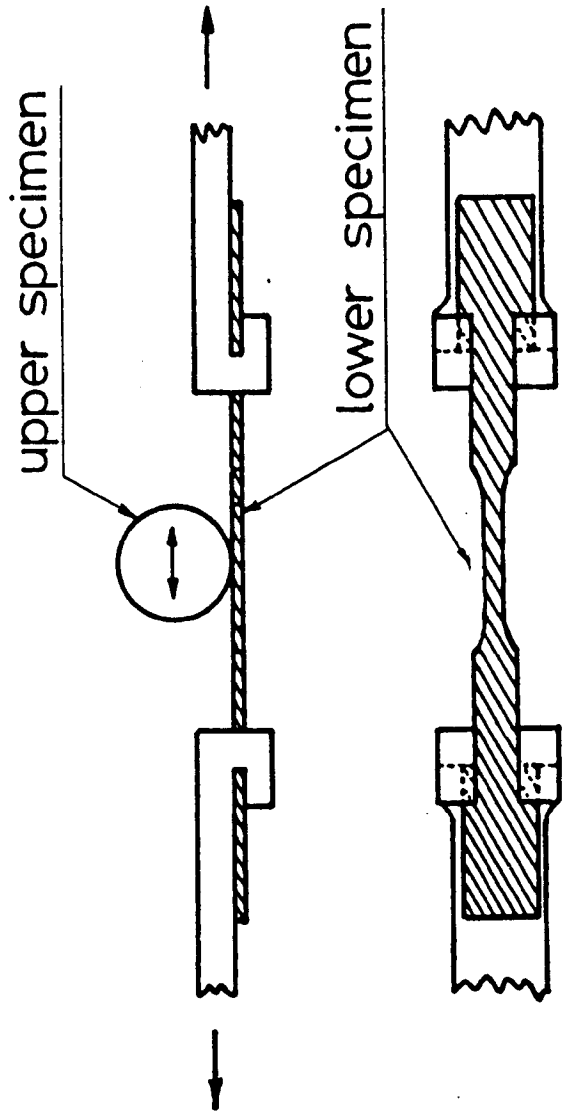


Fig. 6-3 Fretting wear test arrangement

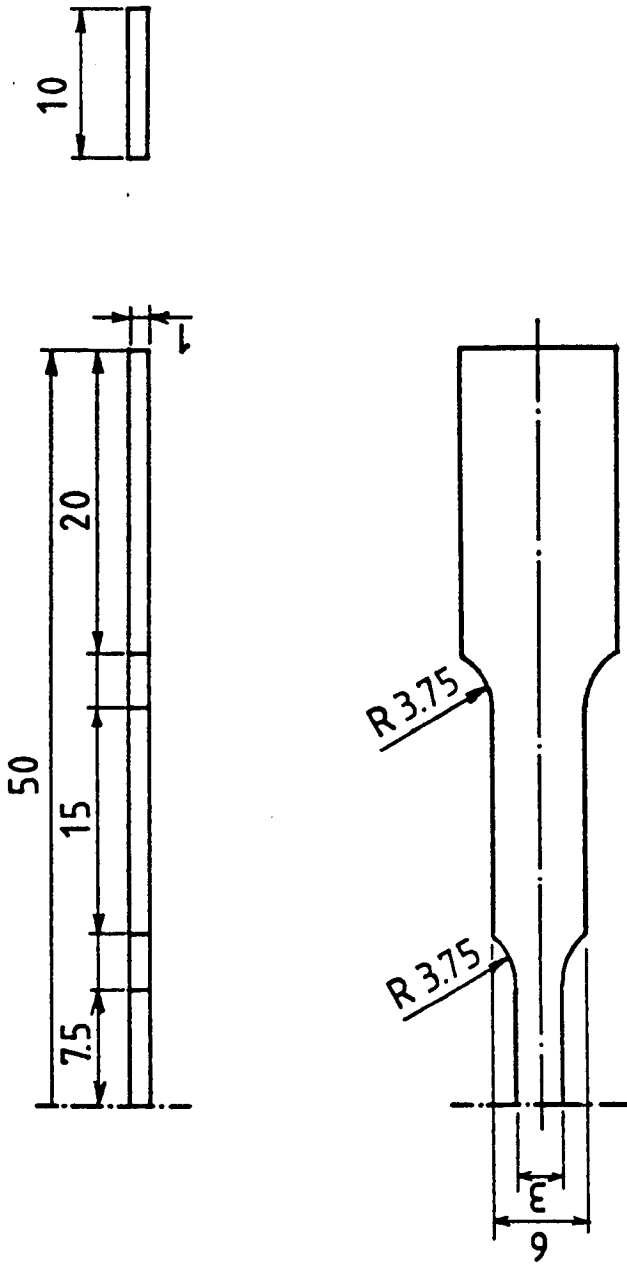


Fig. 6-4 Geometry of the lower stationary specimen

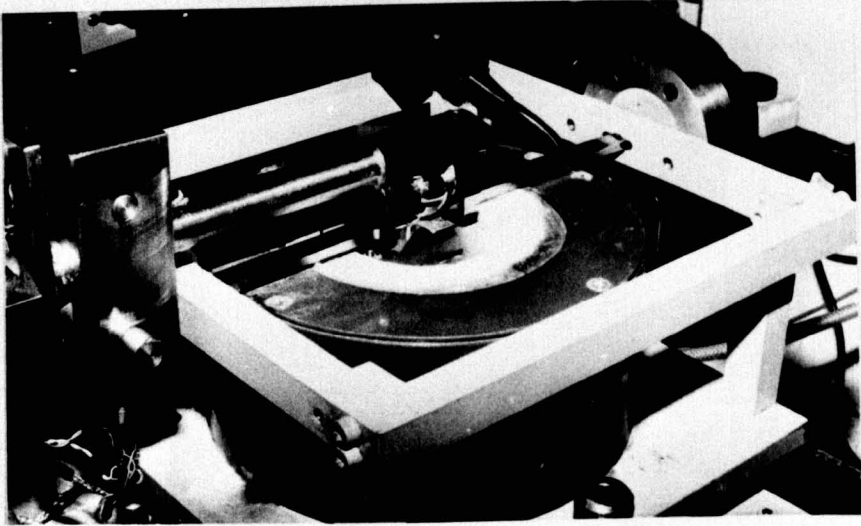


Fig. 6-5 Test arrangement for fretting wear test of the stressed stationary specimen

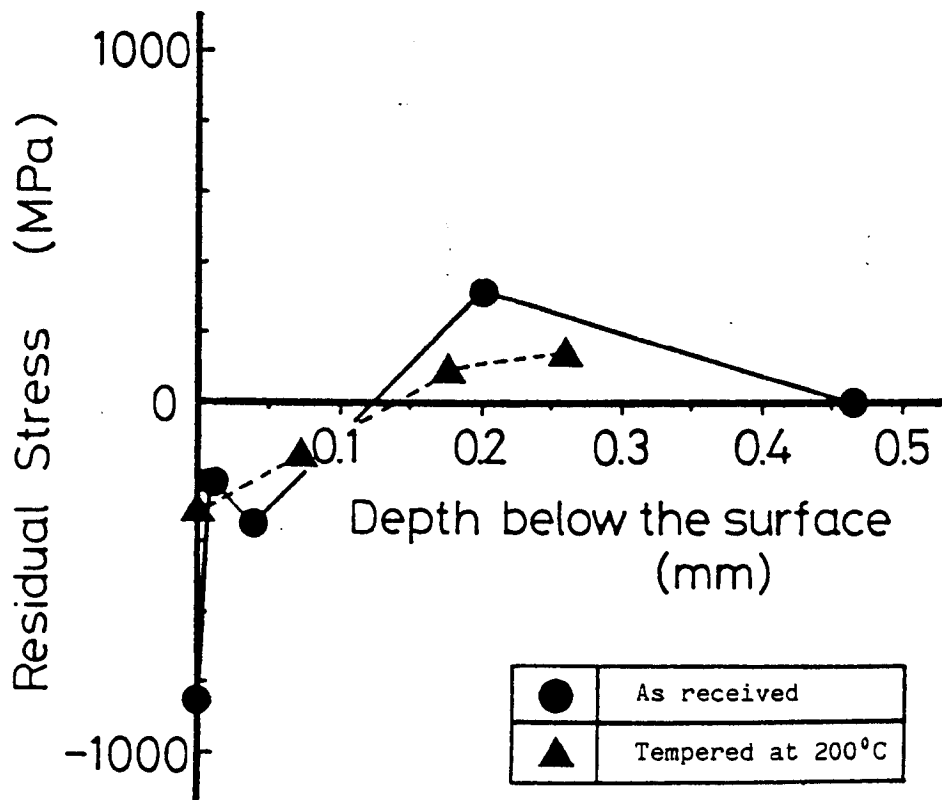
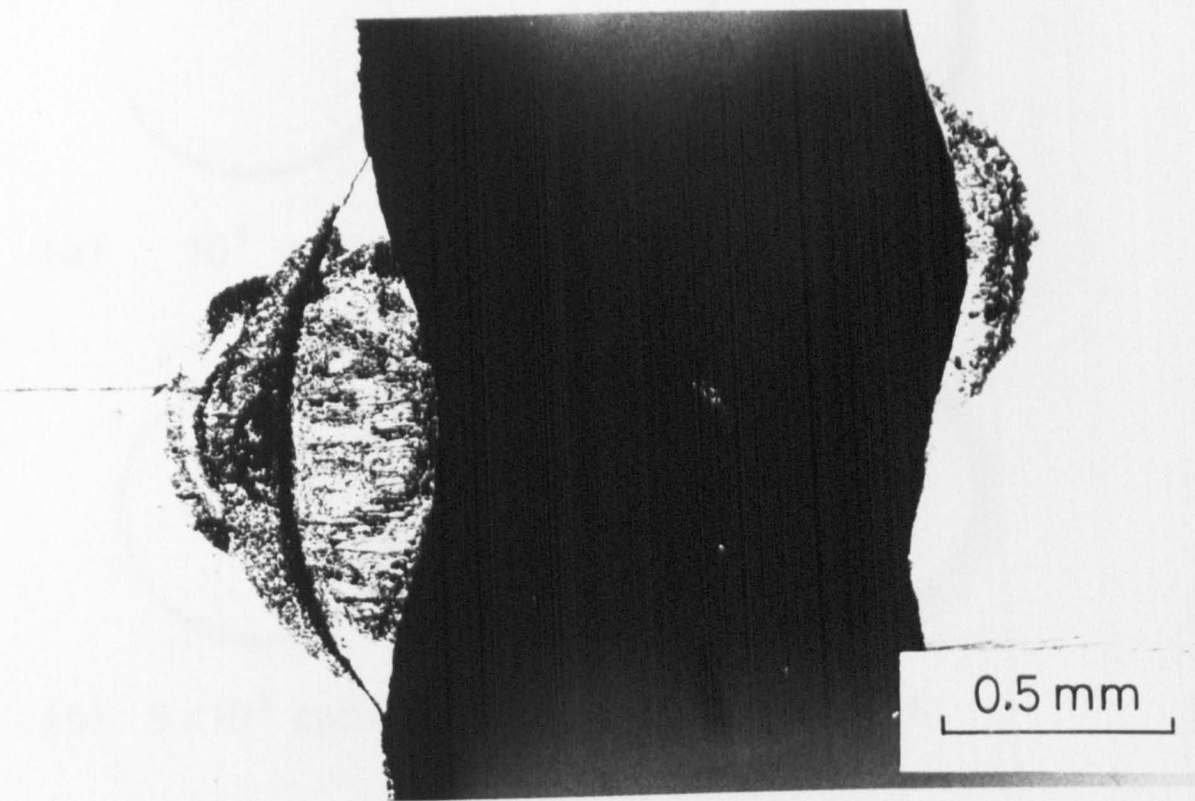
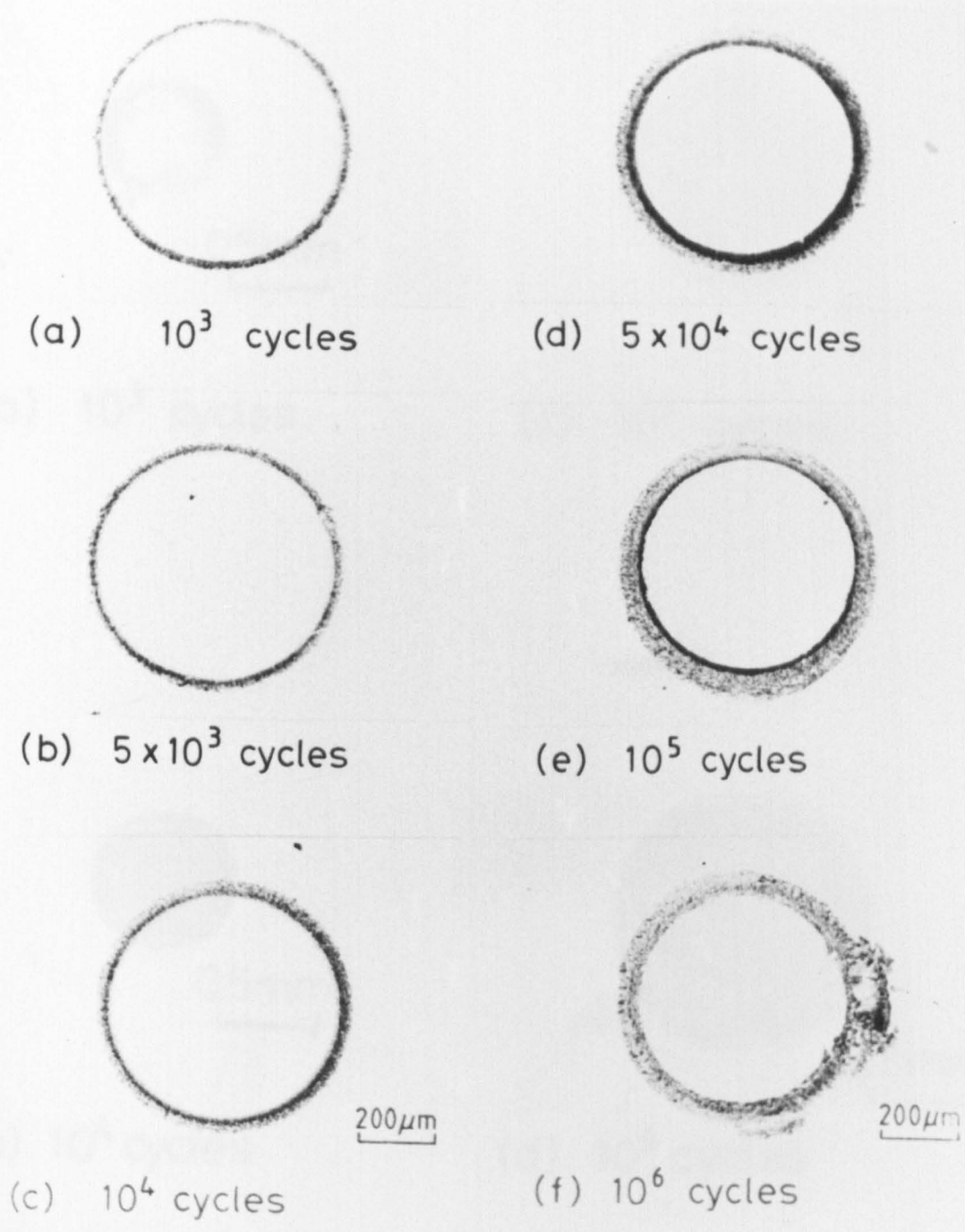


Fig. 7-1 Stress distributions below the surface



437 N ( $P_{max} = 1200$  MPa)  
50 Hz,  $10 \mu\text{m}$ , fractured at  $1.5 \times 10^6$  cycles  
Applied tensile stress : 400 MPa

Fig. 7-2 An example of a failure induced by fretting wear



437 N ( $P_{\text{max}} = 1200 \text{ MPa}$ ), 50 Hz, 8  $\mu\text{m}$

Fig. 7-3a An example of the development of the scar when  $T < \mu P$



0.5mm

(a)  $10^3$  cycles



0.5mm

(c)  $10^5$  cycles



0.5mm

(b)  $10^4$  cycles



0.5mm

(d)  $10^6$  cycles

135N ( $P_{max} = 822\text{MPa}$ ), 60Hz,  $25\mu\text{m}$ , in Lab.

Fig. 7-3b An example of the development of the scar when  $T \geq \mu P$

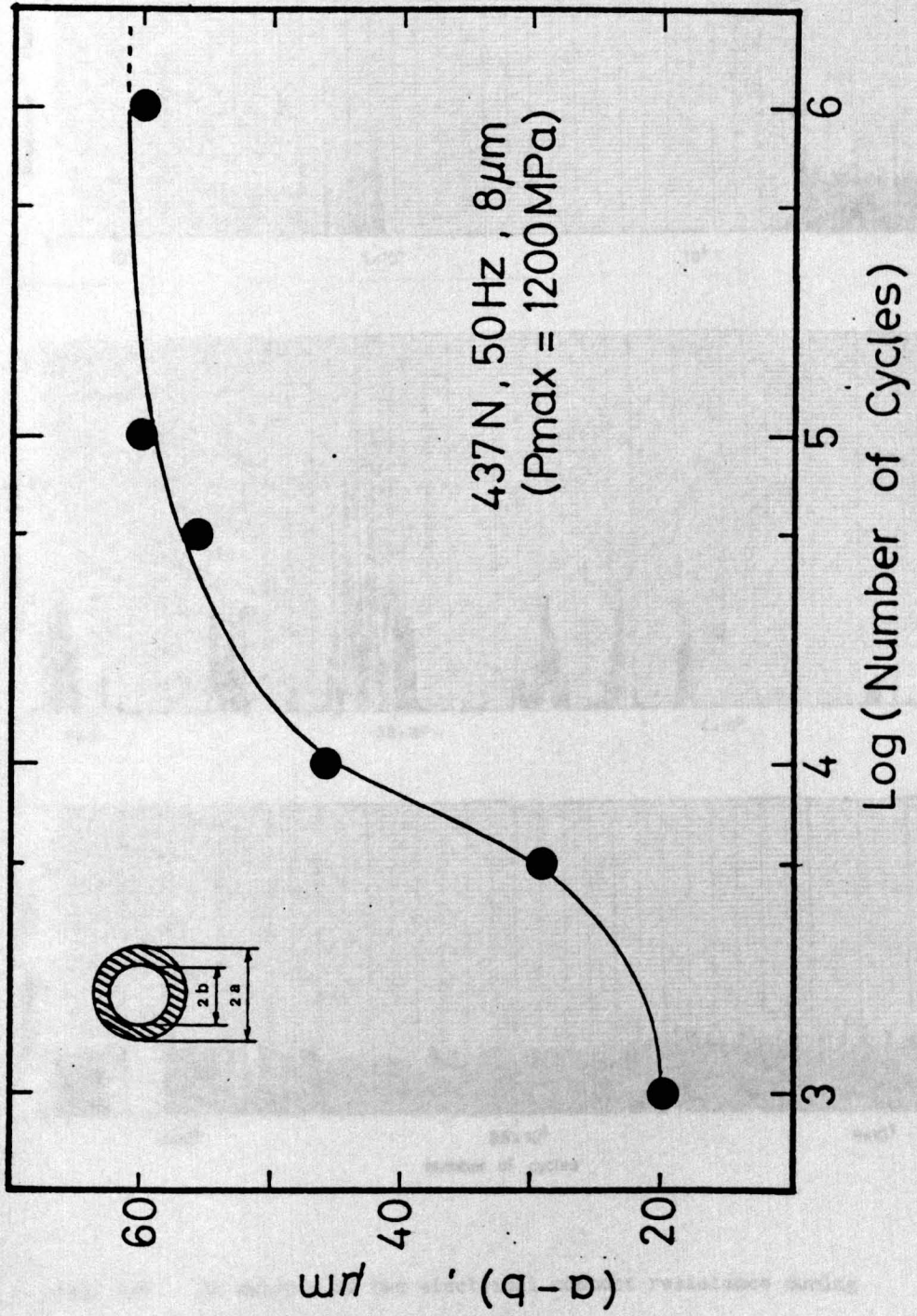


Fig. 7-3c Relationship between the number of cycles and the width of the annulus of the scar, (a-b)

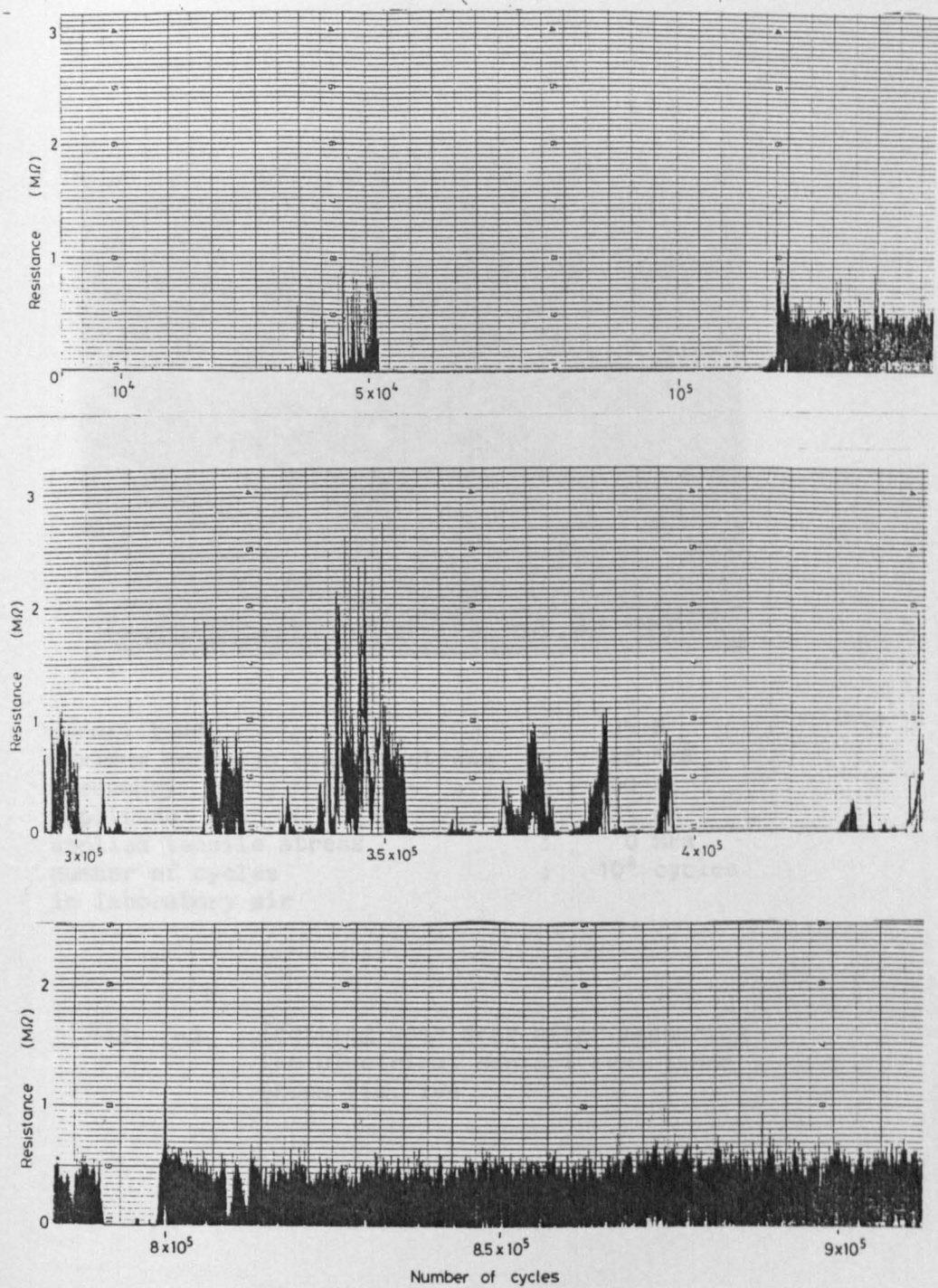
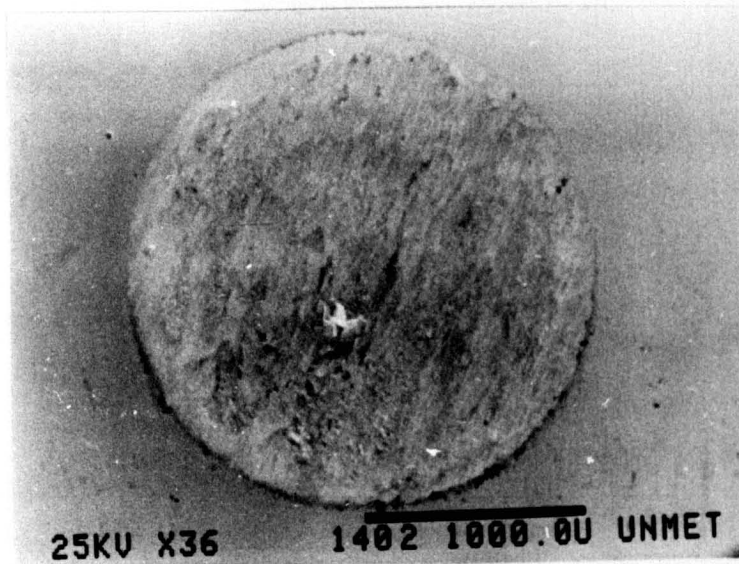


Fig. 7-4 An example of the electrical contact resistance during fretting wear



normal load	:	135 N
maximum Hertzian contact stress	:	822 MPa
frequency	:	60 Hz
amplitude	:	25 $\mu\text{m}$
applied tensile stress	:	0 MPa
number of cycles	:	$10^6$ cycles
in laboratory air		

Fig. 7-5 Fretting wear scar after measuring the electrical contact resistance shown Fig. 7-4

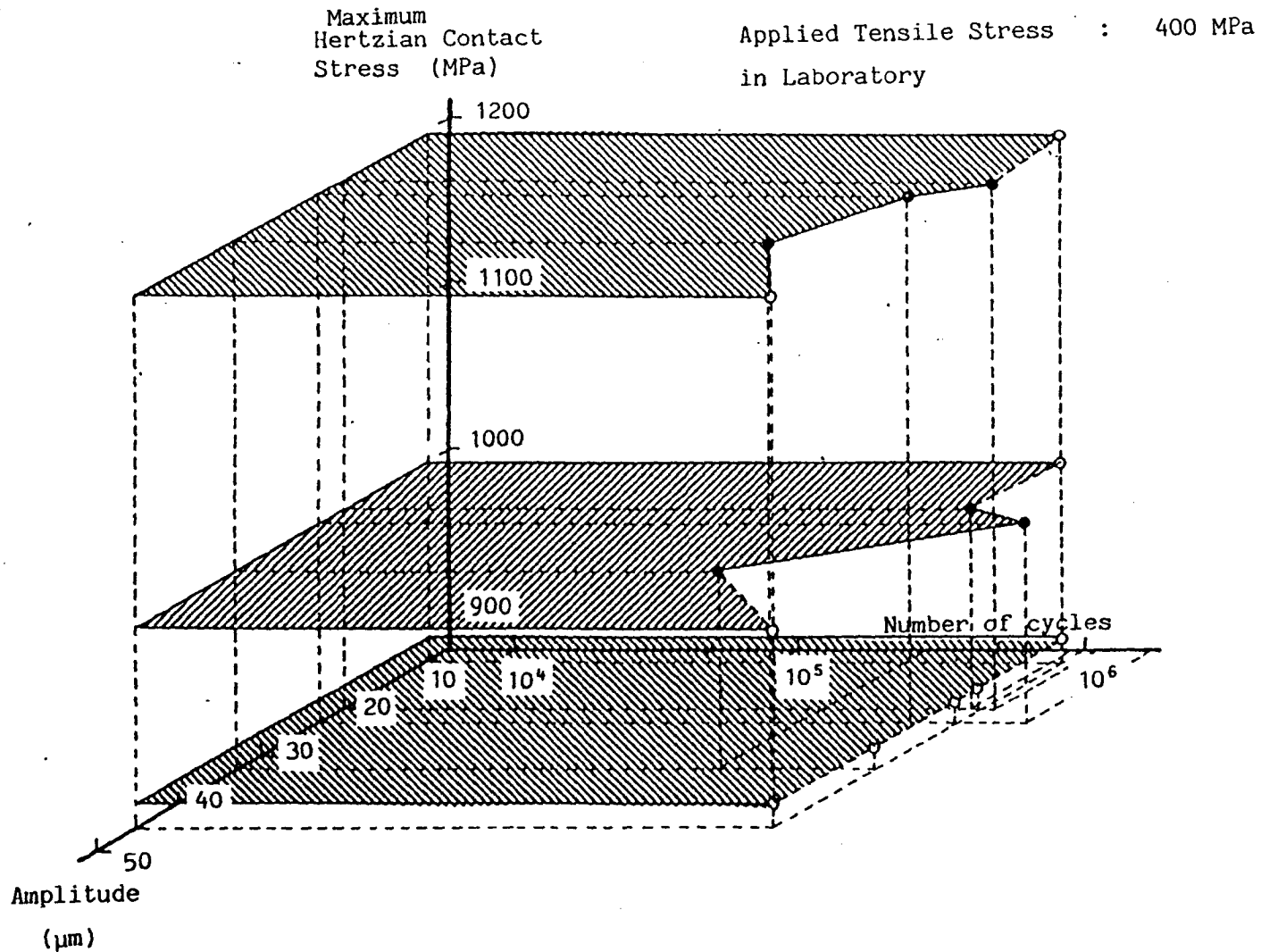


Fig. 7-6a Relationship between maximum Hertzian contact stress, slip amplitude and number of cycles

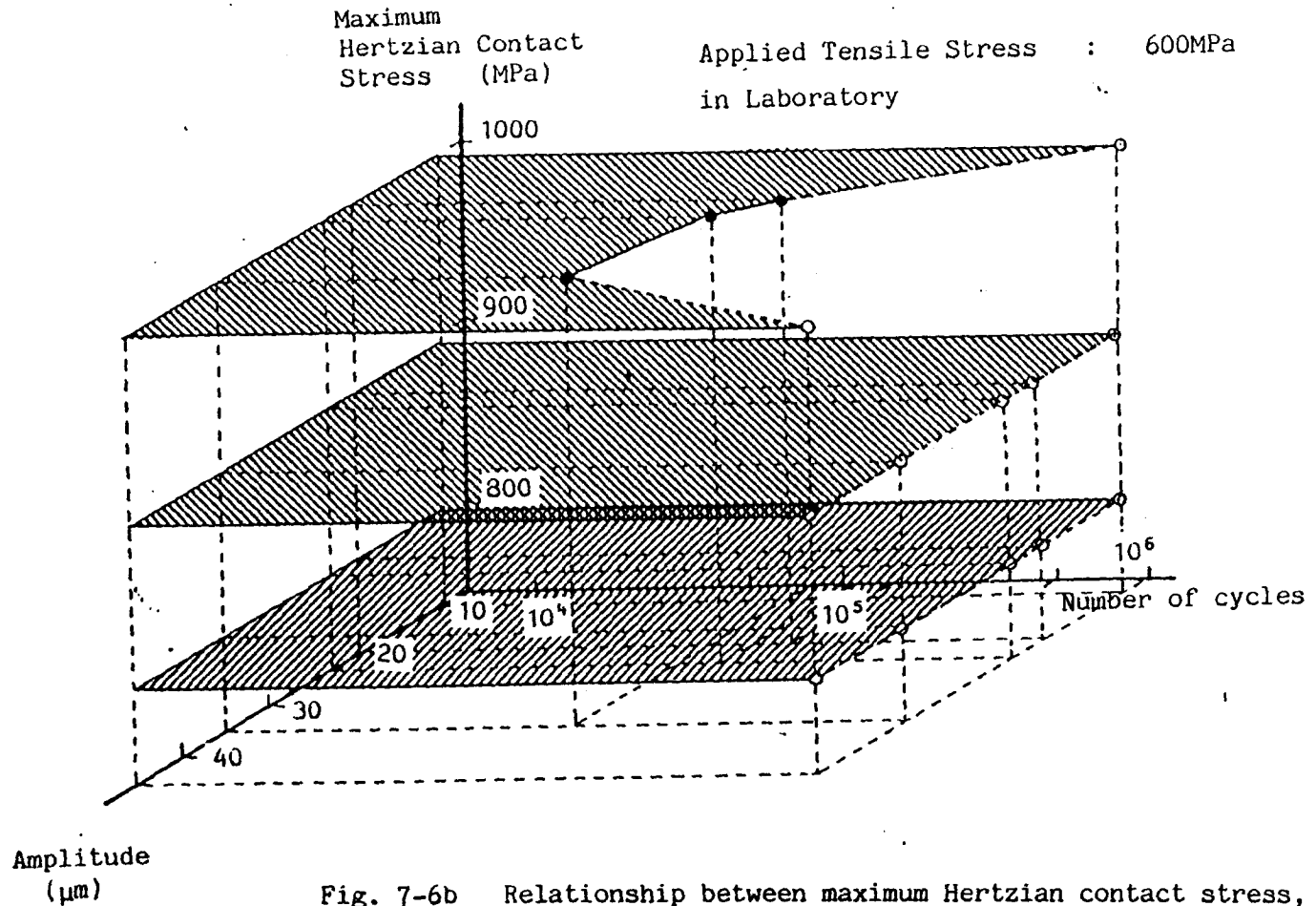


Fig. 7-6b Relationship between maximum Hertzian contact stress, slip amplitude and number of cycles

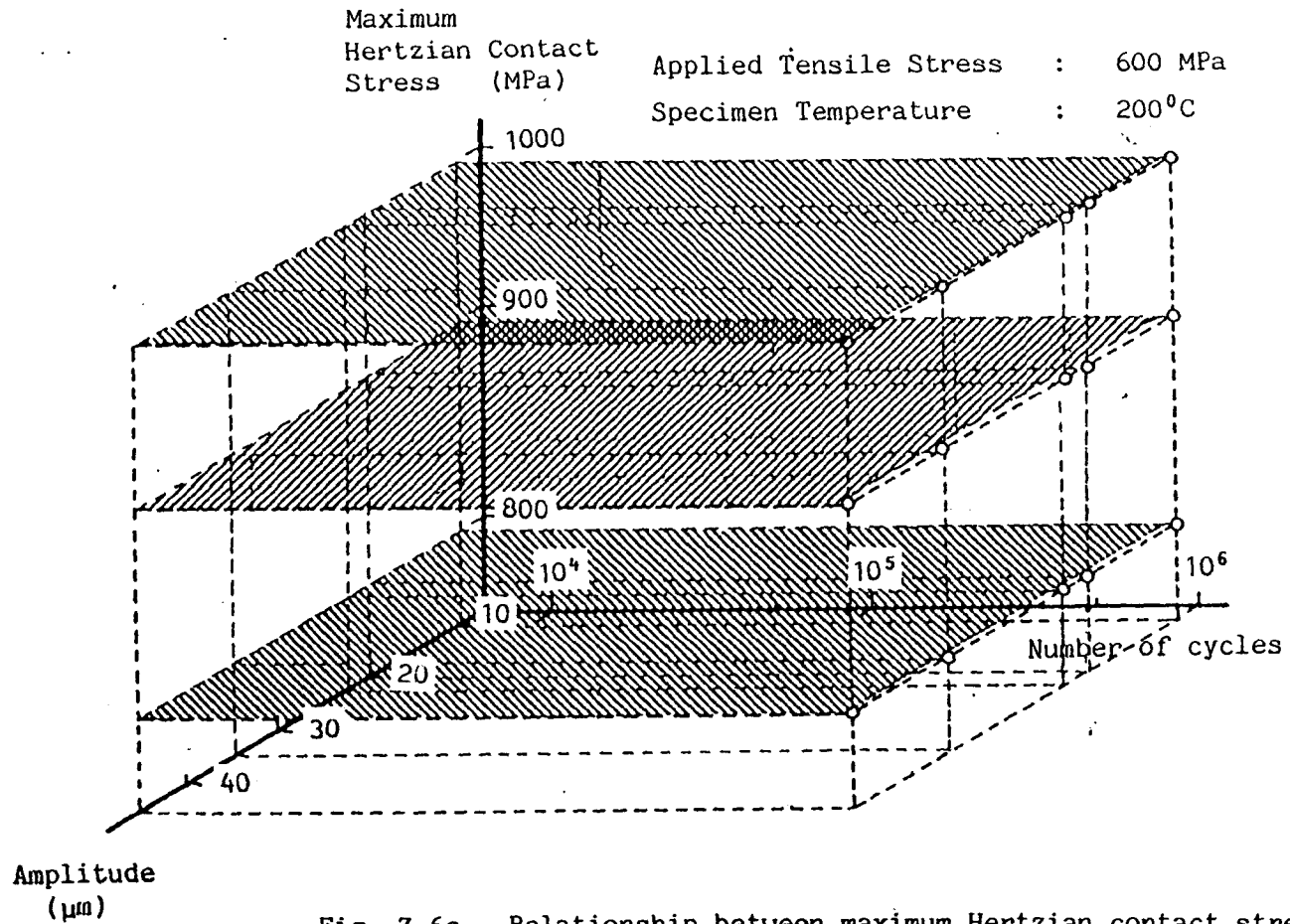


Fig. 7-6c Relationship between maximum Hertzian contact stress, slip amplitude and number of cycles

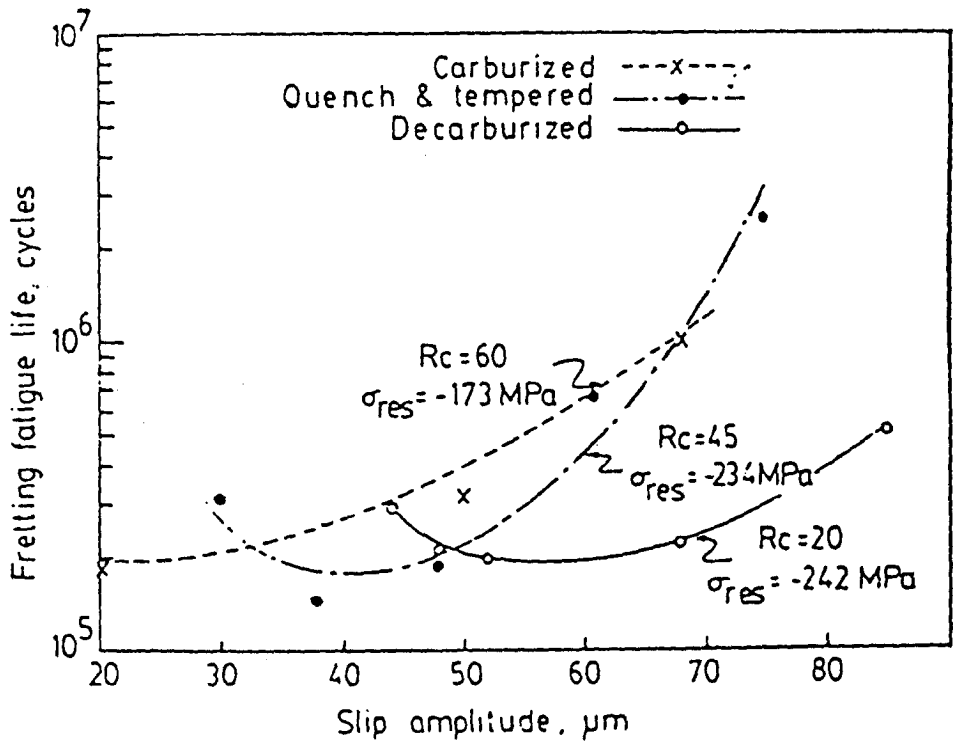
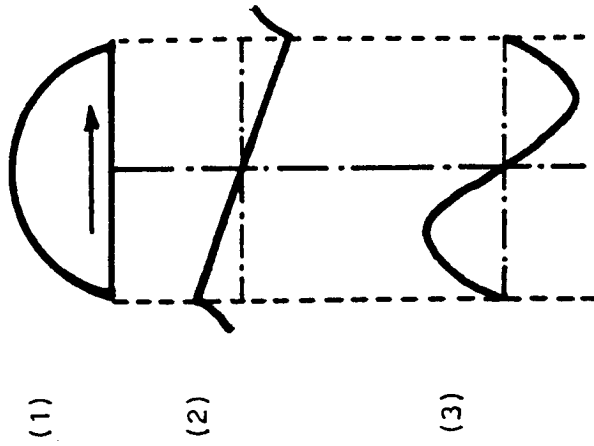


Fig. 7-7 Relationship between fretting fatigue life and slip amplitude obtained by Kudva et al (109)

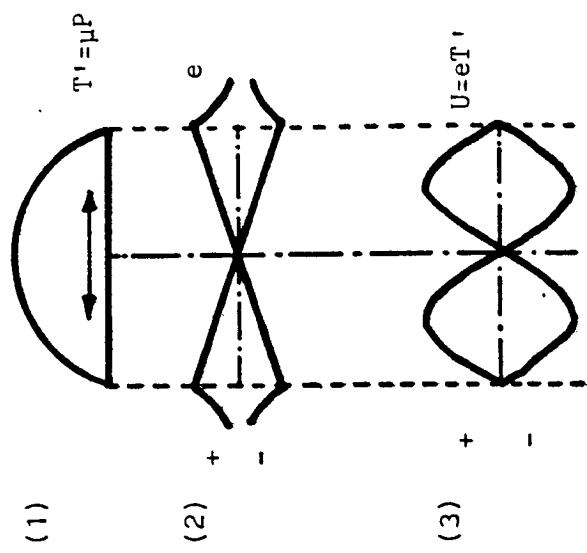
Table 7-1 Relationship between coefficient of friction and slip amplitude

Amplitude	10 $\mu$ m	20 $\mu$ m	25 $\mu$ m	35 $\mu$ m	45 $\mu$ m
Coefficient of Friction	0.50	0.44	0.49	0.72	0.49

normal load : 437N (Pmax = 1200MPa)  
 frequency : 50Hz  
 applied tensile stress : 400MPa  
 coefficient of friction measured at 10<sup>5</sup> cycles

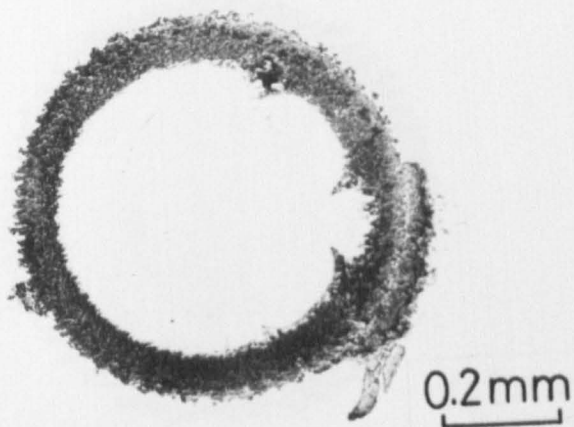


(A)



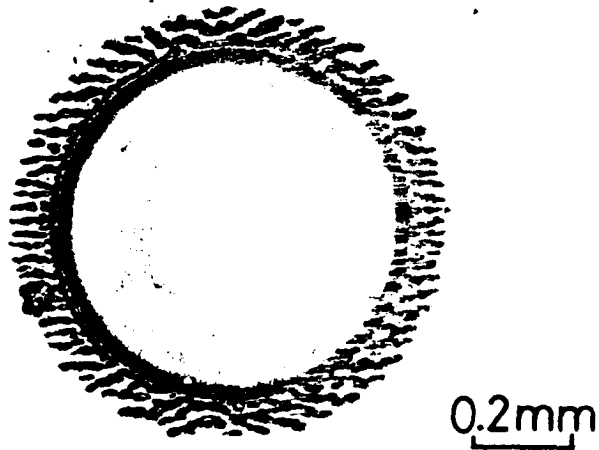
(B)

Fig. 7-8 The distributions of stress, strains and tangential shear strain energy when  $T > \mu P$



normal load	:	437 N
maximum Hertzian contact stress	:	1200 MPa
frequency	:	50 Hz
amplitude	:	8 $\mu\text{m}$
applied tensile stress	:	0 MPa
number of cycles	:	$10^6$ cycles
in laboratory air at R.T.		
coefficient of friction	:	0.5

Fig. 7-9a Fretting wear scar at room temperature



normal load	:	437N
maximum Hertzian Contact stress	:	1200MPa
frequency	:	50Hz
amplitude	:	8 $\mu$ m
applied tensile stress	:	0MPa
number of cycles	:	10 <sup>6</sup> cycles
specimen temperature	:	200 <sup>o</sup> C
coefficient of friction	:	0.21

Fig. 7-9b Fretting wear scar at 200<sup>o</sup>C

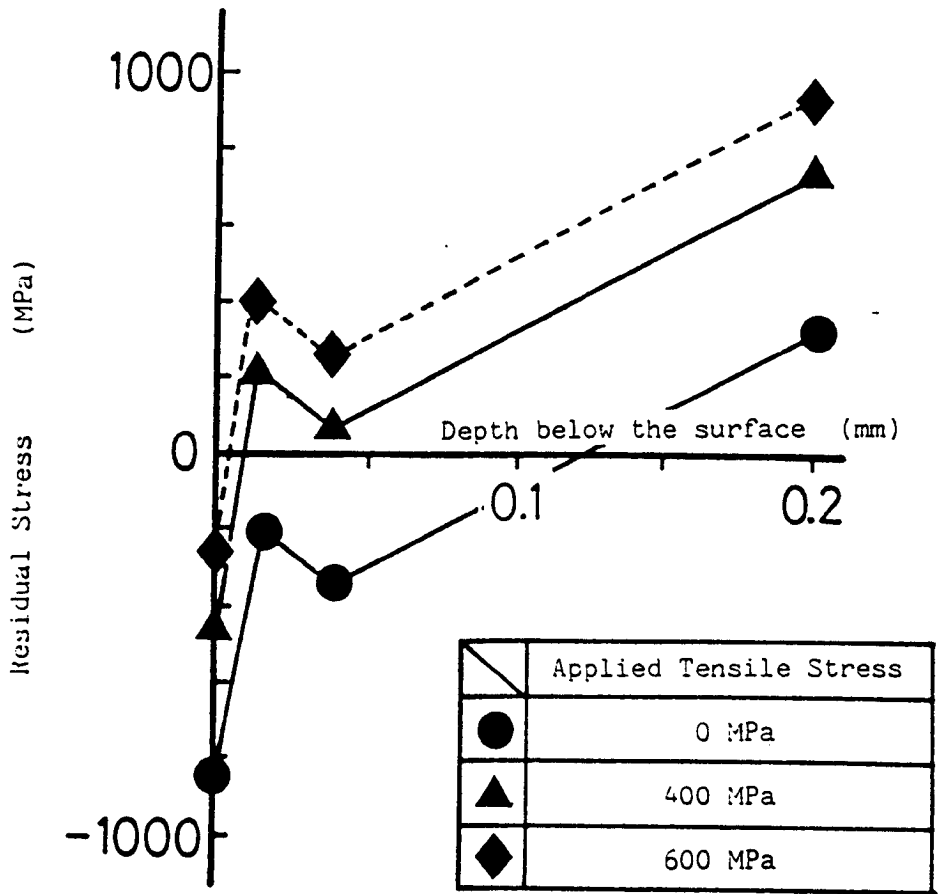
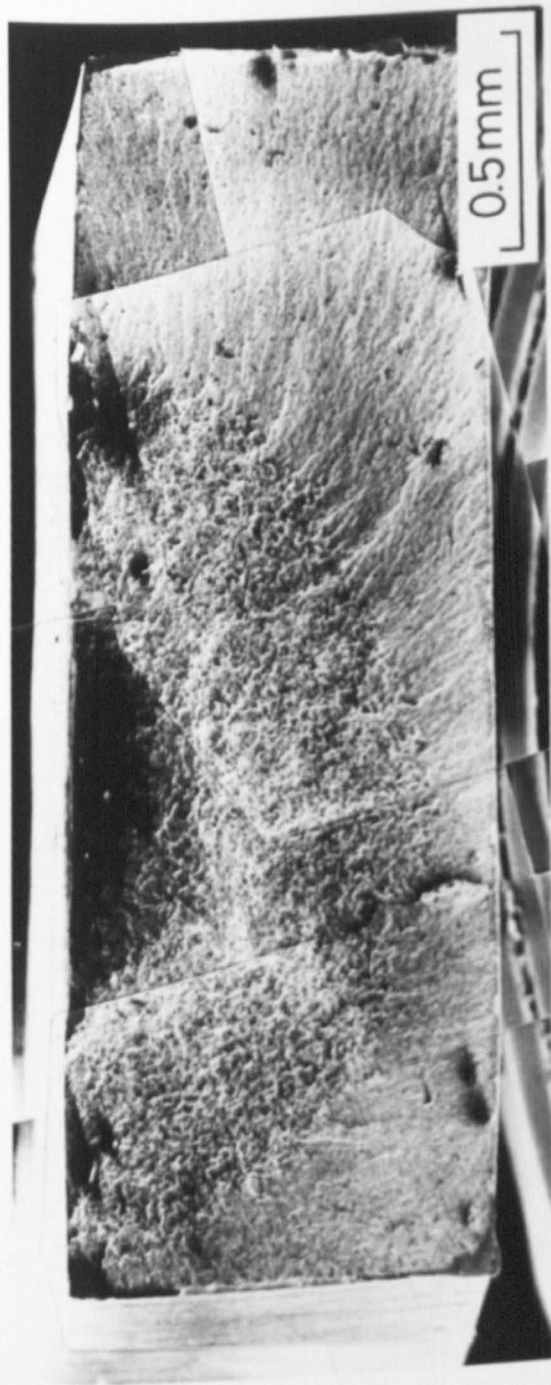


Fig. 7-10 Stress distributions when tensile stresses are applied to the lower stationary specimen



$P_{max} = 1000 \text{ MPa}$   
50 Hz,  $25 \mu\text{m}$   
applied tensile stress  
400 MPa  
fractured at  $1.7 \times 10^6$  cycles

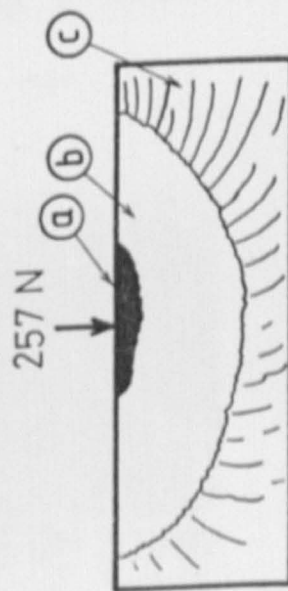
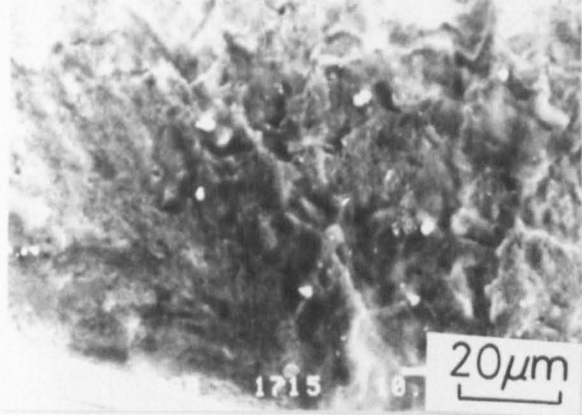
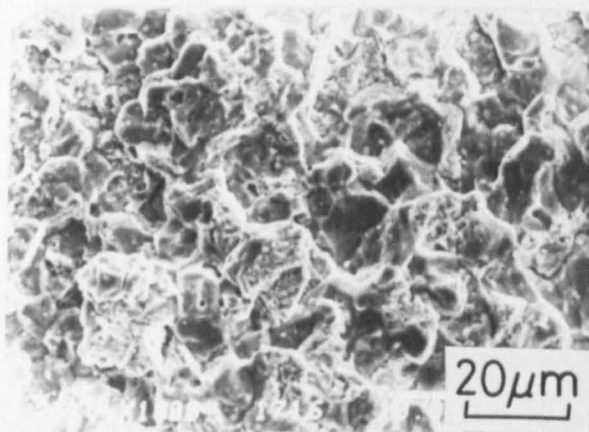


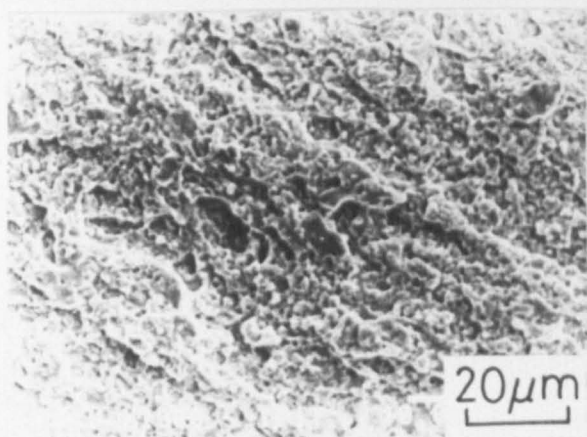
FIG. 7-11 Typical fracture surface



(a) shear mode zone

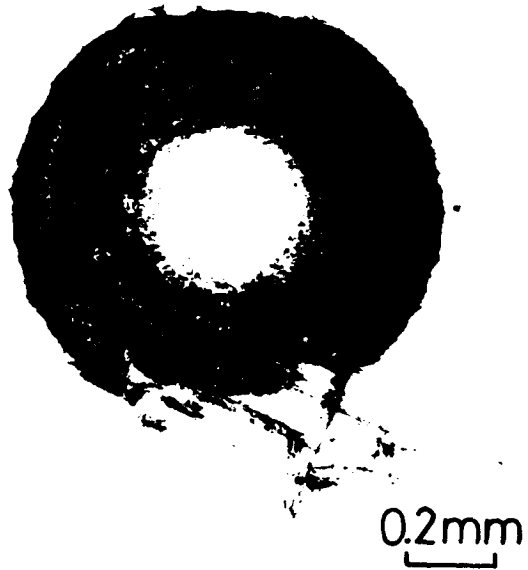


(b) opening mode zone



(c) rapid fracture zone

Fig. 7-12 Three zones in the fracture surface shown in Fig. 7-11



normal load	:	437 N
maximum Hertzian contact stress	:	1200 MPa
frequency	:	50 Hz
amplitude	:	10 $\mu\text{m}$
applied tensile stress	:	400 MPa
number of cycles in laboratory	:	$10^6$ cycles

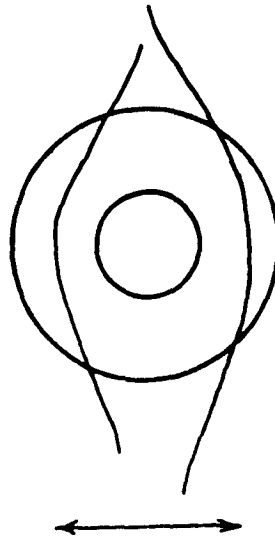
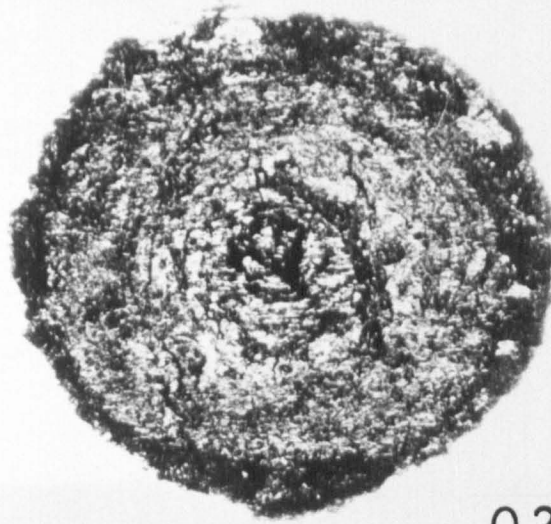


Fig. 7-13a A typical fretting wear scar which has cracks when  $T < \mu P$



0.2mm

normal load	:	257N
maximum Hertzian contact stress	:	1000MPa
frequency	:	50Hz
amplitude	:	35 $\mu$ m
applied tensile stress	:	600MPa
number of cycles in laboratory	:	10 <sup>6</sup> cycles

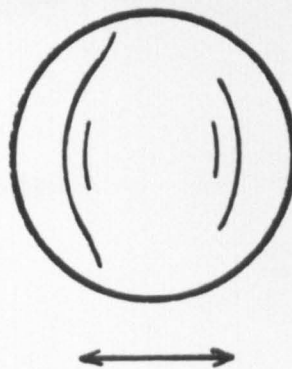
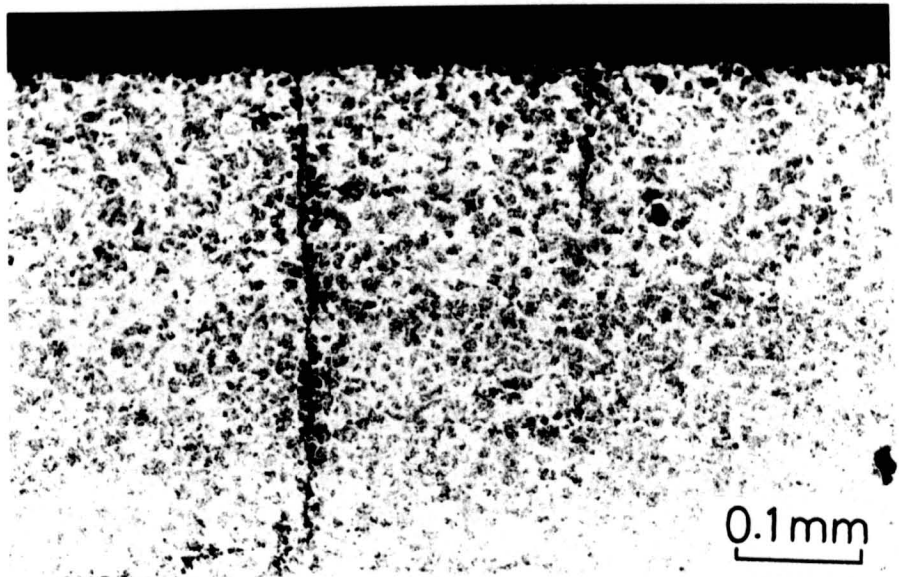
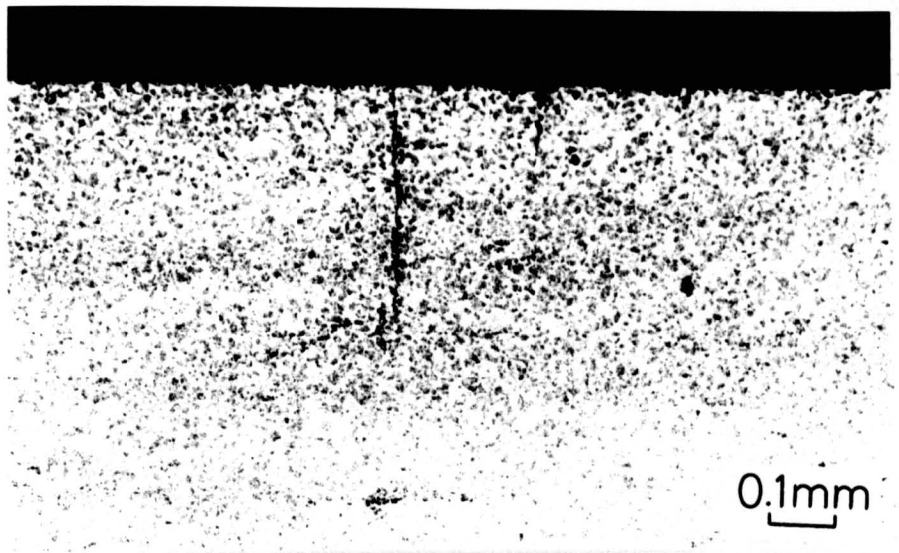


Fig. 7-13b A typical fretting wear scar which has cracks when  $T \geq \mu P$



normal load	:	437 N
maximum Hertzian contact stress	:	1200 MPa
frequency	:	50 Hz
amplitude	:	10 $\mu$ m
applied tensile stress	:	400 MPa
number of cycles	:	$10^6$ cycles
in laboratory		

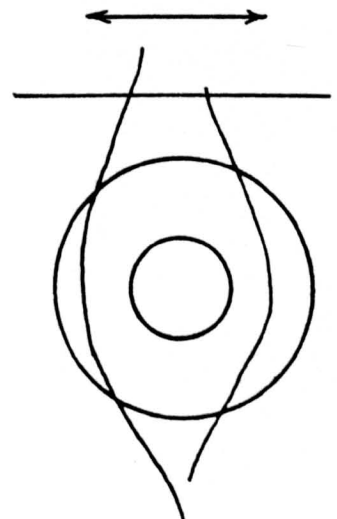
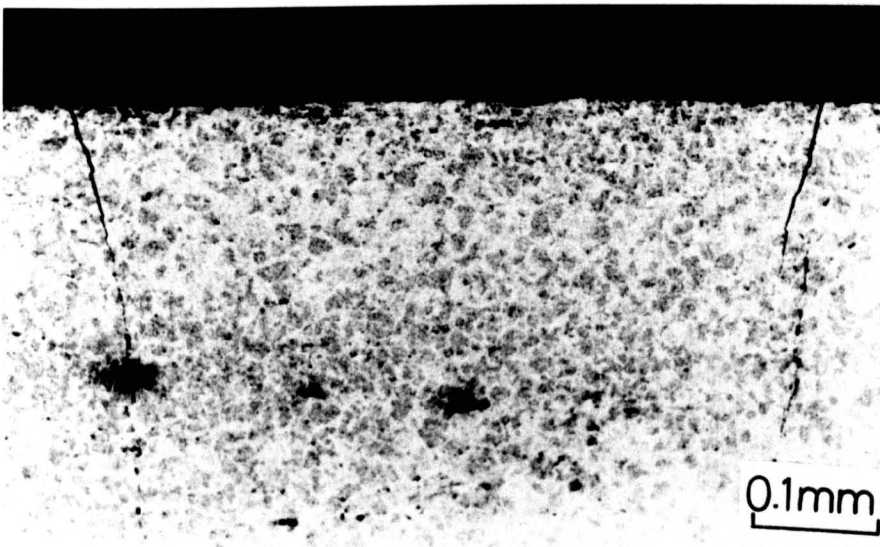
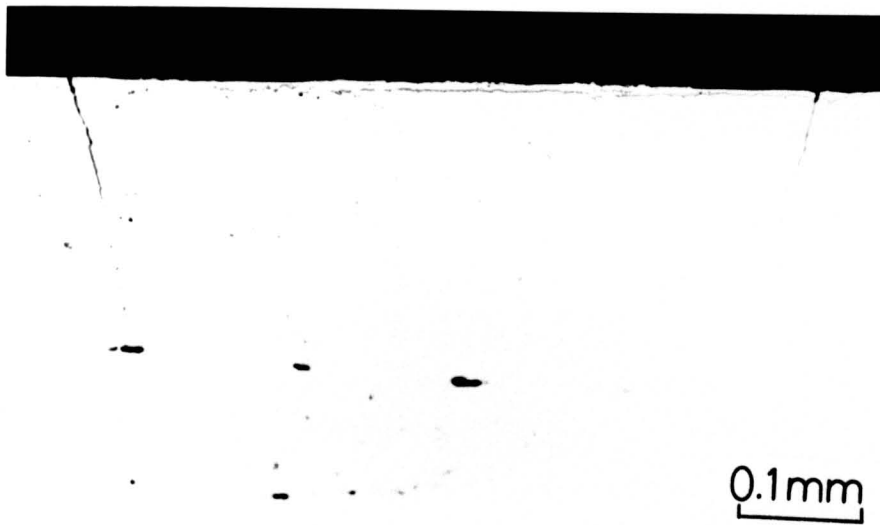


Fig. 7-14a Cracks below the surface



normal load : 437 N  
maximum Hertzian contact stress : 1200 MPa  
frequency : 50 Hz  
amplitude : 10  $\mu$ m  
applied tensile stress : 400 MPa  
number of cycles :  $10^6$  cycles  
in laboratory

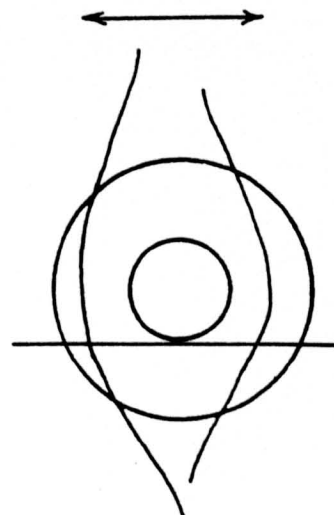
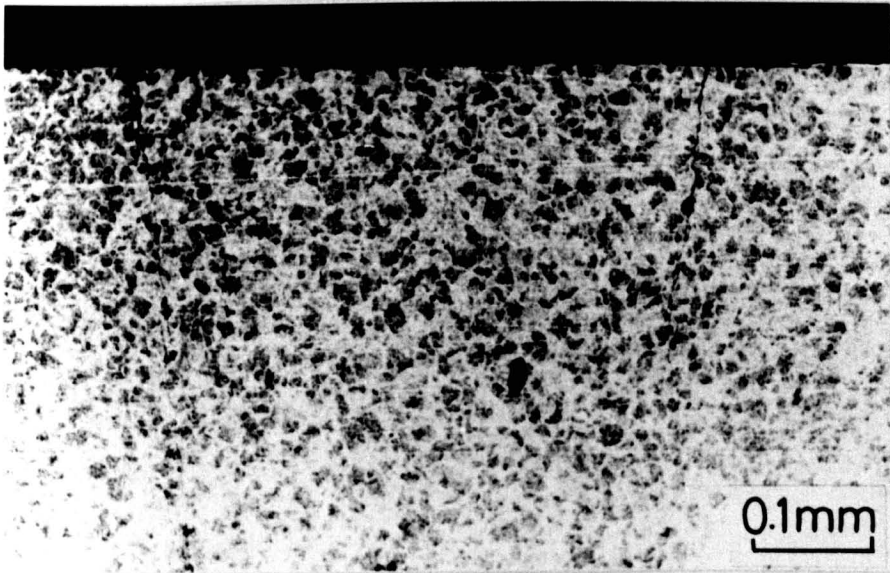
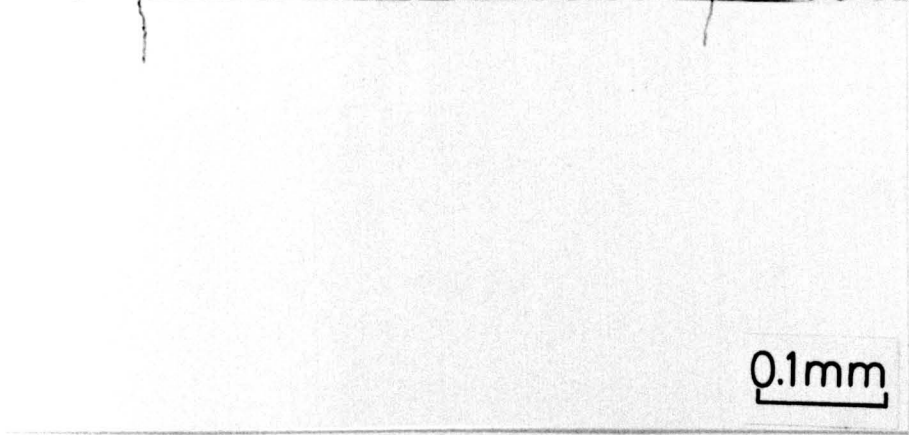


Fig. 7-14b Cracks below the surface



normal load	:	437 N
maximum Hertzian contact stress	:	1200 MPa
frequency	:	50 Hz
amplitude	:	10 $\mu\text{m}$
applied tensile stress	:	400 MPa
number of cycles	:	$10^6$ cycles
in laboratory		

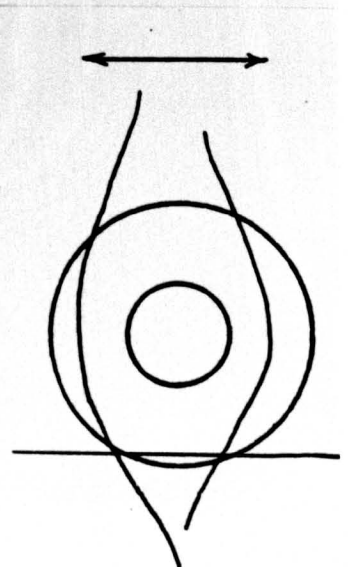
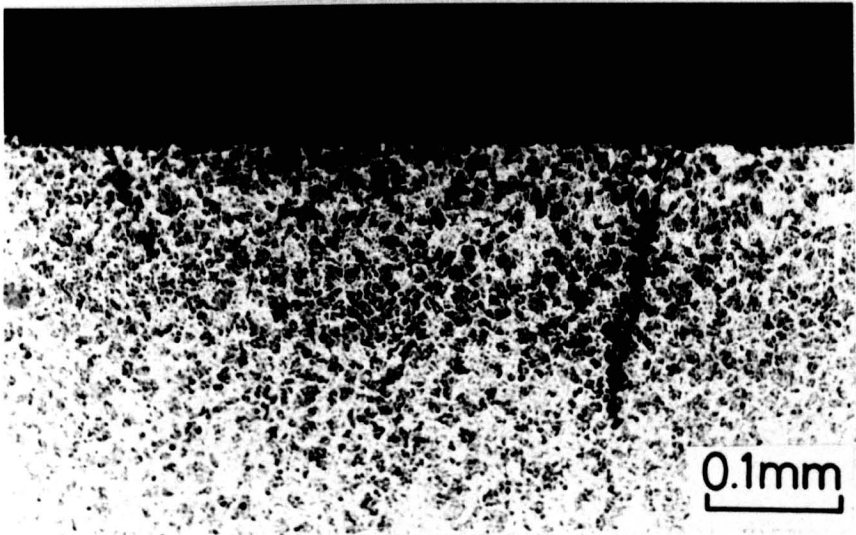


Fig. 7-14c Cracks below the surface



0.1mm



normal load	:	257N
maximum Hertzian contact stress	:	1000MPa
frequency	:	50Hz
amplitude	:	35 $\mu$ m
applied tensile stress	:	600MPa
number of cycles in laboratory	:	10 <sup>6</sup> cycles

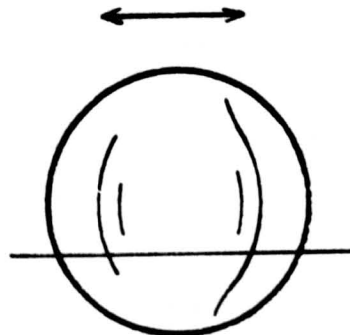
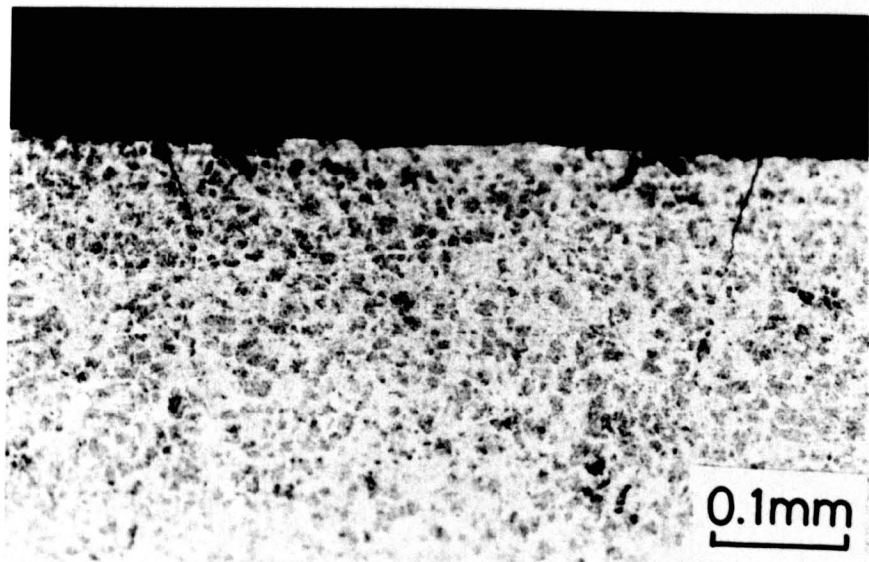


Fig. 7-14d

Cracks below the surface



normal load	:	257N
maximum Hertzian contact stress	:	1000MPa
frequency	:	50Hz
amplitude	:	35 $\mu$ m
applied tensile stress	:	600MPa
number of cycles in laboratory	:	10 <sup>6</sup> cycles

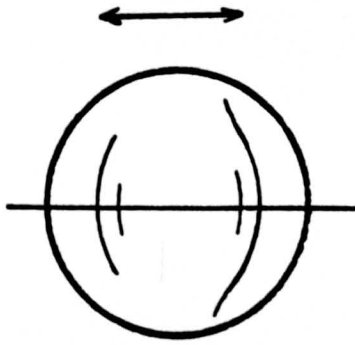
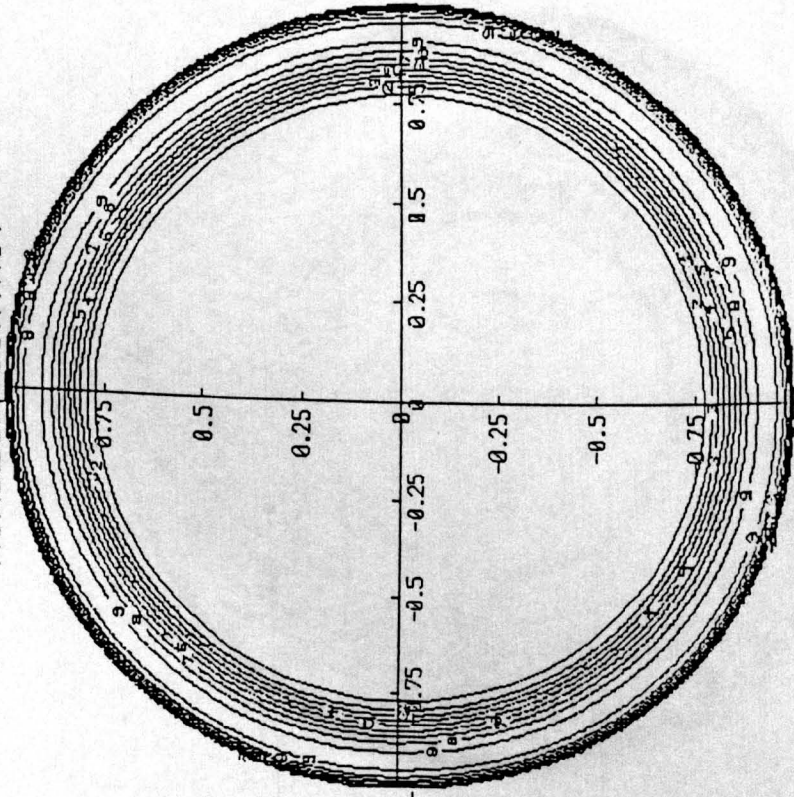


Fig. 7-14e Cracks below the surface

MINDLIN CONTACT



CONTOUR KEY	
1	0.800E+00
2	0.111E-02
3	0.222E-02
4	0.333E-02
5	0.444E-02
6	0.555E-02
7	0.667E-02
8	0.778E-02
9	0.889E-02
10	0.100E-01

Fig. 7-15a The distributions of fretting damage parameter in the fretting wear scar

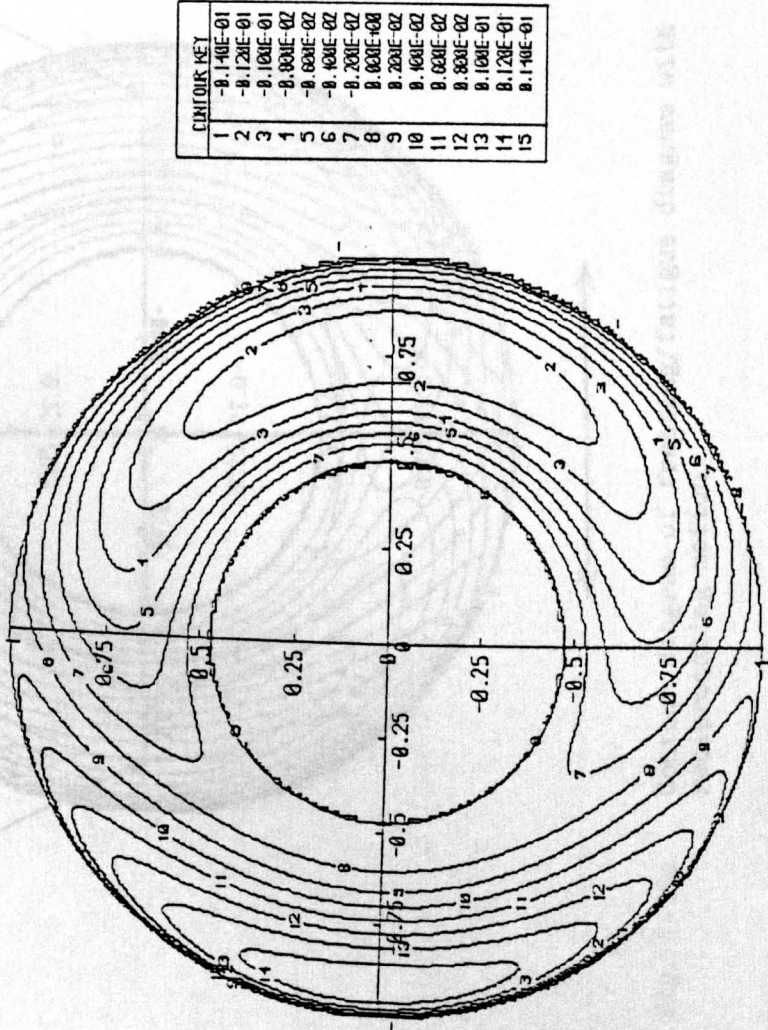


Fig 7-15b Contour diagram of fretting/fatigue damage parameter

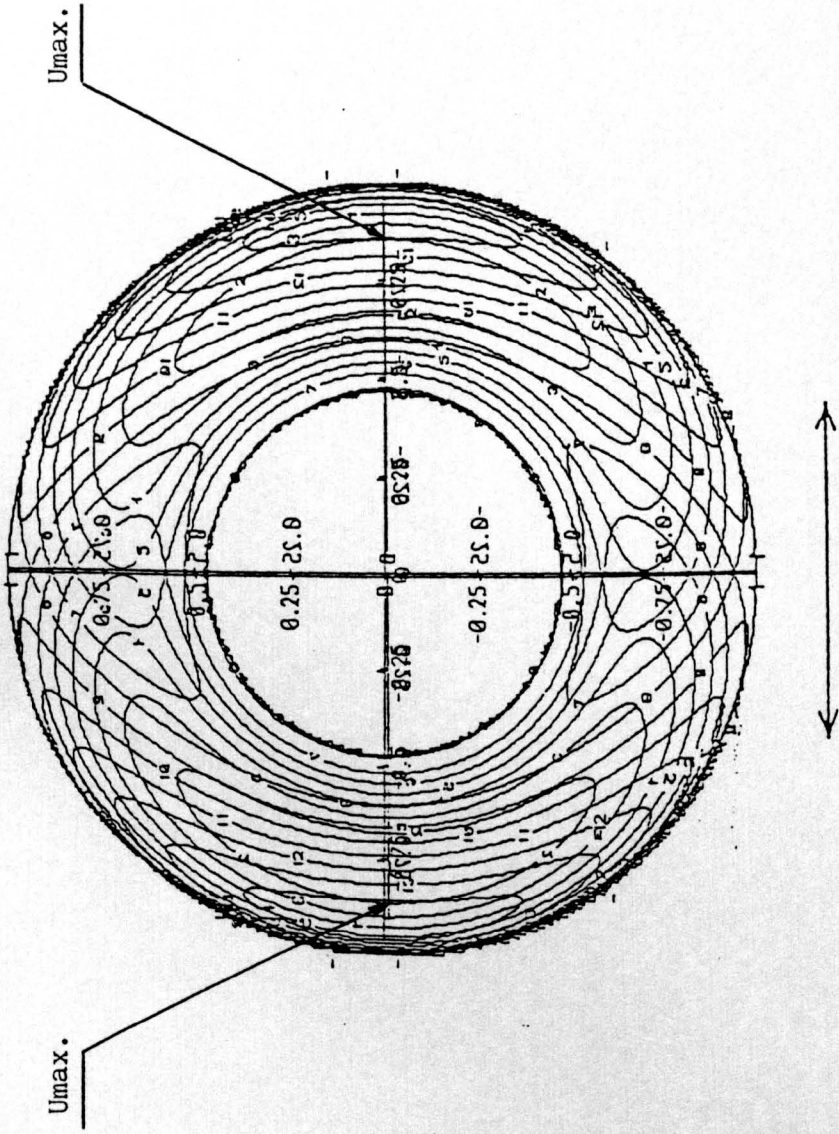


Fig. 7-15c Contour diagram of fretting/fatigue diagram with reciprocating motion